CZECH TECHNICAL UNIVERSITY IN PRAGUE

FACULTY OF ELECTRICAL ENGINEERING

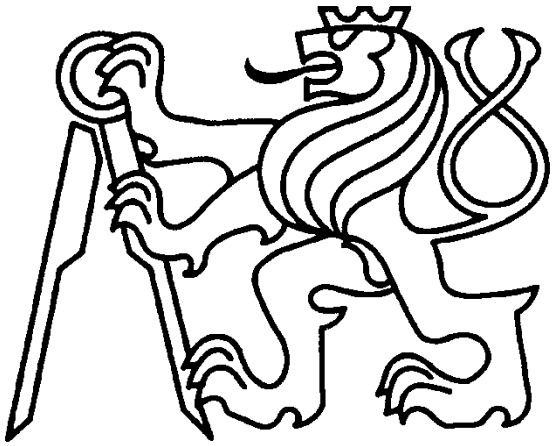

MEASURING WITH MAGNETORESISTIVE SENSORS

HABILITATION THESIS

2014 **Michal Vopálenský**
Vysoká škola polytechnická Jihlava

Acknowledgement

This work was supported by the project "Podpora a individuální rozvoj perspektivních akademických pracovníků na VŠPJ" at the College Of Polytechnics Jihlava.

I would like to express my thanks to my colleagues at the Department of Measurement of the Faculty of Electrical Engineering of Czech Technical University in Prague and at the College of Polytechnics Jihlava, for their wide support.

Special thanks belong to my wife and children for tolerance and patience.

Gloria Patri et Filio et Spiritui Sancto. Sicut erat in principio nunc et semper et in saecula saeculorum.

Contents

Abbreviations

AC	Alternating Current
AMR	Anisotropic Magnetoresistive Effect
DC	Direct Current
FS	Full Scale
GMR	Giant Magnetoresistive Effect
PSD	Power Spectral Density
RMS	Root Mean Square
SDT	Spin Dependent Tunneling Effect
TMR	Tunneling Magnetoresistive Sensor

1. Introduction

Magnetic sensors gained an important role in industrial sensing. Their application range is very wide, encompassing on one hand applications in medicine or geophysical research, on the other hand the automotive industry and automation. Magnetic field is generated and influenced in many ways, so that a lot of processes can be converted into a task where measurement of the magnetic field yields the desired information. This is typically the case of contactless current measurement, where the flowing current causes creation of a magnetic field that can be measured with a magnetic sensor. Sensitive magnetic sensors can be used to determine the gradient (and thus distortion) of the ambient Earth field to detect metal objects such as cars on the road or even metal deposits in human tissues. In navigation, the compass is still a very useful device. Magnetic sensors allowed replacing the mechanical compasses with their electronic alternatives, which nowadays are present in most of mobile "smart" phones. In industrial automation, magnetic sensors are very often used as proximity detectors and rotational encoders.

Of course, there is no a single type of a magnetic sensor that would suit even the limited bundle of applications mentioned above. There are various types of sensors, based on different principles, with different sizes and performances. From the point of view of measurement, the most important parameters of magnetic sensors are the resolution, sensitivity, hysteresis, linearity and measurement range. In many applications, the temperature dependences are also of a big interest. In practice, attention has to be paid to the real meaning of the terms used by individual researchers to avoid false interpretation, for instance the term "sensitivity" is sometimes used instead of "resolution" etc. From the point of resolution, one can line up the most popular magnetic sensors in the following order: for very sensitive measurements (for example in medicine), SQUID (superconducting quantum interference device) allowing measurements of magnetic fields down to femtoTesla ranges are the proper choice. They are followed by fluxgates with the resolution in order of hundreds of picoTesla. Yet in 1970s, the next available sensors in the line would be the Hall probes, with a typical resolution of units of μT. However, thanks to the technological development in the field of deposition of thin layers and in association with the massive expansion of the personal computers, new sensor group became available with the resolution in the order of units to tens of nanoTesla. These devices are based on the magnetoresistive effects in thin layers, i.e., on the change of resistance of a material or more complicated material structure in response to the magnetic field. Although the phenomenon of at least the so-called anisotropic magnetoresistance (AMR) has been known for tens of years, it was first in the last third of the 20th century, when the technology allowed using of this effect in the design of a sensor. The need for miniaturizing the reading heads in hard-drives boosted the development significantly and magnetoresistive reading heads replaced the reading coils. Eventually, sensors for linear measurements have been designed that exploit the anisotropic magnetoresistive effect. These sensors became considerably popular thanks to their miniature size compared to fluxgate and higher sensitivity compared to Hall sensors. Nowadays, they occupy a firm position on the market, serving primarily in contactless current measurement applications, contactless angle detection and in electronic compasses.

In the late decades of 20th century, yet different principles have been employed in magnetic sensing. The magnetoresistive family got new members – sensors based on the Giant Magnetoresistive Effect (GMR) and the Spin Dependent Tunneling (TMR). The design of these sensors is more complicated than that of Anisotropic Magnetoresistors, as it relies on the effects in multilayers. On the

other hand, they can yield higher resolution and sensitivity. Nowadays, there are market-available GMR and TMR sensors for angle measurements.

The magnetoresistive sensors are rather non-typical circuit components and to use them effectively in the particular application requires a specific circuit design. Author of this thesis has spent over 10 years in the field of magnetoresistive sensors, dealing with the design of the sensor itself, developing the appropriate circuits for signal processing and proposing new applications. This thesis summarizes his knowledge, utilizing his published works.

Organization of the thesis

The thesis is submitted as a **series of published works** of the author accompanied with an explaining and unifying text. It would be very demanding for the reader if no basic introduction was given into the principles of the phenomena that are employed in the magnetoresistive sensors. This basic summary is subject of the Chapter 2 and it is yet divided into the sections related to the Anisotropic Magnetoresistance, Giant Magnetoresistance and Spin Dependent Tunneling. Many references to published works are given in the text for the reader's convenience. Basic considerations on the sensor design, indispensable for understanding the advanced techniques used to improve the performance of magnetoresistive sensors, are also presented in Chapter 2.

Chapter 3 is dedicated to the description of the author's own results in the field of magnetoresistive sensors. In section 3.1, issues associated with the development of precise magnetometers with AMR sensors are discussed. A summary is given of the reached parameters of AMR magnetometers. Sections 3.2 and 3.3 give information on the advances in magnetic sensing with GMR and TMR sensors. Chapter 3.4 is dedicated to other applications of magnetoresistive sensors than magnetometry, more concretely to contactless current measurement and power measurement.

To distinguish the referenced pieces of work of the author of this thesis from works of others, the references to the author's texts are typed [underlined] both in the thesis text and in the list of references. The eleven key works of the author are available in the Appendix.

2. Sensors based on anisotropic, giant and tunneling magnetoresistance

2.1 Anisotropic magnetoresistance

2.1.1 Resistivity in magnetoresistive materials

A magnetized ferromagnetic conductor exhibits different resistivity in different directions. The maximum resistivity is imposed to the current flowing along the magnetization of the material, and the minimum resistivity is imposed to the current flowing orthogonally to the magnetization. This phenomenon was firstly reported by William Thomson (also known as Lord Kelvin), who made this discovery in Glasgow before 1856 [1, 2].

In general, magnetic field can affect the conduction of substances in several ways, giving rise to several so-called galvanomagnetic effects. A comprehensive summary of these effects has been presented in [3]. In ferromagnetics, there is a strong influence of the material own magnetization, besides the external magnetic field, making the situation more complicated. Due to their specificity, the galvanomagnetic effects in ferromagnetics are sometimes called the extraordinary galvanomagnetic effects; the effect observed by William Thomson, called extraordinary or anisotropic magnetoresistance (AMR), being one of them.

There are four chemical elements that exhibit ferromagnetic behavior above 0°C – Fe (771°C), Ni (358°C), Co (1127°C) and Gd (16°C). In parentheses, the Curie temperature of these metals is indicated, where the transition from ferromagnetic to paramagnetic state occurs. Various alloys of Ni, Co and Fe are common in magnetoresistive sensors technology. It can be noticed that these elements belong to the group of the so-called transition metals, i.e., they do not have fully occupied 3d-orbitals. Although a phenomenological description of the extraordinary magnetoresistance is possible in rather a non-complicated way, the origin of this effect cannot be explained without applying quantum mechanical principles on the conductivity in transition metals. The primary works in this field were made in the first half of the 20th century, especially by N. F. Mott, who developed a model of the electrical conductivity in transition metals [4, 5]. Later works on electrical transport in transition metals [3, 6, 7] are in fact based on the Mott's two-current model, extending it to the area of ferromagnetic metals. It has been concluded that the primary source of the extraordinary magnetoresistance on the atomic level is the *spin-dependent scattering* of conduction electrons.

Let us designate $\rho_{\parallel}$ the resistivity of a magnetized and saturated ferromagnetic material in the direction of the magnetization, and $\rho_{\perp}$ the resistivity in the direction orthogonal to the magnetization. McGuire and Potter [7] showed that the resistivity ρ_0 of such a material, if fully demagnetized, is

$$\rho_0 = \frac{1}{3}\rho_{\parallel} + \frac{2}{3}\rho_{\perp} \tag{1}$$

From these values, a so-called anisotropic magnetoresistive coefficient or ratio (AMR) is defined as

$$\left(\frac{\Delta\rho}{\rho_0}\right)_{\mathrm{AMR}} = \mathrm{AMR} = \frac{\rho_{\parallel} - \rho_{\perp}}{\frac{1}{3}\rho_{\parallel} + \frac{2}{3}\rho_{\perp}} \tag{2}$$

Some authors use different definition of the AMR coefficient, such as AMR = $\Delta\rho/\rho_{\parallel}$, or AMR = $\Delta\rho/\rho_{\perp}$, so attention has to be paid to the proper interpretation of a particular text. The AMR coefficient reaches units of percent in the ferromagnetic materials, see Table 1. In Table 1, additional material-specific parameters important in the design of AMR sensors are indicated, i.e., characteristic field of anisotropy, magnitude of magnetization in saturation, and magnetostriction coefficient.

Table 1: Parameters of the ferromagnetic materials @ room temperature (after [8]).

Alloy composition	$\Delta\rho/\rho_0$ **(magnetoresistive coef.)**	ρ_0 **(resistivity of demagnetized material)**	H_f **(char. field)**	M_s **(saturated magnetization)**	Λ **(magneto-striction coef.)**
(%)	(%)	($\times 10^{-8}$ Ω.m)	(A.m^{-1})	($\times 10^{-5}$A.m^{-1})	($\times 10^{-6}$)
NiFe 81:19	2.2	22	250	8.7	0
NiFe 86:14	3	15	200	7.6	-12
NiCo 70:30	3.8	26	2500	7.9	-20
NiCo 50:50	2.2	24	2500	10	0
NiFeCo 60:10:30	3.2	18	1900	10.3	-5
NiFeCo 74:10:16	2.8	23	1000	10.1	0
NiFeMo 87:8:5	0.7	72	490	5.1	0
CoFeB 65:15:20	0.07	86	2000	1.03	0

For further considerations, saturated state of a ferromagnetic material will always be assumed, i.e., it will be supposed that the particular magnetic moments of all the magnetic domains within the material are always oriented in the same direction, so that the total magnetization vector $\boldsymbol{M}$ reaches the maximum possible value, saturated magnetization M_s. If there is a reason for $\boldsymbol{M}$ to change its direction, it is always assumed that magnetic moments of all the domains undergo this motion to the new direction. This assumption is referred to as a *coherent rotation of magnetization*. The magnitude of $\boldsymbol{M}$, or saturated magnetization M_s, is dependent on the material (see Table 1).

The magnetization vector can be decomposed into its components along the coordinates *x*, *y* and *z* of the chosen orthogonal Cartesian system, $\boldsymbol{M} = (M_s.\cos\alpha_x, M_s.\cos\alpha_y, M_s.\cos\alpha_z)$, where α_x, α_y, α_z are the angles between $\boldsymbol{M}$ and the respective coordinates. Let $\boldsymbol{\alpha} = (\cos\alpha_x, \cos\alpha_y, \cos\alpha_z)$ be the unit vector in the direction of magnetization $\boldsymbol{M}$. Then the electric field $\boldsymbol{E}$ inside the ferromagnetic material can be described with a general formula [3, 7, 8]

$$\vec{E} = \rho_{\perp}\vec{J} + \Delta\rho\cdot\vec{\alpha}(\vec{\alpha}\cdot\vec{J}) + \rho_{\mathrm{H}}(\vec{\alpha}\times\vec{J}) \tag{3}$$

or in a fully equivalent matrix representation of the Ohm's law

$$\vec{E} = \vec{\rho}\cdot\vec{J} \tag{4}$$

introducing the resistivity tensor $\vec{\rho}$

$$\vec{\rho} = \begin{bmatrix} \rho_{\perp}+\Delta\rho\cdot\cos^2\alpha_x & \Delta\rho\cdot\cos\alpha_x\cdot\cos\alpha_y-\rho_{\mathrm{H}}\cdot\cos\alpha_z & \Delta\rho\cdot\cos\alpha_x\cdot\cos\alpha_z+\rho_{\mathrm{H}}\cdot\cos\alpha_y \\ \Delta\rho\cdot\cos\alpha_x\cdot\cos\alpha_y+\rho_{\mathrm{H}}\cdot\cos\alpha_z & \rho_{\perp}+\Delta\rho\cdot\cos^2\alpha_y & \Delta\rho\cdot\cos\alpha_y\cdot\cos\alpha_z-\rho_{\mathrm{H}}\cdot\cos\alpha_x \\ \Delta\rho\cdot\cos\alpha_x\cdot\cos\alpha_z-\rho_{\mathrm{H}}\cdot\cos\alpha_y & \Delta\rho\cdot\cos\alpha_y\cdot\cos\alpha_z-\rho_{\mathrm{H}}\cdot\cos\alpha_x & \rho_{\perp}+\Delta\rho\cdot\cos^2\alpha_z \end{bmatrix} \tag{5}$$

Here $\boldsymbol{J}$ is the vector of the current density;
ρ_{H} is the Hall coefficient of the material;
meaning of the rest of the quantities has been explained above.

Although the anisotropic magnetoresistive effect has been noticed by Lord Kelvin already, its practical exploitation was possible first in the second half of the 20th century, when the level of technology allowed manufacturing of thin films of ferromagnetic materials. In fact, the design of the present real devices employing the anisotropic magnetoresistive effect is based exclusively on thin film structures. This bears a significant simplification to the formulae for the electric field in the material.

Let us consider a thin film of a material that exhibits anisotropic magnetoresistance. Choosing a coordinate system in a way that *x*-axis coincides with the direction of current propagation and *z*-axis is orthogonal to the plane of the film, the vector of the current density can be written as $\vec{J} = \begin{pmatrix} J_\mathrm{x} \\ 0 \\ 0 \end{pmatrix}$.

As the thickness of the film is very small compared to its width and length, there is a strong so-called demagnetization factor in the *z*-axis direction, thus practically avoiding $\boldsymbol{M}$ to elevate out of the film plane. In other words, it is energetically convenient for $\boldsymbol{M}$ to rotate in the film plane only. Then the angle between *z*-axis and $\boldsymbol{M}$ is always 90° and $\cos\alpha_\mathrm{y} = \sin\alpha_\mathrm{x}$. Considering these facts and using the previously presented formulae, one gets for components of $\boldsymbol{E}$

$$\begin{aligned} E_\mathrm{x} &= \left(\rho_\perp + \Delta\rho\cos^2\alpha_x\right)\cdot J_\mathrm{x} \\ E_\mathrm{y} &= \left(\Delta\rho\cdot\cos\alpha_x\cdot\cos\alpha_y\right)\cdot J_\mathrm{x} = \frac{1}{2}\Delta\rho\sin 2\alpha_x\cdot J_\mathrm{x} \\ E_\mathrm{z} &= -\rho_\mathrm{H}\cdot\sin\alpha_x\cdot J_\mathrm{x} \end{aligned} \tag{6}$$

It can be seen that the electrical current flowing through a saturated film of a magnetoresistive film leads to a creation of the electrical field, whose direction is dependent on the angle of magnetization and which generally has components along all the three axes of the coordinate system. However, E_x, or the field arising in the direction of the current propagation, is of the greatest importance, as it represents the direct manifestation of the anisotropic magnetoresistive effect. The resistivity imposed to the current, or measured in the current propagation direction, is $\rho_\mathrm{meas} = E_\mathrm{x} / J_\mathrm{x}$. Let α_x, or the angle that $\boldsymbol{M}$ contains with the direction of current propagation, be designated φ in the further text. Then

$$\rho_{meas}(\varphi) = \rho_\perp + \Delta\rho\cos^2\varphi = \rho_\parallel - \Delta\rho\sin^2\varphi \tag{7}$$

Equation (7) is usually called *Woigt–Thomson formula* and it remains sufficiently precise even in a real, polycrystalline film with randomly oriented crystallites [7, 8]. Many modifications of this basic formula have been developed to better approximate the real behavior of the resistivity in a ferromagnetic film, e.g. [9], but in fact, the presented formula in its basic form represents a sufficiently good model for the ordinary magnetoresistive sensors; it is even good enough to allow characterization of the behaviour of $\boldsymbol{M}$ inside a magnetoresistive material through the resistance measurement [10].

For completeness, it should be mentioned that the field E_y is a manifestation of the so-called planar or extraordinary Hall effect for its apparent similarity to the regular Hall effect, used in semiconductor-based Hall sensors, where the electric field also arises in the transversal direction to the flowing current. However, it has to be emphasized that the physical origin of this effect is completely different than that of the regular Hall effect [3]. Although papers exist that propose magnetic sensors employing the extraordinary Hall effect [11], there is no real commercially-available sensor that would really be based on this effect. The same applies to the voltage arising along the *z*-axis direction.

2.1.2 Magnetization in magnetoresistive bodies

From the analysis made above it is obvious that the anisotropic magnetoresistive effect is exploitable for the measurement of a magnetic field, if the angle of $\boldsymbol{M}$ inside a saturated film of magnetoresistive material can be influenced by the magnetic field in a defined way. In general, $\boldsymbol{M}$ possesses such a position that the energy of the system is minimized.

The total magnetization-related energy in a ferromagnetic stripe used in magnetoresistors consists of several terms. In basic considerations, the magnetostatic energy, related to the mutual orientation of an external magnetic field $\boldsymbol{H}$ and $\boldsymbol{M}$ and being minimal for $\boldsymbol{M}$ coinciding with $\boldsymbol{H}$, and energy terms associated with the uniaxial anisotropies in the material, are taken into account. Uniaxial anisotropy manifests itself by the existence of the so-called easy axis, where $\boldsymbol{M}$ tends to orient to. The energy associated with the uniaxial anisotropy is minimal when $\boldsymbol{M}$ is oriented along the easy axis (in one of the two possible directions), all other directions of $\boldsymbol{M}$ lead to a state with a higher energy. The "strength" of the uniaxial anisotropy is quantified by its characteristic field H_k. The higher H_k, the stronger affinity of $\boldsymbol{M}$ to the easy axis, or the higher energy needed to incline $\boldsymbol{M}$ out of the easy axis. There are several origins of uniaxial anisotropies in magnetoresistive stripes, as will be discussed later. It can be shown that, in the first approximation, several uniaxial anisotropies with different easy axes and H_k values result in an equivalent uniaxial anisotropy, whose H_k and direction of easy axis can be derived from the parameters of the original uniaxial anisotropies [12].

The practical exploitation of anisotropic magnetoresistive effect in magnetoresistive sensors rely on narrow stripes formed out of a thin film of magnetoresistive material deposited onto an appropriate substrate. In practice, alloy of nickel and iron, NiFe 81:19 (called permalloy) is mostly used as a material for fabrication of the magnetoresistive stripes. Its magnetoresistive coefficient is high enough to allow its exploitation in sensors and it has very low magnetostriction (see Table 1), i.e., its magnetic properties are not sensitive to the mechanical stresses. The width of magnetoresistive stripes is usually in the order of tens of micrometers, the thickness is tens of nanometers, the length reaches hundreds to thousands of micrometers. The stripes are mostly sputtered onto a passivated silicon substrate. To save the space in the sensor, the stripes are almost exclusively realized as meanders [13, 14, 15]. The magnetoresistive ratio is rather small, reaching units of percent (see Table 1). This ratio can additionally be affected by high background resistivity ρ_0, caused among others by the charge carrier scattering on the material grain boundaries. The amount of the material grains can be reduced by annealing of the sputtered films, lowering thus ρ_0. Annealing must be done in an inert atmosphere (mostly argon); even a small amount of oxygen present during annealing process can depreciate the anisotropic material due to surface oxidation. A homogeneous magnetic field is usually applied during annealing in the direction of the intended longitudinal axis of the stripes. This measure is performed in order to reduce the anisotropy dispersion in the material, but it also leads to creation of a uniaxial anisotropy with the easy axis along the direction of the applied field. In further text, this anisotropy will be called the *induced anisotropy*. The characteristic field $H_{k,f}$ of this anisotropy in NiFe 81:19 is around 250 A/m. Altogether, annealing reduces the background resistivity ρ_0, lowers the mechanical stresses in the material and leads to creation of the induced anisotropy with a low dispersion.

The shape of a saturated ferromagnetic body heavily influences behavior of its magnetization. The divergence of magnetization on the surfaces of a spatially limited ferromagnetic body leads to existence of the so-called demagnetization field [16]. In a simplified way, it can be said that it is harder to magnetize a (non-spherical) ferromagnetic body in certain direction compared to other directions. Thus, the magnetization in a saturated ferromagnetic body can have preferred directions of orientation, depending on the shape of the body. The theory of demagnetization effects have been described thoroughly in the general textbooks on magnetism [17], so in this work, a basic knowledge on the topic is assumed, and only the case of thin narrow ferromagnetic stripes will be discussed. More detailed analysis has been made in [18]. It can be shown [11, 13, 19] that the demagnetization effects in a thin ferromagnetic stripe have two consequences:

(1) vector of magnetization $\boldsymbol{M}$ does not leave the plane of the stripe under normal conditions due to a huge demagnetization factor in the perpendicular direction to the stripe plane (z-axis), and

(2) ***M*** tends to orient itself along the longitudinal axis of the stripe (*x*-axis). This tendency can be described, in the first approximation, as a uniaxial anisotropy with the easy axis along the longitudinal axis of the stripe. This anisotropy is called the *shape* or *form anisotropy*.

The characteristic field $H_{k,s}$ of the shape anisotropy is associated with the so-called demagnetization factor N_y in the *y*-axis direction and with saturation magnetization M_s through the relation [12]

$$H_{k,s} = N_y M_s \tag{8}$$

A known problem in this regard is that only in ellipsoidal specimens the demagnetization field is uniform, resulting in single-number demagnetization factors along the axes [20]. In rectangular bodies, however, the demagnetization field is not uniform in the entire volume of the specimen and thus the demagnetization factor in any axis cannot be represented with a single number. However, due to its practical importance, considerable effort has been made to develop suitable models that would allow making a proper estimation of single-number demagnetization factors even in rectangular bodies [16, 21–24]. In the case of thin magnetoresistive stripes, an assumption is usually made that the demagnetization factor $N_x \approx 0$, $N_z \approx 1$ and N_y is approximated as $N_y = t / (t + w) \approx t / w$, where w is the width and t is the thickness of the stripe [8, 11, 19].

In a typical AMR sensor, the annealing is performed in a way that the easy axis of induced anisotropy lies along the longitudinal axis of the stripes, coinciding thus with the easy axis of the shape anisotropy. The resultant anisotropy has the easy axis along the longitudinal axis of the stripe and its characteristic field is [12] $H_a = H_{k,f} + H_{k,s}$. As $H_{k,f}$ can hardly be influenced, being rather a material property (see Table 1), the anisotropy can practically be controlled through $H_{k,s}$, or the thickness and width of the stripe. However, stripe thickness cannot be chosen arbitrarily, because thickness bigger than approx. 50 nm can lead to formation of domains in more than one layer, which leads to degradation of the magnetoresistive effect. Thus, the width of the stripe is a decisive parameter in determination of the strength of the uniaxial anisotropy H_a within the stripe, and consequently the sensitivity of the sensor, as will be shown soon.

Let us consider a saturated ferromagnetic stripe made of a magnetoresistive material, with a uniaxial anisotropy H_a along the longitudinal axis of the stripe. Let an external field $\boldsymbol{H} = (H_x, H_y)$ be applied in an arbitrary direction in the stripe plane – see figure 1. The external field ***H*** disturbs ***M*** from its idle position along the easy axis, but due to anisotropy, ***M*** does not rotate fully into the direction of ***H***. The orientation of ***M*** is thus a result of the competition between the magnetostatic energy, associated with the external magnetic field ***H***, and energy associated with the affinity of ***M*** to the easy axis of anisotropy.

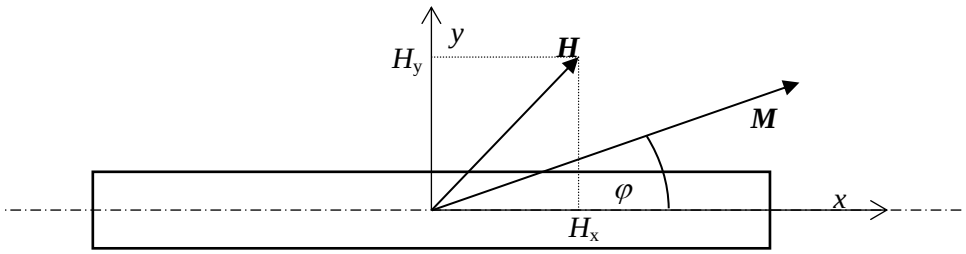

Figure 1: Ferromagnetic stripe with inclined ***M***.

Introducing the reduced fields $h_x = \frac{H_x}{H_a}$, $h_y = \frac{H_y}{H_a}$, it can be shown [8] that the angle φ of inclination of ***M*** from the longitudinal axis of the stripe in the state of minimum system energy satisfies the formula

$$h_x \sin\varphi - h_y \cos\varphi + \sin\varphi\cos\varphi = 0 \tag{9}$$

Unfortunately, there is no (simple) analytic solution for φ (although a way how to find φ analytically has been presented recently [25]). It means that there is no simple equation for the angle of $\boldsymbol{M}$ when the stripe is exposed to an arbitrary external field $\boldsymbol{H}$. Nevertheless, the angle of $\boldsymbol{M}$ for an arbitrary $\boldsymbol{H}$ can be found geometrically, exploiting the so-called Stoner-Wohlfahrt diagram [26, 27].

However, there exist simple solutions for some particular cases, from which the most important one in magnetoresistive sensors is that of $\boldsymbol{H}$ applied in the *y*–axis direction, called in that case the *sensitive axis*. Then h_x is zero and for $H_y \leq H_a$, it can be written

$$\sin\varphi = \frac{H_y}{H_a} \tag{10}$$

For $H_y > H_a$, $\boldsymbol{M}$ is rotated fully to the H_y direction and further increasing of $\boldsymbol{H}$ does not change φ.

2.1.3 Exploitation of AMR effect in sensors

Considering a ferromagnetic stripe contacted on its short edges, so that the current flows along the longitudinal axis that coincides with the easy axis of anisotropy, exposed to an external field applied in the *y*-axis only, the measured resistivity can be obtained combining (10) and Woigt-Thomson formula (7):

$$\begin{aligned} \rho_{\mathrm{meas}}\left(H_y\right) &= \rho_{\parallel} - \Delta\rho\left(\frac{H_y}{H_a}\right)^2, \quad \left|H_y\right| \leq H_a \\ \rho_{\mathrm{meas}}\left(H_y\right) &= \rho_{\perp}, \qquad\qquad\quad \left|H_y\right| > H_a \end{aligned} \tag{11}$$

Expressions (11) are visualized in figure 2. Solid line is the theoretically expected dependence; dashed line corresponds better to the real stripe, where mainly the nonuniformity of demagnetizing fields [11] and higher terms of anisotropy [28] cause significant differences in the response for bigger inclinations of $\boldsymbol{M}$ out of the easy axis.

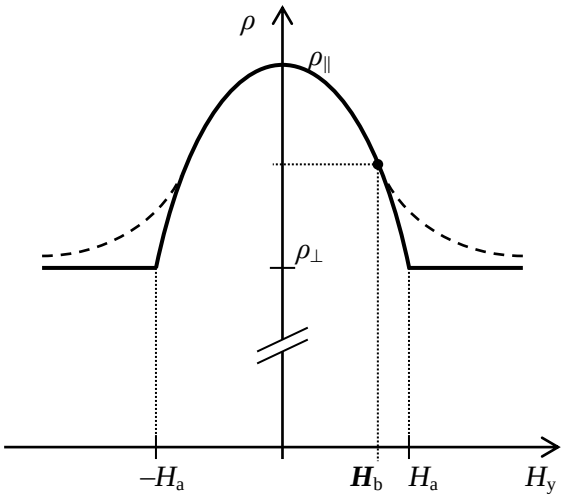

Figure 2: Theoretical (solid line) and real (dashed line) dependence of the resistivity in the longitudinal direction of AMR stripe on the field applied in the orthogonal direction.

Obviously the dependence of the resistivity ρ on the applied field H_y is quadratic and unipolar, making thus impossible the detection of the polarity of the applied field. Linearization and bipolar

response can be achieved in several ways. The most straightforward is to shift the initial orientation of magnetization $\boldsymbol{M}$ to an appropriate angle with an additional, bias field H_b, applied in the direction of sensitive axis, see figure 2. Then one direction of H_y causes enlargement of the angle φ between $\boldsymbol{M}$ and x-axis, whereas the opposite direction causes its decreasing. In [29], an analysis has been presented showing that it is reasonable to set the initial angle of $\boldsymbol{M}$ to 30°, which can be done with $H_b = 0.5 \cdot H_a$.

Using the biasing field leads to a bipolar response of the magnetoresistive stripe, but this response is considerably nonlinear – external field H_y applied in one direction causes different change in resistivity than the same field applied in opposite direction. This fact can be beneficial in some applications [29], as will be discussed later, but in most applications it is an undesired behavior.

Non-zero initial angle between $\boldsymbol{M}$ and the flowing current is usually achieved by inclining the current path through the stripe. This is done by depositing shorting bars of aluminum or gold through the angle of 45° directly onto the surface of magnetoresistive stripe. As the conductivity of aluminum or gold is much higher than that of the magnetoresistive material, the current tries to minimize the length of flow through the magnetoresistive material, flowing from one shorting bar to another one in the shortest possible way, i.e., with inclination of 45° to the longitudinal axis of the stripe. Magnetoresistive structures with shorting bars are commonly called the "Barber poles" [8, 30]. The dependence of ρ_{meas} on the field H_y in a system with current flow inclined through 45° can be again derived from (7) and (11):

$$\rho_{\mathrm{meas}}(H_y) = \frac{\rho_{||} + \rho_{\perp}}{2} \pm \Delta\rho \frac{H_y}{H_a} \sqrt{1 - \left(\frac{H_y}{H_a}\right)^2} \tag{12}$$

With barber poles, the response of the magnetoresistive stripe gets linearized and symmetrical. There are two possible geometrical configuration of barber poles (+45° and -45° with respect to the x-axis) and the response of ρ to the same external field in these two configurations is opposite, see figure 3. This is very convenient for the design of the bridge-based sensors, as the availability of pairs of elements with bipolar and complementary (mutually opposite) response is a necessary requirement for the full-bridge sensor configuration.

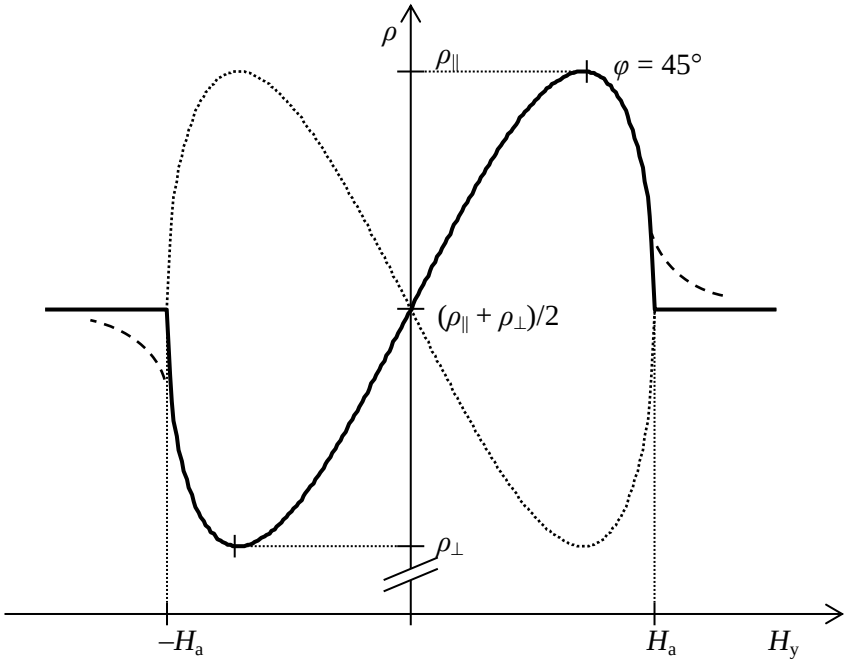

Figure 3: Theoretical (solid line) and real (dashed line) dependence of the resistivity of an AMR strip with barber poles at –45° (solid line) and 45° (dotted line) on the field applied in the orthogonal direction.

2.2 Giant Magnetoresistance

Giant Magnetoresistive Effect (GMR) is an effect of a dramatic change (tens of percent) of resistivity in thin film ferromagnetic / nonmagnetic sandwich structures in dependence on the mutual orientation of magnetization of ferromagnetic (FM) layers. The GMR effect is of quantum-mechanical origin and it is associated with the spin-dependent scattering of electrons propagating in ferromagnetic layers. Albert Fert and Peter Grünberg discovered this effect in 1988 and their discovery was awarded by the Nobel Prize in Physics in 2007. Various structures have been invented exploiting the same physical phenomenon.

Structures exhibiting the GMR effect always take a form of sandwiches of thin films of FM materials separated with a thin (tens of nanometers, [31]) conductive layer, so-called spacer. The resistivity of such a structure, measured usually in-plane for the technological reasons, is dependent on the mutual angle of magnetization vectors in the ferromagnetic layers, being the highest for antiparallel alignment of magnetization vectors ($\rho\uparrow\downarrow$) and the lowest for their parallel alignment ($\rho\uparrow\uparrow$). The GMR coefficient, being of 10 – 20 % @ room temperature, is usually defined as

$$\left(\frac{\Delta\rho}{\rho}\right)_{\mathrm{GMR}} = \mathrm{GMR} = \frac{\rho_{\uparrow\downarrow} - \rho_{\uparrow\uparrow}}{\rho_{\uparrow\uparrow}} \tag{13}$$

Let ξ be the mutual angle of magnetization vectors in the adjacent FM layers. The resistivity ρ_{GMR} of the structure is given as

$$\rho_{\mathrm{GMR}}(\xi) = \rho_0 - \frac{\Delta\rho}{2}\cos\xi \tag{14}$$

Here $\Delta\rho = \rho_{\uparrow\downarrow} - \rho_{\uparrow\uparrow}$;

$\rho_0 = \frac{\rho_{\uparrow\downarrow} + \rho_{\uparrow\uparrow}}{2}$ (in fact, the resistivity of the structure with orthogonally oriented magnetization vectors).

It has to be emphasized that the resistance of a GMR structure is dependent on the angle of ***M*** in the FM layers only, regardless to the direction of flowing current. This is a significant difference of GMR structures to AMR elements.

In the so-called "unpinned sandwich" GMR structure, the exchange coupling effect between the layers is exploited, which can lead to a spontaneous antiparallel alignment of the ***M*** vectors in the adjacent layers in absence of an external field [13]. To ensure this behavior, the spacer thickness is a critical factor, as the spontaneous antiparallel orientation arises for certain thicknesses only (the origin of this phenomenon has not been fully explained yet, see e.g. [8], p. 166), and additionally the GMR effect diminishes for too thick spacers. The mutual orientation of magnetization can be influenced by the external field applied in the orthogonal direction to the initial alignment of magnetization vectors, causing thus both magnetization vectors to incline from their initial position towards the acting field. To enlarge the GMR ratio, more unpinned sandwiches are stacked one upon another, forming thus the so-called "multilayer" structure, with more ferromagnetic layers always separated with a conductive layer.

The influence of the acting field on the direction of magnetization vectors in ferromagnetic layers is in general governed by the same principles as the rotation of magnetization in the AMR thin stripes (see section 2.1.2). However, the exchange coupling field adds to the characteristic field of the shape anisotropy. Exchange coupling field is considerably high in multilayer structures, resulting in a need of high magnetic fields to move the magnetization vectors of the layers from the initial antiparallel

alignment. This fact results in high operating range, but lower sensitivity of the GMR sensors and represents a basic drawback of exchange-coupling based structures.

Alternatively, a pinned structure, or spin-valve, uses a spacer of the thickness that still allows manifestation of the GMR effect, but the exchange coupling of the layers is very weak. Magnetization of one layer is held in a constant direction by an adjacent antiferromagnetic "pinning" layer, magnetization in the second layer is free to rotate in dependence of the acting field. In spin valves, rather weak fields are sufficient to move the magnetization in the free layer, allowing thus high sensitivity of spin-valve based sensors. Spin valve structures are ideal for angle measurements, but they can also be used for linear magnetic field measurements. In fact, most of the market-available GMR and TMR (see below) structures rely on the spin-valve structures [32].

2.3 Spin Dependent Tunneling

The Spin Dependent Tunneling (SDT) effect arises in structures of thin ferromagnetic layers separated with a very thin non-conductive spacer. The electrons can tunnel through the barrier from one ferromagnetic layer to the other one and the probability of tunneling is dependent on the electron spin and orientation of magnetization vectors. The SDT effect is thus again of a quantum-mechanical origin. The SDT effect at room temperatures has been proposed in 80's of 20th century, the first realization was achieved in the middle 90's. The magnetoresistive sensors based on the SDT effect are usually called the Tunneling Magnetoresistors or TMR. This technology is very promising thanks to high magneto-resistance at room temperature (tens of percent) and very low noise [33]. Authors of [33] also state that the sensitivity of a well-designed SDT structure is the highest reported for MR sensors without the flux concentrators (for flux concentrators see section 2.4).

The practical realization of a TMR device is generally based on the same structures as GMR devices (i.e., unpinned sandwiches and spin valves), with some significant differences:

(1) The spacer between the ferromagnetic layers is non-conductive. It is usually realized as Al_2O_3 layer of the thickness of max. units of nanometers. Vopalensky et al. [34] refer about a spin-valve sensor based on SDT with the spacer thickness of 1.5 nm. Consequently, devices employing SDT effect are very sensitive to electrostatic discharge that can destroy the spacer.

(2) The resistance of a TMR element allows the current to be led perpendicularly to the sensor plane, forcing thus all the electrons to undergo the spin dependent tunneling through the barrier. This is not possible in GMR based elements because of their low resistance, therefore the current is led in the plane of a GMR element, which results in lower GMR coefficient, as the electrons can propagate entirely within one ferromagnetic layer and only a minor part of the current-leading electrons undergo the spin dependent scattering.

(3) Using serially connected SDT junctions to realize a TMR sensor. This configuration can lead to significant noise suppression [33]. Thanks to the insulating spacer and perpendicular current flow, the TMR sensors can be designed as to have rather high resistances, with values of units of MΩ easily achievable. This can be an important advantage over the GMR sensors from the point of view of power consumption.

The definition of the TMR coefficient as well as the dependence of the resistivity of a TMR device on the mutual angle of magnetization is analogical to those of GMR devices.

2.4 Design of GMR and TMR sensors

Both the unpinned and spin-valve configuration of GMR and TMR elements generally provide a unipolar response to the applied field. Hence it is impossible to form a bridge out of these components with a bipolar response to the measured field. Nevertheless, there are market-available sensors with declared unipolar mode of operation [32].

The basic condition for obtaining a bipolar-response bridge is the bipolar response to the measured field of the particular bridge legs. Moreover, for a configuration of a full-bridge, elements with

opposite response to the same measured field (complementary pairs) must be available. In the case of the AMR sensors, the complementary pairs can be easily provided with inclining the current path by means of shorting bars – barber poles. In the case of unpinned structures and spin valves made of GMR and TMR elements, the situation is much more complicated.

In an unpinned GMR or TMR structure, the magnetization vectors of the ferromagnetic layers are antiparallel in the idle state. The measured field is applied in-plane in the orthogonal direction, lowering the mutual angle of magnetization vectors and consequently lowering the resistivity. Changing the polarity of the measured field, the magnetization vectors rotate to the opposite direction, but the mutual angle, and thus the resistivity, remains equal. It is however possible to apply an auxiliary bias field in the sensitive direction that would set an initial mutual angle of magnetization vectors. Then the measured field sums with the bias field and increases or decreases the mutual angle of magnetizations depending on its polarity. Thus a bipolar response of a single element is achieved. The bias field is usually generated with an integrated flat coil (strap). It is possible to make such a geometrical configuration of the GMR / TMR elements that the bias field direction is opposite in two bridge elements with regard to the other two bridge elements. Thus the measured field, acting in the same direction on all the bridge elements, adds to the bias field in two bridge elements and subtracts from the bias field in the other two elements. In this way, formation of complementary pairs is possible and a bipolar operation of the bridge can be achieved, as visualized e.g. in [8], p. 292.

The magnetization of the free layer in a general spin-valve structure aligns antiparallel to that in pinned layer in an ideal state, thanks to a weak, but still existing exchange coupling. The measured field, applied in the orthogonal direction, makes the magnetization rotate towards its direction, changing the mutual angle of magnetizations and thus the resistivity of the structure. For a strong enough field, the magnetization of the free layer is fully rotated into the direction of the measured field, the mutual angle between magnetization vectors reaches 90° and further increasing of the measured field does not have further effect (not considering extremely strong fields that can decouple the pinned layer and damage the sensor). Measured field with an opposite polarity rotates the magnetization to the opposite direction, but the mutual angle between magnetizations, and thus the resistivity, is the same for both field polarities. Hence the response is unipolar again.

Auxiliary bias field is used for obtaining a bipolar response of a spin-valve structure. The technique and configuration is described in more detail for example in [34]. The bias field is applied orthogonally to the magnetization of the pinned layer and it is high enough to rotate the magnetization of the free layer fully to its direction, setting thus the initial angle of magnetizations to 90°. The measured field is then applied in the direction of the magnetization of the pinned layer and the magnetization of the free layer inclines from its 90° angle towards the measured field. In this way, a bipolar response of a spin-valve element is achieved. In this case, however, it is complicated to form a complementary pair of bridge elements. Changing the polarity of the orthogonal bias field does not lead in reversion of the response to the measured field and the only way how to achieve the complementary behavior of the elements would be to provide opposite directions of the magnetizations of the pinned layers in the complementary elements, which is technologically complicated. Therefore, a half-bridge configuration is commonly used to form bipolar bridges with spin-valve elements. Only two diagonally opposite bridge elements are exposed to the measured field, whereas the other two elements are shielded from the field by relatively thick (units of micrometers) permalloy formations, deposited on the chip, that at the same time act as magnetic flux concentrators for the two active elements, which are placed in the gap between the flux concentrators. This technique allows to achieve a bipolar response to the measured field at the bridge diagonal even when both the active elements react in the same way to the applied field. Another benefit of flux concentrators is the increased immunity of the sensor to the components of the field acting out of the sensing axis [35, 36]. On the other hand, flux concentrators can contribute to the overall nonlinearity and hysteresis of the sensor. At present, half-bridge based on the spin-valve structures with flux concentrators is the most popular configuration of market-available GMR and TMR sensors.

3. Magnetic field measurement with AMR, GMR and TMR sensors

3.1 Magnetometers with AMR sensors

3.1.1 Basic considerations

Nowadays, there are many market-available sensors based on the AMR effect. Sensors based on GMR and TMR effects are not so widely spread, but still they have been available on the market recently [32, 37]. Additionally, AMR effect is used in sensors for compasses and angle measurement [38, 39].

AMR sensors compete with Hall sensors, which have been used for years in many applications. Although the AMRs are more sensitive, their remaining problem is a problematical possibility of integration of the sensor and processing electronics onto a single chip. In the case of Hall sensors, the situation is simpler, as the material of the sensor is a semiconductor. In the case of AMR, however, the sensor material contains iron, which is fatal for the silicon-based electronic structures due to possible contamination of conducting channels caused by iron diffusion. Thus, the smart sensors employing AMR effect and containing the processing electronics are usually realized as a hybrid, multi-die system in one package.

A basic AMR sensor for the weak field measurement comprises a full Wheatstone bridge of four magnetoresistive meanders made usually from permalloy NiFe 81:19, with barber poles deposited in such a way that the same field causes opposite effect on resistivity in the adjacent magnetoresistive legs of the bridge [8, 30]. Together with the magnetoresistive bridge, there are usually two flat-coils, or straps, integrated on the chip, one for creation of a field along the sensitive, or transversal, axis of the stripes (compensation coil), the second one for creation of a field along the longitudinal axis of the stripes (flipping or set/reset coil).

The flipping coil serves for (periodical) remagnetizing of the ferromagnetic material. As was explained in section 2.1.2, magnetization has two stable states along the easy axis of anisotropy in the absence of an external field. A strong field applied in the direction of easy axis can cause the magnetization to change its initial orientation into the opposite direction along the easy axis. In a sensor with barber poles, this leads to a reversed sensor characteristics. In a typical sensor that employs a full bridge of the magnetoresistive elements, this means that for the same field, the polarity of the output voltage of the bridge gets reversed. Periodical remagnetization of the ferromagnetic material in the sensor has many benefits: deep saturation of the material significantly reduces the hysteresis and noise and it increases the resistance of the sensor against field shocks. A proper signal processing of a periodically remagnetized, or flipped, sensor can also reduce the temperature dependence of the sensor offset.

The magnitude of the field needed for a deep saturation can be estimated from an energetic model of the magnetization reversal of the thin ferromagnetic film. Author of this thesis cooperated on a development of such a model and its verification on the AMR sensor KMZ51 from Philips, now NXP Semiconductors [14]. The results were published in [40]. The energetic model predicts the appropriate flipping field to be of 940 A/m. In the particular case of KMZ51, this field means a current pulse of approx. 2.8 A flowing through the flipping strap. The manufacturer recommends significantly lower pulses (1.5 A max.), but ensuring that the total power dissipation of the sensor is not exceeded, the pulse can be higher without destroying the flipping strap. As the flipping circuit is usually realized

with a switched capacitor and flipping is made periodically, an energetic consideration must be done to determine the maximum allowed capacity of the switched capacitor on the chosen working frequency.

The effects of the magnitude of flipping pulses has been reported in [40], showing a significant reduction of noise for higher flipping pulses. It has been verified that the saturation of material has also a significant influence on the offset stability. The offset of the bridge output can generally vary after each flipping pulse, if the saturation of the material is not sufficient. In [40], the offset variance is presented for various flipping field amplitudes, showing that the higher the flipping field, the better the offset stability. This effect is also discussed in more detail in a subsequent work [41].

It is reasonable to perform flipping of the magnetization periodically. This leads, however, to an alternating rectangular output signal from a sensor bridge, where amplitude of the signal carries the information about the measured field. This is convenient, because the offset of the bridge can effectively be eliminated with a high-pass filtering of the bridge output signal. On the other hand, the signal has to be demodulated to get the value of the measured field. In [42], a typical circuit used for a signal processing in an AMR magnetometer is presented. After amplification of the sensor signal, a synchronous detector, or phase-sensitive rectifier, is employed to get a DC signal corresponding to the measured field. However, it was eventually found out by the author of this thesis that the sensor output is not stable immediately after the flipping pulse. Therefore, a modified circuit is used as a synchronous demodulator. The short periods of transients immediately after the flip are ignored, and the synchronous detection is applied just to the stable areas of the output. A timing diagram is presented in [42]. The demodulator is followed by a sample-hold circuit.

To suppress the temperature dependence of the sensitivity of an AMR sensor, it is convenient to operate the sensor in the feedback compensation mode. An integrated compensation strap is usually used for this purpose. The demodulated signal from the sensor is integrated and the resulting signal is led back to the sensor to its compensation coil. If properly connected, a negative feedback is formed in this way: in presence of the measured field the integrator integrates the sensor output, magnetic field with the opposite orientation to the measured field is generated in the compensation coil, which after stabilizing is of the same magnitude as the measured field, compensating thus the measured field and maintaining the sensor in a zero magnetic field. Thus, the sensor acts as a zero indicator, which leads to significant improvement of linearity (the linearity is determined by the linearity of the feedback loop only) and reduction of the temperature dependence of the sensor. The parameters achieved with this magnetometer design are concluded in [42] and in [43].

3.1.2 Temperature dependences of AMR magnetometers

An important parameter of each measuring device, including a magnetometer, is the temperature dependence of offset and sensitivity. Since the resistivity of the AMR elements is temperature-dependent, as in most metallic materials, both the offset and sensitivity of an AMR bridge are influenced by temperature. Moreover, the anisotropy field H_a and the difference of resistivity $\Delta\rho$ are both temperature dependent [8]. For the basic considerations, only the temperature dependence of resistivity can be taken into account.

In the case of the magnetometer using an AMR sensor, an important question arises, what is the proper supply for the measurement bridge. An analysis on the topic has been done by the author of this thesis and published in [44]. It has been shown that in an ideal case, the voltage supply of the magnetoresistive bridge leads to theoretically temperature-independent offset of the bridge and the current supply theoretically eliminates the temperature dependence of the sensitivity of the bridge. These findings have also been verified on the KMZ52 [45] magnetoresistive sensor. The sensor was placed into a heated magnetic-shielded chamber with the dc attenuation of approx. 75 dB @ 100 μT (hence the Earth's field is attenuated by the factor of 5600 to a residual level of about 10 nT). The temperature changed in between 25°C and 45°C. First, the temperature dependence of the resistivity of a single element was measured, giving the value of the temperature coefficient $\alpha = 0.0026°C^{-1}$, which is in a good agreement with [46]. Then the dependences of the offset and sensitivity of the sensor bridge supplied with a constant voltage and constant current source have been measured.

It has been found out that the results are basically in accordance with the developed model. The coefficient of the offset temperature drift in the case of constant voltage supply was about -0.0003°C^{-1}. This means that offset is still temperature dependent, but the coefficient of its temperature drift is almost by an order lower than the temperature coefficient of the magnetoresistive elements. In the case of a constant current supply, coefficient of the offset temperature drift was approx. 0.0025°C^{-1}, very close to the temperature coefficient of resistivity of the magnetoresistive elements. Hence, the offset behavior corresponds very well to the proposed theoretical model. The temperature coefficient of sensitivity in the case of a constant voltage source was about -0.0023°C^{-1}, which again fits very well with the proposed hypothesis, and it reduces to approx. -0.001°C in the case of a constant current supply. Although the hypothesis expected the temperature coefficient of sensitivity to be zero in this case, it can be seen that it reduced significantly with respect to the case of a constant voltage supply, supporting thus the developed simplified mathematical model.

The findings made in [44] are very important for the design of circuitry for AMR magnetometers. As the periodical remagnetization of the material (flipping) is usually employed in the magnetometers with AMR sensors, the offset temperature dependence does not represent a big problem, because it is rather easy to eliminate the offset of the bridge by a careful design of the circuit (high-pass filter and synchronous demodulation). However, the temperature dependence of the sensitivity remains a problem, although it can be reduced using the compensation mode. Therefore, it is well justified to use a constant current supply for AMR sensors. This solution may be easier than that proposed in [47].

The influence of the flipping and compensation mode on the temperature dependences of offset and sensitivity has been investigated. KMZ51 sensor supplied with a constant-current source was used. First, the long term stability of the offset of the flipped sensor in compensation mode under virtually constant temperature has been determined. During the test, the sensor was placed into a magnetic shielding with a dc attenuation of 75 dB for 48 hours. The variation of offset was between 0 nT and 60 nT. For the evaluation of temperature dependences of offset and sensitivity, the sensor was placed into an 8 layer permalloy cylindrical shielding with an internal thermostat. The offset dependence of an unflipped and uncompensated sensor has been evaluated. In the temperature range of -20°C to 65°C, the offset changed through 3600 nT to -4000 nT, i.e., with the coefficient of approx. -90 nT/°C. In the case of a flipped and compensated sensor, the temperature coefficient of the offset drift was strongly reduced to approx. 2.1 nT/°C.

For the measurement of the sensitivity temperature dependence, the AMR sensor was placed into a temperature-controlled chamber inside the Helmholtz coils. The sensor without flipping and compensation showed the temperature coefficient of sensitivity of approx. 600 ppm/°C. In the case of periodically remagnetized (flipped) and compensated sensor, the temperature dependence of sensitivity lowered to approx. 20 ppm/°C.

The results have been published in [48]. It has been shown that flipping and compensation modes of an AMR sensor heavily improve the temperature dependences of its basic properties, i.e., offset and sensitivity.

A summary of the achieved temperature-related parameters of KMZ51 / KMZ52, reported in [43, 44, 48], can be done and compared to the datasheets [14, 45]. The parameters of KMZ51 / KMZ52 are identical, as KMZ52 in fact integrates two bridges used in KMZ51 into a single package. The datasheets do not contain all the data needed, but the temperature coefficient of offset and sensitivity without flipping and compensation is mentioned there. The maximum offset of KMZ51 / KMZ52 is guaranteed to be 1.5 mV on each supplying volt (i.e., for a bridge supplied by 6 V, the maximum offset is 9 mV etc.) The offset temperature drift coefficient is stated as 3 μV/V/°C, but it is not clear from the datasheet, what supplying method is assumed, although the supplying method has a crucial influence on the offset temperature drift, as it has been shown in [44]. Considering the datasheets, the offset of the bridge can be described as V_{off} = 1.5 mV/V ± 0.003 mV/V/°C and hence V_{off} = 1.5·(1 ± 0.002·Δϑ) mV/V. The temperature coefficient of offset is then α = 0.002 °C^{-1}. This value fits very well with that presented in [44] for current supply, being α = 0.0025 °C^{-1}. In constant-current supplied sensor, reported in [48], the initial offset was equivalent to 36500 nT and its drift was 90 nT/°C without flipping and compensation. Hence, B_{off} = 36500 nT ± 90 nT/°C, or B_{off} = 36500·(1 ± 0.0025·Δϑ), i.e., α = 0.0025 °C^{-1}, in an exact accordance with the value reported in [44]. A conclusion can be made that the **offset temperature drift** coefficient of an **unflipped and**

uncompensated AMR sensor KMZ51 / KMZ52 supplied with a constant-current source can be expected to be approx. 0.0025 $°C^{-1}$, or 90 nT/°C.

The sensitivity temperature coefficient of KMZ52 [45] declared by the producer is 3100 ppm/°C. In [44], the temperature coefficient of the KMZ52 sensor under voltage supply was found to be -0.0023 $°C^{-1}$, which can be expressed as -2300 ppm/°C. The sign is not important in this regard; it can be seen that the measured value is in a considerably good agreement with the producer's data. In [48], the **temperature coefficient** of the **unflipped and uncompensated sensor** under current supply was measured, being approx. -600 ppm/°C. In [44], the respective value was of approx. -1000 ppm/°C. It can be concluded that in the case of current supply of an unflipped and uncompensated bridge, the temperature coefficient of sensitivity can be expected around -1000 ppm/°C.

Periodical remagnetization, or **flipping, and feedback compensation** can lead to a huge suppression of the offset and sensitivity temperature coefficients. This fact has been demonstrated in [43] already, where the temperature coefficient of 100 ppm/°C for a flipped and compensated sensor is reported. With further development, this value has been suppressed to 20 ppm/°C [48], which is the area of sensitivity temperature coefficient of cheap fluxgates [30, 42].

The value of **offset drift** (expressed in the reading change per degree Celsius rather than by α) of a **flipped and compensated sensor** achieved in [43] was 10 nT/°C, but this value has been improved to 2.1 nT / °C, as reported in [48], by a careful design of remagnetization process, described in more detail in [41]. This is a good result, although this drift is by order higher than that of fluxgates (typically 0.1 nT/°C, [42]).

3.1.3 Noise, linearity and hysteresis of AMR magnetometers

For precise applications, the magnetometer noise can be a crucial property. The noise is normally superposed to the useful signal and therefore masks the weak signals. In other words, the noise, among other factors, determines the resolution of a magnetometer. Power spectral density (PSD) of the noise at low frequencies, such as 1 Hz, is usually of interest in the area of magnetic measurements. Author of this thesis cooperated on the research works [40] and [41], which showed that the amplitude of the flipping pulses has a strong effect on the sensor noise. The reason for this is that the deeper saturation of the material, the better defined the magnetic parameters after remagnetization (flip), or the better restoring of the magnetic properties of the ferromagnetic stripe. The magnetometer with AMR sensor, reported in [43], used pulses of 2.8 A for flipping. The noise PSD was about 2 nT / √Hz @ 1 Hz, the RMS value in the 100 mHz to 10 Hz range was approx. 7 nT and the noise peak-to-peak value was approx. 15 nT. In [42], slightly higher values are reported, with noise PSD value about 3.2 nT / √Hz @ 1 Hz. It can be concluded that the noise of a flipped magnetoresistive sensor can be expected under 10 nT / √Hz @ 1 Hz. This value is significantly higher than that of fluxgate sensor, which can be as low as 10 pT / √Hz @ 1 Hz [49].

A basic property of a magnetometer is, besides the sensitivity, the linearity of the transfer curve. The linearity of a magnetometer with AMR sensor can be improved by using the feedback compensation. In [42, 43], the results obtained both in compensated and uncompensated mode are discussed. Without compensation, the linearity of the characteristic of a single sensor was about ±0.3% in the range of ±200 μT. In accordance with the expectations, feedback compensation highly improves the linearity of measurement. In [42], the reported linearity error is ±200 ppm in the range of ±200 μT. With the further development, the linearity was yet improved to ±40 ppm in the range of ±300 μT, as reported in [48]

Hysteresis of the characteristic is an inherent property of most magnetic sensors. In anisotropic magnetoresistors, hysteresis can be highly suppressed by means of remagnetization (flipping). This fact represents another reason for periodical flipping. In [42] and [43], hysteresis of a magnetometer with AMR sensor is presented both in unflipped and flipped mode, reaching about ±0.3% in the range of ±200 μT without flipping. With flipping, the hysteresis lowers to ±0.04% in the same measurement range. Combined linearity & hysteresis error below ±40 ppm in the range of ±300 μT represents the best achieved result with an optimized design of the magnetometer circuitry [48].

Table 2 summarizes the results achieved with a magnetometer with AMR sensor [42, 43, 48]:

Table 2: Parameters of magnetometer with AMR sensor.

Parameter	Best result achieved	Typical value
Measuring range	---	±300 μT
Linearity error & hysteresis	±24 nT (±40 ppm @ ±300 μT)	±48 nT (±80 ppm @ ±300 μT)
Long-term zero stability	---	±30 nT
Offset temperature drift	2.1 nT / °C	2.1 nT / °C
Temperature coefficient of sensitivity	20 ppm / °C	20 ppm / °C
Noise PSD	2 nT / √Hz @ 1 Hz	5 nT / √Hz @ 1 Hz

3.1.4 AMR sensors for compass applications

A typical application of magnetic sensors is an electronic compass. Thanks to their miniature size and high sensitivity, anisotropic magnetoresistors are a logical choice for realization of such a device. Honeywell company offers ready solutions for compassing with AMR sensors [50, 51]. A question arises, what parameters of a compass can be expected using AMR sensors as the Earth's field detectors. Let only the azimuth be of interest and let the compass be used in a geographical position, where the horizontal component of the Earth's field is approx. 20 μT (Middle Europe). At least two sensors have to be used, usually with orthogonal mutual position of sensitive axes [13].

Two-axis KMZ52 is a typical sensor that can conveniently be used for a compass design [52]. The external field applied in any direction can be decomposed into its components along the two orthogonal sensitive axes of the sensor. If H_{ext} is the measured field tilted through the angle α from the sensitive axis of sensor 1, then its components are $H_{ext}\cdot\cos(\alpha)$ in axis 1 and $H_{ext}\cdot\sin(\alpha)$ in axis 2. Hence, the ratio of the sensor outputs V_{out2} / V_{out1} = tan(α) and the angle of the applied field can be thus calculated applying arctan function on the ratio of the sensor outputs. If 20 μT is the field magnitude, 350 nT must be reliably detected to ensure the resolution of 1 degree within the whole angle range.

The resolution of the magnetometer developed above is determined by its noise. As the noise rms value in the range of 100 mHz to 10 Hz is lower than 10 nT [42], field changes bigger than 10 nT should be distinguished from the noise, so that 10 nT can be declared as the best possible magnetometer resolution in a short-term mode of operation. This value corresponds to a theoretical angle resolution of approx. 0.03 degrees.

However, the linearity and hysteresis error measured both in the full range of ±300 μT and restricted range of ±60 μT (important for compassing applications) is typically about ±50 nT in both cases, as reported in [48] and [42], respectively. This value corresponds to the angle variation of approx. ±0.14 degrees, which is therefore the best theoretically achievable reproducible precision of a compass realized with the described magnetometer in a short-term mode of operation. For a long-term operation, the offset stability matters. As has been noticed above already, the magnetometer possesses the long-term offset variance of ±30 nT, which worsens the theoretical compass precision to approx. ±0.23 degrees.

The temperature coefficient of sensitivity does not represent a big complication, as the outputs of the both sensors are processed ratiometrically. Nevertheless, the temperature drift of the offset is a serious problem. In a compass intended for use within the temperature range of -20°C to 40°C, the offset changes by almost 130 nT in the best circuitry of magnetometer that has been developed, limiting the theoretical precision of the compass to approx. ±0.42 degrees.

An important problem associated with the use of AMRs in compass applications is the so-called cross-field effect. In an ideal vector sensor of a magnetic field, the output should be proportional exclusively to the field component in the sensitive axis. However, it is a common situation in magnetic sensors that the sensor response is influenced by the orthogonal field component. The associated effects are usually called the cross-field effects. In the case of AMR sensors, the cross-axis component of the field directly influences the angle of magnetization of the magnetoresitive material, as can be

easily understood from section (2.1.2). Thus the resistivity of the magnetoresistive stripe, and consequently the sensitivity of the sensor, is strongly affected with the orthogonal field component. In a magnetometer application, it may be possible to minimize the cross-field effect by a careful adjustment of the sensitive axis and the acting field direction. In a compassing application, however, the existence of the orthogonal field component is inevitable, leading thus to the cross-field effect on sensitivity, which represents further source of compass inaccuracy. Fortunately, cross-field effect can be highly suppressed by periodical flipping and feedback compensation. Additionally, knowing the value of characteristic field of anisotropy in an AMR sensor, the cross-field effect on sensitivity can be numerically compensated. In [48], basic considerations associated with this topic are made.

A conclusion can be made [42] that if 0.5 degrees compass accuracy is sufficient, the AMR is a proper choice for its realization. Honeywell Inc. is the market leader of commercially available magnetic compasses with AMR sensors, delivered both as electronic components and ready-to-use modules. The typical accuracy of the modules is 0.5 degree with the resolution of around 0.1 degree [51, 53, 54].

3.2 GMR sensors for magnetic measurements

In cooperation with US based NVE Coorporation, which nowadays is the world market leader in the area of Giant Magnetoresistance and Spin-dependent Tunnelling sensors, an investigation has been performed on the possibilities of improvement of GMR and TMR measurement characteristics.

Properties of a prototype of an unpinned multilayer GMR structure have been measured. The sensor comprises of four GMR elements configured to a full bridge. Each GMR element has a unipolar symmetrical response, but it is possible to shift the operating point of each element to a proper position on its characteristic with a biasing field applied along the sensitive axis. For this purpose, a flat strap is integrated together with the sensing elements in a way that biasing field adds to the measured field in two elements and subtracts from the measured field in the remaining two elements, making thus possible to achieve a response to the measured field at the output of the bridge – see section 2.4. Although applying a DC biasing field is sufficient for the sensor to work, it has been shown in [55] that AC biasing field can improve the measurement characteristics of the GMR sensor. The idea of AC biasing was presented by Ripka et al. in [56] already. Ripka et al. used a sinewave excitation current for generation of the biasing field; the sensor output was processed with a lock-in amplifier.

In [55], Vopalensky et al. used a squarewave biasing field at 1 kHz. Changing the polarity of the biasing field leads to the change of the polarity of the bridge output. Consequently, with a squarewave biasing, the output is also a squarewave signal, whose magnitude bears the information of the measured field. Hence a synchronous demodulation has to be used for the signal recovery. For this purpose, the modified design of AMR magnetometer circuitry, reported in section 3.1, was used. Instabilities of the output have been observed immediately after the change of orientation of the biasing field. Therefore, the useful signal is taken from the stabilized areas of the output only, ignoring short time-periods immediately after the change of the biasing field polarity, where the magnetic properties of the material are not settled yet. It has been shown in [55] that the squarewave AC biasing of a GMR sensor leads to a considerable reduction of hysteresis. With the DC biasing the hysteresis was about 2% of the FS of ±375 μT. With an AC biasing made with a field of the same magnitude as in the DC biasing case, the hysteresis diminished to 0.5 % of the FS, due to periodical restoring of the magnetization orientation in the multilayer structure. The linearity of the characteristic was about 3 % of the full scale with DC as well as AC biasing, the sensitivity was approx. 20 mV/V/kA/m. Nowadays, commercially available GMR sensors are usually designed as unbiased structures with two operational bridge legs and flux concentrators (see section 2.4). Typical guaranteed linearity is of 2 % FS and hysteresis of 4 % FS in a unipolar mode of operation, with wide range of available ranges and sensitivities [57].

The noise of the sensor was measured both in DC biasing and AC biasing mode. In both cases, the sensor was placed into a six-layer permalloy magnetic shielding. With DC biasing, the recalculated noise PSD value is 20 nT / √Hz @ 1 Hz, with the noise RMS value approx. 44 nT in the range of 100 mHz to 10 Hz and the noise peak-to-peak value about 225 nT. With AC biasing, the noise parameters worsen: the recalculated noise PSD value is 37 nT / √Hz @ 1 Hz, with noise RMS value approx. 100 nT in the range of 100 mHz to 10 Hz and the noise peak-to-peak value about 450 nT.

3.3 TMR sensors for magnetic measurements

A structure with a pinned layer, or spin-valve (see section 2.4), based on the Spin-dependent Tunneling or Tunneling Magnetoresistance Effect was used in the research of possibilities of improvements of the measurement characteristics of these sensors. The research was performed in cooperation with the NVE Corporation, who provided prototypes of TMR sensors.

Each of the four legs of the measurement bridge is formed out of more serial-connected TMR elements. The magnetization of one ferromagnetic layer is pinned by means of an adjacent antiferromagnetic layer, so its direction is fixed. The magnetization of the next ferromagnetic layer is free to move in response to the external magnetic field. To obtain a bipolar response of each element, the initial mutual angle of the magnetization vectors in ferromagnetic layers can be set with a biasing magnetic field applied orthogonally to the direction of magnetization in the pinned layer. Then, an external magnetic field applied in the direction of magnetization of the pinned layer changes the mutual angle of magnetization vectors, which leads to a change in resistance of individual TMR elements. The resistance response of the particular elements to the measured field is bipolar, but the change has the same sign in all the elements. To achieve a bipolar output of the sensor bridge, flux concentrators are used that also serve as a magnetic shielding of two bridge elements (see section 2.4).

The orthogonal biasing field is generated with an integrated flat strap. Changing the field polarity does not result in a change of the mutual angle of magnetization vectors in ferromagnetic layers and thus it does not reverse the sensor transfer curve. However, it can be beneficial to periodically change the orientation of the biasing field to recover the magnetic properties of the free ferromagnetic layer and thus to reduce the hysteresis of the sensor. The results of investigation on AC orthogonal biasing of the TMR sensors were reported by Vopalensky et al. in [34]. The sensor was biased with a DC and AC squarewave current of 13.5 mA at 1000 Hz. The transfer curve of the sensor is not symmetrical due to high offsets in both axes. In the range of 50–100 μT, the sensitivity of the device reaches 1750 mV/V/kA/m, with the linearity error of about 10% FS in the case of DC biasing and 5% in the case of AC biasing. The hysteresis is reduced to 12% in the case of AC biasing, compared to 60% achieved with DC biasing.

The noise of the sensor was measured both in DC biasing and AC biasing mode. In both cases, the sensor was placed into a six-layer permalloy magnetic shielding. With DC biasing, the recalculated noise PSD value is 750 pT / √Hz @ 1 Hz, with noise RMS value approx. 3.5 nT in the range of 100 mHz to 10 Hz and the noise peak-to-peak value about 16 nT. With AC biasing, the recalculated noise PSD value is 5 nT / √Hz @ 1 Hz, with noise RMS value approx. 12 nT in the range of 100 mHz to 10 Hz and the noise peak-to-peak value about 50 nT.

The research reported in [34] showed that TMR technology is promising from the point of view of sensitivity and noise parameters, but the linearity, hysteresis and offset remains a big issue for weak field measurements. However, there are market-available angle sensors based on TMR effect, such as AAT001-10E [58].

The results achieved with AMR, GMR and TMR sensors are summarized and compared to the fluxgates in [42].

3.4 Applications of AMRs for current and power measurements

3.4.1 AMR current measuring device

Contactless current measurement is a classical task where the magnetic sensors find their application. Hall sensors are commonly used for this purpose, placed into a gap of a ring-shaped flux concentrator, or yoke, through which the current wire is led [59]. Using a flux concentrator has indisputable advantages: the magnetic field is concentrated into the gap, so lower sensitivity of magnetic field sensor is sufficient, the error caused by un-centered wire is highly suppressed thanks to the concentration of the field in the yoke, for similar reasons the impact of the out-of-hole currents or other ambient magnetic fields is highly reduced. On the other hand, the measurement can be influenced by the nonlinear behavior of the magnetic material of the yoke (hysteresis, saturation). The magnetic properties of the yoke and thus a careful choice of the yoke material are of a principal importance in these devices.

AMR sensors are much more sensitive than common Hall sensors. The measurement range of the Hall sensors is between units to thousands of millitesla, with the resolution of tenths of percent of the full scale. For example a sensitive Hall sensor for contactless current measurement CSA-1VG has a measurement range of ±8 mT with the resolution of ±8 μT [60]. The measurement range of AMR sensors is in order of hundreds of μT, making it possible to design a current measurement device without the flux concentrator. A rose-like array of magnetoresistive sensors configured in a way that the sensitive axes follow the flux lines of a wire led through the center has been reported by Ripka et al. in 1996 [61].

This idea has been further developed by Mlejnek et al. in 2007 [62]. Eight KMZ51 sensors have been placed to form a circle with the diameter of 25.4 mm. All the knowledge of the author of this thesis related to the development of AMR magnetometer and reported in [40, 42, 43, 48] have been used to achieve the best possible performance. Hence, the sensors are periodically remagnetized, or flipped, with high currents and feedback compensation is used to reduce the temperature dependence of the sensitivity and improve the linearity [42]. The theoretically achievable parameters of a current measuring device using AMR sensors can be determined from Table 2. If the magnetic field in the distance of 12.7 mm from the wire can reach 300 μT, or 240 A/m, the maximum measurable current derived using the Amper's law is approx. 19 A. The current resolution is approx. 0.65 mA, considering the field resolution of 10 nT. Linearity error is approx. ±3 mA and the long-term stability is better than ±2 mA. Hence, the current measurement device should provide the accuracy of ±5 mA (≈ ±150 ppm) with the resolution better than 1 mA in the range of ±19 A, in the case of a perfectly centered wire. For comparison, the common market-available contactless ammeters possess errors in range of units of percent (2% typically).

However, omitting the flux concentrator leads to a significant problem with the influence of the position of the wire on the measured value. An analysis of this displacement error is given in [62], showing that the more sensors are used around the measurement hole, the lower the influence of the non-centrical position of the wire. For the hole diameter 10 mm and 8 sensor used, the maximum error due to the wire displacement is around 0.06 % [62].

The above given consideration of the theoretically achievable parameters assumes that each sensor in the rose-like array works as a single magnetometer. This arrangement would require using of eight fully-equipped magnetometers, which would be very demanding especially as for the amount of components. In [62], the outputs of the eight sensors are summed together, processed with a single processing chain, and the compensation of all the sensors is performed with one resulting current. Consequently, the individual sensors may operate in a not fully compensated mode, especially if the wire is not centered perfectly. Moreover, the field factors of compensation straps can differ, so even in a case of a centered wire the full compensation of each sensor may not be achieved with a single current value.

The current measurement device was successfully built and its function has been verified. In the range of ±8 A, the linearity error was approx. ±0.05 %. The error due to uncentered wire was of ±0.5 % (due to common compensation of all the sensors much worse than theoretically possible), an

external current of 5 A led in the distance of 40 mm from the center caused an absolute error of 25 mA.

3.4.2 Power measurement with AMR sensors

Power measurement is a principal task in energetics. Recently, electronic wattmeters have been constantly replacing the electromechanical devices. The instantaneous power is defined as the product of instantaneous values of current and voltage on the line. The active power is the mean value of the instantaneous power over one period and for harmonic signals, it is given as $P = U \cdot I \cdot \cos\varphi$, where U, I are the RMS values of voltage and current and φ is the phase shift between them. However, it is often required to measure active power of non-harmonic and distorted signals with high content of higher harmonic frequencies. Hence, the bandwidth of a wattmeter is an important parameter. In electronic wattmeters, the voltage and current are either sampled and digitized and the power is calculated fully digitally, or an analog multiplier is employed.

Hall sensors are commonly used as the core elements of such multipliers [59, 63, 64]. Vopalensky et al. [65] present an AMR sensor in the function of an analog multiplier. The Wheatstone bridge of the AMR sensor is supplied with the voltage that is proportional to the voltage of the measured signal. The current proportional to the current of the measured signal generates a field that is measured with the sensor. As the output of the Wheatstone bridge is proportional both to the supply voltage and the acting field, it is actually a multiple of the two signals.

The coil for field generation may be external, wound around the sensor [8]. Vopalensky et al. in [65] use the integrated compensation coil of a standard market-available AMR sensor as the field-generating coil. Since the coil is very close to the magnetoresistive elements, the sensitivity to the current led through is large. KMZ51 sensor [14] was used for realization of the multiplier. Measurement was performed with harmonic signals up to 5 V RMS at the bridge and 10 mA RMS through the coil, the active power range was of 3.6 μW to 50 mW.

Influence of the phase shift between the voltage and current signals has been investigated. In the range of ±70°, the relative error of the reading was below 0.1%. The ratio of the output voltage to the product of the input RMS values, or simply the sensitivity of the multiplier, has been measured for the zero phase-shift of the signals. A sensitivity map is visualized in [65]. It has been found out that the sensitivity differs for various values of the current, which is probably a consequence of the intrinsic nonlinearity of the field response of the sensor and internal heating of the sensor. The frequency range of the multiplier was about 100 kHz, for details see [65].

It has been demonstrated that an AMR sensor can be used as an analog multiplier for power measurements. Further improvement could be reached with compensation of the measured current, but there are no market-available sensors that would contain two integrated coils in the field-sensitive direction. The main benefit of using an AMR sensor as an analog multiplier is the expectable wide frequency range. The sensor can measure magnetic fields up to 1 MHz, so with a careful design, a multiplier with this measurement range would probably be constructible.

In [65], the described use of a linear magnetoresistive sensor for power measurement is rather straightforward. There is yet a different way how to take advantage of the anisotropic magnetoresistive effect for the power measurement, proposed by the author of this thesis. Let a stripe of a magnetoresistive material be contacted at its short edges and the current with density J_x be led along its longitudinal axis. Then the electric field E_x, measured as a voltage drop on the stripe, can be expressed from the Woigt-Thomson formula (7) as

$$E_x = \rho_l J_x - \Delta\rho J_x \sin^2\varphi \tag{14}$$

where φ is the angle between the longitudinal axis of the stripe and the magnetization vector. The voltage along the stripe is then dependent on the flowing current and $\sin^2\varphi$, which in turn is dependent on the magnetic field, which the stripe is exposed to. If the current of the measured signal is used to generate the magnetic field and the voltage of the signal is converted to the current which is led through the stripe, the voltage drop measured along the stripe is dependent on both. Unfortunately,

$\sin^2\varphi$ is not linearly proportional to the acting field. Nevertheless, a sensor configuration has been proposed [66] that overcomes this problem and can measure signal power in audio frequency range. The configuration used in [66] neglects the anisotropy in the material, supposing that the magnetization vector aligns its direction fully with the acting magnetic field.

A configuration that includes the influence of anisotropy on magnetization and allows measurement of active power was proposed by Vopalensky in [29]. In this configuration, magnetization is inclined from the easy axis with a DC bias field H_b applied in the orthogonal direction. The current of the measured signal creates a magnetic field that is applied again in the orthogonal direction, and thus adds to H_b. The voltage of the measured signal is converted to current led through the stripe in the longitudinal direction. It has been shown in [29] that, in the particular case of a strictly harmonic signal, the mean value of E_x is proportional to the active power of the signal. A prototype of a power convertor proposed in [29] has not been manufactured yet. However, the idea is very promising from the point of view of frequency range of such a convertor. Theoretically, the convertor could measure active power of signals up to RF range.

4. Conclusion

4.1 Thesis summary

The thesis deals with magnetoresistive sensors based on anisotropic magnetoresistive effect, giant magnetoresistive effect and spin dependent tunneling effect, mainly – but not only – used for magnetic field measurement. The improvement of the performance of circuits and operation methods used in magnetometers with the mentioned sensors, as well as testing novel approaches and applications, represent the main contribution of the author in this field of science and technology. In the thesis, a brief introduction is given into the principles of the magnetoresistive effects and basic considerations are made on the operation techniques used in magnetic field sensors based on the above mentioned effects. The scientific core of the thesis, however, lies in the published articles, involved in the Appendix.

Several magnetometers have been realized, using commercially-available anisotropic magnetoresistors. Continuous improvement of the magnetometer circuitry allowed exploiting the sensor performance in the best possible way. Thus the development proceeded in several steps and more physical devices have been built, using the knowledge from the previous models. The influence of the supply method on the temperature dependences of the offset and sensitivity of the sensor has been analyzed and verified, leading to a finding that current source supply is preferable – see section 3.1.2 and [44]. Periodical remagnetizing, or flipping, has been optimized by using very high pulses that deeply saturate the magnetic material of the sensor. This technique led to improvement of the offset stability and noise of the device, as described in section 3.1.1 and in related papers [40, 41]. With a periodical remagnetization, the output of the sensor is a rectangular signal with the amplitude proportional to the measured field. Transients occurring in short time periods after changing the polarity of the output signal have been observed. Therefore, the processing circuit for the signal demodulation was developed that ignores these short time periods using a controlled rectifier and sample-hold circuit. The timing of the flipping and synchronous demodulation has been discussed in section 3.1.1 and in [42]. To suppress the temperature dependence of sensitivity and linearize the magnetometer characteristic, it is convenient to use the sensor in the compensated mode. The feedback compensation loop consists of an integrator, on-chip compensation strap and a sensing resistor. With feedback compensation, magnetic field is created with an on-chip compensation coil of the magnitude equal to the measured field, but with opposite direction, so that the sensor itself operates in the near-to-zero region. The best results obtained with an optimized magnetometer design are summarized in section 3.1.3 and in related papers [42, 43, 48]. Linearity, hysteresis, noise, temperature dependence of offset and sensitivity have been thoroughly characterized. The best magnetometer with anisotropic magnetoresistor reaches repeatedly the linearity and hysteresis error below ±80 ppm in the range of ±300 μT, with the long-term zero stability of ±30 nT, offset temperature drift of 2.1 nT / °C, temperature coefficient of sensitivity of 20 ppm / °C and noise PSD value below 5 nT / √Hz @ 1 Hz.

The parameters of anisotropic magnetoresistive sensors allow their usage in the compassing applications. Closer description on this topic is given in section 3.1.4 and in [48]. It has been shown that anisotropic magnetoresistor-based compass can reach the long-term precision of 0.5 degree.

Prototypes of giant magnetoresistors have been tested for the magnetic field measurement applications. A method of alternating biasing of the sensor has been proposed and verified that reduces the hysteresis of the characteristic of the sensor. The results have been published in [55] and are

described in more detail in section 3.2. The hysteresis was suppressed from 2 % with the DC biasing to 0.5 % with AC biasing in the range of ±375 μT. The linearity error was about 3 % in both cases with the sensitivity of approx. 20 mV/V/kA/m. The noise PSD value was 20 nT / √Hz @ 1 Hz with the DC biasing and 37 nT / √Hz @ 1 Hz with the AC biasing, so that AC biasing, besides its beneficial effect on the hysteresis, bears worsening of noise parameters.

Similar characterization has been performed with a TMR spin-valve prototype sensor. The results are discussed in section 3.3 and in the related paper [34]. The sensor was biased with a DC and AC squarewave current. The sensitivity of the sensor is very high, about 1750 mV/V/kA/m, but the characteristic suffers from a big hysteresis and offsets both in *x* and *y* axis. The hysteresis in the non-symmetrical range of 50–100 μT was reduced from 60 % with DC biasing to 12 % with AC biasing, the linearity error reaches 10 % with DC biasing and 5 % with AC biasing. The noise PSD value is about 5 nT / √Hz @ 1 Hz with AC biasing, but as low as 750 pT / √Hz @ 1 Hz with DC biasing. Although the linearity and hysteresis of the measured prototype do not allow to use the sensor for linear magnetic field measurements in a conventional way, the noise parameters and high sensitivity are very promising for specific applications.

Contactless current measurement is usually based on exploitation of Hall sensors. It has been shown that anisotropic magnetoresistors, thanks to their sensitivity, can also serve in this application field. A device has been developed with eight anisotropic magnetoresistors placed around the measurement hole in a rose-like array. The device is capable of measurement of electrical currents in the range of ±8 A with the linearity error of approx. ±0.05 %. Since the device does not employ a flux concentrator, or yoke, as it is usual at Hall-probe based devices, the non-concentricity of the current-leading wire causes significant errors. In the realized device this error was below ±0.5 % of the measuring range. The device is described in more detail in section 3.4.1 and in the related paper [62].

Experiments have been performed with anisotropic magnetoresistor used as an analog multiplier. The principle is straightforward: if one signal is used for supplying the sensor bridge and the second signal generates magnetic field in the sensitive axis direction, the output of the sensor is proportional to the product of these two signals. Thanks to their frequency range, the anisotropic magnetoresistors used in this operation mode can represent a very interesting alternative for active power measurements, where it is necessary to multiply voltage and current of the signal. In the performed experiment, the sensor bridge was supplied with a voltage proportional to the voltage of the signal, and the current proportional to the current of the measured signal was led through the internal coil or strap used for compensation in the normal mode of operation. Hence, the sensitivity to the current is very high. The function of such a multiplier has been verified in the range of 3.6 μW to 50 mW and with the phase shift ±70° between the voltage and the current signal. It has been found that the sensitivity is not constant for different values of the current led through the internal coil. However, the relative error due to phase shift was below 0.1 % in the frequency range up to 100 kHz. These experiments are described in section 3.4.2 and in the related paper [65].

A novel application that could be used for active power measurements of strictly harmonic signals with a single magnetoresistive stripe has been proposed. This application can be interesting from the point of view of frequency range, going supposedly up to radio frequency values. The method is described in section 3.4.2 and in the related paper [29].

4.2 Outlooks & further research

It has been shown that anisotropic magnetoresistive sensors are capable of considerably precise measurement of magnetic fields, with the sensitivity allowing compassing applications. They can also be successfully used in current or power measurement devices. Further research will be focused on possibilities of digital processing of the sensor signal. A microcontroller unit is in any case a part of a magnetometer with AMR sensors, if the described advanced timing of synchronous demodulation is used (although it is possible to realize these circuits using discrete logical parts, the microcontroller based solution is much simpler). The analog processing chain of magnetometers described in the thesis is rather complicated. If an A/D convertor with sufficient precision is available, the signal of the sensor can be digitized directly and the synchronous demodulation, offset elimination etc. can be

performed by an appropriate digital processing. Although some analog parts, such as the input amplifier or flipping circuits, would remain in the circuitry, the design as a whole would be markedly simplified.

The best performance of the magnetometer with anisotropic magnetoresistors has been achieved in flipped and compensated mode of operation. However, it would be possible to perform flipping on much lower frequencies under normal conditions. High enough flipping pulse restores the magnetic properties of the sensor, as has been shown, but especially in a compensated mode, there might be no need of making this restoration with kHz frequencies. Lower flipping frequency would result in lower consumption and possibly also in lower noise. On the other hand, the benefits of periodical remagnetizing, such as cross-field effect reduction and offset temperature drift elimination would be partially sacrificed. Therefore, different technique would probably have to be used for periodical cross-field and offset compensation.

An important parameter of a magnetometer used as an autonomous device is its consumption. In the case of the developed device, the main part of overall consumption is caused by the feedback compensation loop, driving current of the sensor bridge, and flipping circuits. The consumption could be lowered, if the sensor was not compensated constantly, but rather only for the moment when the measured value is desired. This mode could be interesting in automated applications with periodical or random data reading. In between readings, the magnetometer could be set in an "idle" mode, with no supply to the measurement bridge, no flipping and no compensation. Nevertheless, the reading would always have to be preceded with a strong flipping pulse to restore the magnetic properties of the sensor. An important question in this case of a "low power" magnetometer would be the reading stability.

Nowadays, there are several market-available types of GMR and TMR sensors. These sensors are intended mainly for automotive applications with modest requirements on precision. Nevertheless, further development in the field of these sensors can be expected, which can probably lead to construction of low-noise sensors for linear measurements.

Presented current and power measurement applications can be extended in many ways. The principle of single-stripe power convertor has not been fully verified yet. The analog multiplier with AMR sensor could be improved, given that there is a possibility of field compensation. This would be realizable even with an external coil wound around the sensor. In the case of compensation, the improvement of linearity of the multiplier can be expected. Additionally, periodical remagnetization of the sensor could also result in better performance, although a more complicated signal processing would have to be used.

5. References

The works of the author of this thesis typed [underlined]. These papers, excepting research report [18], can be found in Appendix A.

[1] Thomson W.: On the Electro-dynamic Properties of Metals. *Proceedings of Royal Society London, iss. 8 (1856), 50–55*

[2] Thomson W.: On the Electro-dynamic Properties of Metals – Effects of Magnetization on the Electric Conductivity of Nickel and of Iron. *Proceedings of Royal Society London, iss. 8 (1856), 546–550*

[3] Jan J. P.: Galvanomagnetic and thermomagnetic effects in metals. *Solid State Physics, No. 5 (1957), 1–96*

[4] Mott N. F.: A discussion of the transition metals on the basis of quantum mechanics. *Proceedings of the Physical Society, Vol. 47 (1975), 571–588*

[5] Mott N. F.: The electrical conductivity of transition metals. *Proceedings of the Royal Society of London, Vol. A153 (1936), 699–726*

[6] Smit J.: Magnetoresistance of ferromagnetic metals and alloys at low temperatures. *Physica XVII (1951), No. 6, 612–627*

[7] McGuire T. R. and Potter R. I.: Anisotropic magnetoresistance in ferromagnetic 3d alloys. *IEEE Transactions on Magnetics, Vol. Mag-11 (1975), No. 4, 1018–1038*

[8] Tumanski S.: Thin film magnetoresistive sensors. *Institute of Physics Publishing, 2001, ISBN 0 7503 0702 1*

[9] Haji-Sheikh M. J., Morales G., Altuncevahir B, Koymen A. R.: Anisotropic magneto-resistive model for saturated sensor elements. *IEEE Sensors Journal, Vol. 5 (2005), No. 6, 1258–1263*

[10] Aumentado J. and Chandrasekhar V: Magnetoresistance of single-domain ferromagnetic particles. *Applied Physics Letters, Vol. 74 (1999), No. 13, 1898–1900*

[11] Groenland J. P. J., Eijkel C. J. M., Fluitman J. H. J., de Ridder R. M.: Permalloy thin-film magnetic sensors. *Sensor and Actuators A, Vol. 30 (1992), Iss. 1–2, 89–100*

[12] Sczaniecki Z., Stobiecki F, Gontrarz R., Ratajczak H.: Anisotropy of narrow stripes of thin ferromagnetic film. *Acta Physica Polonica, 1974*

[13] Tumanski S.: Handbook of Magnetic Measurements (Series in Sensors). *CRC Press, Taylor & Francis Group, 2011, ISBN 1439829519*

[14] Philips Semiconductors: KMZ51 Magnetic field sensor. *Product datasheet*

[15] Honeywell: Magnetic Sensor Products – HMC/HMR Series. *Application note*

[16] Joseph R. I. and Schlömann E.: Demagnetizing field in nonellipsoidal bodies. *Journal of Applied Physics, Vol. 36 (1965), No. 5, 1579–1593*

[17] Buschow K. H. J. and de Boer F. R.: Physics of Magnetism and Magnetic Materials. *Kluwer Academic Publishers, New York 2004, ISBN 0-306-47421-2*

[18] Vopalensky M.: Sensores de Potencia con Películas Delgadas Magnetorresistivas para Mediciones de Potencia RF Activa „in situ". *Research report, Universidad Nacional Autónoma de México, 2003 (in Spanish, unpublished)*

[19] Dibbern, U: Magnetic field sensors using the magnetoresistive effect. *Sensors and Actuators A, Vol. 10 (1986), 127–140*

[20] Osborn J. A.: Demagnetizing factors of a general ellipsoid. *Physical Review, Vol. 67 (1945), No. 11–12, 351–357*

[21] Schlömann E.: A sum rule concerning the inhomogeneous demagnetizing field in non-ellipsoidal samples. *Journal of Applied Physics, Vol. 33 (1962), No. 9, 2825–2826*

[22] Aharoni A.: Demagnetizing factors for rectangular ferromagnetic prisms. *Journal of Applied Physics, Vol. 83 (1998), No. 6, 3432–3434*

[23] Aharoni A., Pust L., Kief M.: Comparing theoretical demagnetizing factors with the observed saturation process in rectangular shields. *Journal of Applied Physics, Vol. 87 (2000), No. 9, 6564–6566*

[24] Fluitman J. H. J: The influence of sample geometry on the magnetoresistance of Ni-Fe films. *Thin Solid Films, Vol. 16 (1973), Iss. 3, 269–276*

[25] Wood R.: Exact Solution for a Stoner–Wohlfarth Particle in an Applied Field and a New Approximation for the Energy Barrier. *IEEE Transactions on Magnetics, Vol. 45 (2009), No. 1, 100–103*

[26] Stoner E. S. and Wohlfarth E. P.: A mechanism of magnetic hysteresis in heterogeneous alloys. *Philos. Trans. R. Soc. Lond., vol. A240 (1948), 599–642*

[27] Thiaville A.: Extensions of the geometric solution of the two dimensional coherent magnetization rotation model. *Journal of Magnetism and Magnetic Materials, Vol. 182 (1998), 5–18*

[28] Stancu A. and Chiorescu I.: Crossover Condition in the Coherent Rotation Model and the Preisach-Type Models. *IEEE Transansction on Magnetics, Vol. 33 (1997), No. 4, 2573–257*

[29] Vopalensky M.: A Single Magnetoresistive Strip as a Power Convertor. *Journal of Electrical Engineering – Elektrotechnický časopis, Vol. 63 (7 suppl), 2012, 114–117*

[30] Ripka P. (ed.): Magnetic sensors and magnetometers. *Artech House Publishers, 2001, ISBN 1-58053-057-5*

[31] White, R. L.: Giant magnetoresistance: A primer. *IEEE Transactions on Magnetics, Vol. 28 (1992), No. 5, 2482–2486*

[32] NVE Corporation: GMR Sensor Catalog. *Product catalog*

[33] Tondra M., Daughton J. M., Wang D., Beech R. S., Fink A., Taylor J. A.: Picotesla field sensor design using spin-dependent tunneling devices. *Journal of Applied Physics, Vol. 83 (1998), Iss. 11, 6688–6690*

[34] Vopalensky M., Ripka P., Kubik J., Tondra M.: Alternating biasing of SDT sensors. *Sensors and Actuators A, Vol. 110, Iss. 1-3 (2004), 182–186*

[35] Smith N., Jeffers F., Freeman J.: A high-sensitivity magnetoresistive magnetometer. *Journal of Applied Physics B, Vol. 69 (1991), 5082–5084*

[36] Cheng S.F., Lubitz P., Zheng Y., Edelstein A. S.: Effects of spacer layer on growth, stress and magnetic properties of sputtered permalloy film. *Journal of Magnetism and Magnetic Materials, Vol. 282 (2004), 109–114*

[37] Infineon Technologies AG: TLE5041plusC, Differential iGMR Wheel Speed Sensor for Indirect TPMS Systems. *Product datasheet*

[38] NXP Semiconductors: KMZ60 – Angle sensor with integrated amplifier. *Product datasheet*

[39] Honeywell: AN214 – Reference Design: Low Cost Compass. *Application note*

[40] Hauser H., Fulmek P. L., Haumer P., Vopalensky M., Ripka P.: Flipping field and stability in anisotropic magnetoresistive sensors. *Sensors and Actuators A, Vol. 106, Iss. 1-3 (2003), 121-125*

[41] Platil A., Vopálenský M., Ripka P., Kašpar P., Hauser H.: Improvement of AMR Magnetometer Precision. *Eurosensors XVI - Proceedings, Prague, 2002, 612-613*

[42] Vopálenský M., Ripka P., Platil A.: Precise magnetic sensors. *Sensors and Actuators A, Vol. 106, Iss. 1–3 (2003), 38–42*

[43] Ripka P., Vopálenský M., Platil A., Döscher M., Lenssen K. M. H., Hauser H.: AMR magnetometer. *Journal of Magnetism and Magnetic Materials, Vol. 254 (2003), 639–641*

[44] Vopalensky M., Platil A.: Temperature Drift of Offset and Sensitivity in Full-Bridge Magneto-resistive Sensors. *IEEE Transactions on Magnetics, Vol. 49, Iss. 1 (2013), 136-139*

[45] Philips Semiconductors: KMZ 52 Magnetic field sensor. *Product datasheet.*

[46] Counil G., Devolder T., Kim J.-V., Crozat P., Chappert C., Zoll S., Fournel R.: Temperature dependences of the resistivity and the ferromagnetic resonance linewidth in permalloy thin films. *IEEE Transactions on Magnetics, Vol. 42, Iss. 10 (2006), 3323–3325*

[47] Mũoz D. R., Moreno J. S., Berga S. C., Montero E. C., Escrìv C. R., Antón A. E. N.: Temperature compensation of Wheatstone bridge magnetoresistive sensors based on generalized impedance converter with input reference current. *Review of Scientific Instruments, Vol. 77, Iss. 10 (2006), art. number 105102*

[48] Platil A., Kubík J., Vopálenský M., Ripka P.: Precise AMR Magnetometer for Compass**.** *IEEE SENSORS 2003, p. 472-476, Toronto 2003, ISBN 0-7803-8134-3*

[49] Ripka P.: Noise and stability of magnetic sensors. *Journal of Magnetism and Magnetic Materials, Vol. 157-158 (1996), 424-427*

[50] Honeywell: HMC5883L – 3-axis Digital Compass IC. *Product datasheet*

[51] Honeywell: HMR3000 – Digital Compass Solution. *Product datasheet*

[52] Philips Semiconductors: AN00022 – Electronic Compass Design using KMZ51 and KMZ52. *Application note*

[53] Honeywell: HMR3300 Digital Compass Solutions. *Product datasheet*

[54] Honeywell: HMR3600 uPoint Gyro-Stabilized Digital Magnetic Compass Module. *Product datasheet*

[55] Vopalensky M., Ripka P., Kubik J., Tondra M.: Improved GMR sensor biasing design. *Sensors and Actuators A, Vol. 110, Iss. 1-3 (2004), 254-258*

[56] Ripka P., Tondra M., Stokes J., Beech R.: AC driven AMR and GMR magnetoresistors. *Sensors and Actuators A, Vol. 76, Iss. 1-3 (1999), 225-230*

[57] NVE Corporation: AA and AB-Series Analog Sensors. *Product catalog*

[58] NVE Corporation: AAT001-10E: TMR Angle Sensor. *Product datasheet*

[59] Iwansson K., Sinapius G., Hoornaert W. (Eds.): Measuring Current, Voltage and Power. *1st ed., Elsevier, Amsterdam, 1999, ISBN 9780444720016*

[60] GMW Associates: Hall IC Current Sensor, CSA-1VG-SO. *Product datasheet*

[61] Ripka P., Kejík P., Kašpar P., Draxler K.: Precise DC Current Sensors. *IEEE Instrumentation and Measurement Technology Conference, Brussels, Belgium, 1996, 1479-1483*

[62] Vopálenský M., Mlejnek P., Ripka P.: AMR current measurement device. *Sensors and Actuators A, Vol. 141, Iss. 2 (2008), 649-653*

[63] Patent US 4,199,696: Multiplier using Hall element

[64] Chasmar R.P., Cohen E., Holmes D.P.: The design and performance of a Hall-effect multiplier. *Proceedings of the IEE - Part B: Electronic and Communication Engineering, Vol. 106, Iss. 16 (1959), 702-705*

[65] Vopálenský M., Platil A., Kašpar P.: Wattmeter with AMR sensor. *Sensors and Actuators A, Vol. 123-124 (2005), 303-307*

[66] Vountesmeri V.: Audio Frequency Magnetoresistive Watt-Converter, *IEEE Transactions on Instrumentation and Measurement, Vol. 51, No. 1 (2002), 63-66*

Appendix
Selected papers of the author related to the thesis

[29] Vopalensky M.: A Single Magnetoresistive Strip as a Power Convertor. *Journal of Electrical Engineering – Elektrotechnický časopis, Vol. 63 (7 suppl), 2012, 114–117*

Journal of ELECTRICAL ENGINEERING, VOL 63. NO 7s, 2012, 114-117

A SINGLE MAGNETORESISTIVE STRIP AS A POWER CONVERTOR

Michal Vopálenský*

Magnetoresistive effect can be exploited for the measurement of an active power of harmonic signals. A single stripe of a magnetoresistive material is capable of converting active power to voltage drop on the stripe. The current flowing through the stripe is proportional to the voltage of the measured signal, whereas the signal current produces magnetic field that influences the orientation of magnetization and thus the resistivity of the stripe. The convertor requires a biasing DC magnetic field for a proper operation. The range and sensitivity of the measurement can be determined by the shape anisotropy of the stripe. A theoretical description of a configuration of an active power convertor based on a magnetoresistive stripe with uniaxial anisotropy is given in the paper.

Keywords: anisotropic magnetoresistance, thin ferromagnetic films, active power measurement

1 INTRODUCTION

Measurement of active power is one of the basic tasks in electrical engineering. Considering a signal with the voltage and current given as functions of time, $u(t)$ and $i(t)$, the instantaneous power is given as

$$p(t) = u(t).i(t) \tag{1}$$

If the voltage and current are harmonic functions with the period T, angular frequency $\omega = 2\pi/T$, and mutual phase shift φ, the active power is defined as the mean value of the instantaneous power

$$\begin{aligned} P &= \frac{1}{T}\int_0^T u(t)\cdot i(t)dt = \\ &= \frac{1}{T}\int_0^T U_m \sin(\omega t+\varphi)\cdot I_m \sin(\omega t)dt = UI\cos\varphi \end{aligned} \tag{2}$$

In (2), U_m, I_m are the amplitudes and U, I are the effective (RMS) values of $u(t)$, $i(t)$. From (2) it is obvious that a crucial task when measuring the active power of a continuous harmonic signal is analogous multiplication of two signals. Obtaining the mean value of the resulting signal is rather a simple task.

Sensors of magnetic field are often used in power convertors as contactless current-voltage convertors. In particular Hall sensors are widely spread in this field, designed specifically as a signal multiplier: the sensor is supplied with a current proportional to the signal voltage, the current of the signal produces magnetic field sensed by the sensor. Thus the Hall voltage at the sensor output is proportional to the product of voltage and current of the signal [1].

Linearized magnetoresistive sensors can be used in fact in the same way, as the Hall sensors. However, the magnetoresistive phenomenon can be yet differently exploited for measuring of active power of harmonic signals, using a single thin stripe of a magnetoresistive material with uniaxial anisotropy.

2 PHENOMENOLOGICAL DESCRIPTION OF MAGNETORESISTIVE EFFECT

Let a body of a saturated ferromagnetic magnetoresistive material be considered. The resistivity of such a body is not uniform, but it is dependent on the direction in which it is measured; more specifically on the mutual orientation of the direction of measurement and the magnetization vector. The current flowing through the material generates electric field, which in a compact form can be written as [2, 3]:

$$\vec{E} = \rho_t \vec{J} + \Delta\rho\cdot\vec{\alpha}(\vec{\alpha}\cdot\vec{J}) + \rho_H(\vec{\alpha}\times\vec{J}) \tag{3}$$

Here,

- $\vec{E}$ (V/m) is the vector of the electric field intensity;
- $\vec{J}$ (A/m^2) is the vector of the current density;
- $\vec{\alpha}$ (-) $\vec{\alpha}$ (-) = (cos α_1, cos α_2, cos α_3) is the vector of directional cosines of magnetization $\vec{M}$, where $\alpha_{1,2,3}$ are the angles between $\vec{M}$ and the individual axes of the coordinate system;
- ρ_t (Ω.m) is the resistivity in the orthogonal direction to $\vec{M}$;
- $\Delta\rho$ (Ω.m) is the difference between the resistivity ρ_l measured in parallel with $\vec{M}$ and ρ_t, $\Delta\rho = \rho_l - \rho_t$
- ρ_H (Ω.m) is the Hall coefficient of the material.

In most of the real cases, only the resistivity in the current direction is important. When we fix the vectors to an orthogonal coordinate system with the current flowing along the x-axis direction, *ie* $\vec{J} = (J_x, 0, 0)$, the intensity of the field in x-axis direction is

$$E_x = (\rho_t + \Delta\rho\cos^2\alpha_1)J_x \tag{4}$$

The magnetoresistive body used in sensors takes usually the form of a narrow thin stripe contacted on the short edges. For further considerations, let the longitudinal axis be aligned with the x-axis of the orthogonal coordinate

* College of Polytechnics Jihlava, Department of Electrical Engineering and Computer Science, Tolstého 16, 586 01 Jihlava, Czech Republic, vopalensky@vspj.cz

ISSN 1335-3632 © 2012 FEI STU

system and let the sensor lie in the *xy* plane. Due to the strong demagnetization factor in the direction orthogonal to the stripe plane, vector $\vec{M}$ cannot in fact leave the stripe plane. Therefore, its orientation can be described with a single angle α_1, meaning the inclination of $\vec{M}$ out of the x-axis in a counterclock direction. For the sake of better legibility, let this angle be designated as ψ, $\psi = \alpha_1$. Using the fact $\Delta\rho = \rho_l - \rho_t$, the so-called Woigt-Thomson formula (4) can be rewritten as

$$E_x = \rho_l J_x - \Delta\rho J_x \sin^2\psi \tag{5}$$

From Eq. (5) it is obvious that the electric field component along the longitudinal axis of a magnetoresistive stripe (which is measurable as the voltage drop on the stripe) is dependent on the material constants ρ_l, $\Delta\rho$, and on two physical quantities that can be influenced externally, namely the current density J_x and inclination of magnetization from the *x*-axis, ψ. The presence of the product of J_x and $\sin^2\psi$ gives a chance of using a magnetoresistive stripe as an analog multiplier.

3 MAGNETORESISTIVE STRIPE AS AN ANALOG MULTIPLIER

Basic configuration of a multiplier with a magnetoresistive stripe is illustrated in Fig. 1. Current flowing through the magnetoresistive stripe is proportional to the signal voltage. The signal-leading wire is led in the vicinity of the stripe and the magnetic field generated by the flowing current influences the angle of $\vec{M}$ and thus the resistivity of the stripe. The voltage drop on the stripe is then a function both of the signal current and voltage. Unfortunately, $\sin^2\psi$ is not linearly proportional to the applied magnetic field.

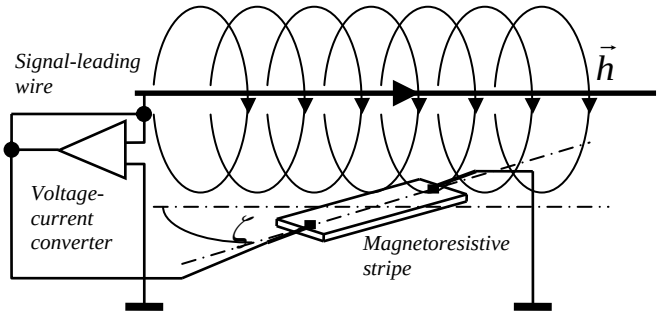

Fig. 1. General configuration of a magnetoresistive stripe for a multiplier application

Magnetization vector in a ferromagnetic body takes the orientation determined by the competition of the external acting field and affinity of $\vec{M}$ to the easy axes of anisotropy, whereas the prevalent one is usually the shape anisotropy of the stripe. Minimizing the shape anisotropy by an appropriate design of the stripe and neglecting the technologically induced anisotropy, it can be assumed that there are no easy axes in the material and $\vec{M}$ takes the orientation of the external field. Based on this assumption, active power convertors have been developed, overcoming the problem with the non-linear dependence of $\sin^2\psi$ on the external field by a suitable sensor configuration [4].

A narrow thin stripe of a magnetoresistive material used in magnetoresistive sensors is usually designed in order to exhibit a strong shape anisotropy, which then determines the sensor's range and sensitivity [3]. In addition, the material of a magnetoresistive sensor is usually annealed in a homogenous magnetic field to reduce the anisotropy dispersion and lower the background resistance in order to enlarge the magnetoresistive coefficient [3]. Annealing in the magnetic field causes formation of an induced anisotropy with the easy axis along the direction of the magnetic field. The value of the characteristic field of this anisotropy is dependent on the material [3]. In practice, the magnetoresistive stripes used in sensors have the longitudinal axis aligned to the induced anisotropy direction, so that the induced and shape anisotropy sum together and make an easy axis along the longitudinal axis of the stripe. The strength of the shape anisotropy can be determined by the dimensions of the stripe, mainly by its length and width [5].

In a stripe with a uniaxial anisotropy, the $\vec{M}$ orients along the easy axis in absence of any external field. If an external field H_{ext} is applied, $\vec{M}$ leaves the easy axis and orients to a direction determined by the angle and magnitude of H_{ext} and strength of the anisotropy. Unfortunately, there is no analytical solution for the angle of $\vec{M}$ for a general magnitude and angle of H_{ext}.

A simple solution for the angle of $\vec{M}$ exists in the case of H_{ext} acting in the plane of the stripe and in orthogonal direction to the easy axis of uniaxial anisotropy. In this particular, but very important case, the angle ψ of $\vec{M}$, determined by the minimization of the free system energy is given as [3]

$$\sin\psi = \frac{H_{ext}}{H_c} \tag{6}$$

Here H_c is the characteristic field of the anisotropy along the longitudinal axis of the stripe (consisting of induced and shape anisotropy).

Let a magnetoresistive stripe be fixed to an orthogonal coordinate system as described below the Eq. (4). Let the easy axis lie along the longitudinal axis of the stripe (*ie* in the *x*-axis direction). Let the stripe be connected as in Fig.1 with $\zeta = 0$, so that the produced field acts in *y*-axis direction. Finally, let a DC magnetic field H_b be applied in *y*-axis direction (superposing with H_{ext}, generated by the signal current). This field serves for establishing of the appropriate initial angle of $\vec{M}$, as will be discussed further. The whole configuration is shown in Fig. 2.

Combining (5) and (6), the electric field in the *x*-axis takes the form

$$E_x = \left(\rho_l - \Delta\rho\left(\frac{H_b + H_{ext}}{H_c}\right)^2\right) J_x \tag{7}$$

Let it be supposed that the voltage and current of the processed signal are harmonic functions, and that J_x is proportional to the signal voltage with the coefficient c_u and the H_{ext} proportional to the signal current with the coefficient c_i. The J_x and H_{ext} as functions of t will be designated in lower case, ie

$$\begin{aligned} j_x &= c_u U \sin(\omega t + \varphi) = J_x \sin(\omega t + \varphi) \\ h_{ext} &= c_i I \sin \omega t = H_{ext} \sin \omega t \end{aligned} \tag{8}$$

Then

$$E_x(t) = \left(\rho_l - \Delta\rho \left(\frac{H_b + H_{ext} \sin \omega t}{H_c} \right)^2 \right) J_x \sin(\omega t + \varphi) \tag{9}$$

It is obvious that the instantaneous value of $E_x(t)$ is not a product of instantaneous values of $i(t)$ and $u(t)$. However, let us concentrate on the mean value of E_x:

$$\begin{aligned} \overline{E}_x &= \rho_l J_x \frac{1}{T} \int_{-T/2}^{T/2} \sin(\omega t + \varphi) dt \\ &- \Delta\rho J_x \left(\frac{H_b}{H_c} \right)^2 \cdot \frac{1}{T} \int_{-T/2}^{T/2} \sin(\omega t + \varphi) dt \\ &- 2\Delta\rho J_x \cdot \frac{H_b H_{ext}}{H_c^2} \cdot \frac{1}{T} \int_{-T/2}^{T/2} \sin \omega t \sin(\omega t + \varphi) dt \\ &- \Delta\rho J_x \cdot \left(\frac{H_{ext}}{H_c} \right)^2 \cdot \frac{1}{T} \int_{-T/2}^{T/2} \sin^2 \omega t \sin(\omega t + \varphi) dt \end{aligned} \tag{10}$$

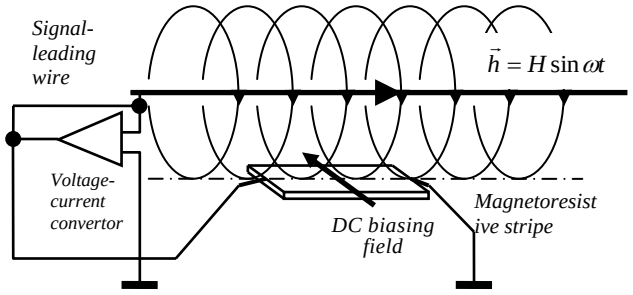

Fig. 2. Novel configuration of an active power convertor proposed in this paper.

Obviously the first and second member in (10) is equal to zero, because of integration of the sine function over one whole period. The integral in the fourth member can be written as

$$\begin{aligned} &\int_{-T/2}^{T/2} \sin^2 \omega t \sin(\omega t + \varphi) dt \\ &= \cos\varphi \int_{-T/2}^{T/2} \sin^2 \omega t \sin \omega t dt + \sin\varphi \int_{-T/2}^{T/2} \sin^2 \omega t \cos \omega t dt \end{aligned} \tag{11}$$

The first integral in (11) is the integral of an odd function in a symmetrical interval and is therefore equal to zero. The indefinite integral of the function in the second member is

$$\int \sin^2 \omega t \cos \omega t dt = \frac{\sin\varphi}{3\omega} \sin^3 \omega t + C \tag{12}$$

so that the definite integral over $-T/2$, $T/2$ is equal to zero.

The last unsolved member of (10) resembles directly the formula for the active power (2) of a harmonic signal. After modification,

$$\begin{aligned} \overline{E}_x &= -2\Delta\rho J_x \cdot \frac{H_b H_{ext}}{H_c^2} \cdot \frac{1}{T} \int_{-T/2}^{T/2} \sin \omega t \sin(\omega t + \varphi) dt \\ &= -\frac{\Delta\rho H_b}{H_c^2} \cdot J_x \cdot H_{ext} \cdot \cos\varphi = -\frac{\Delta\rho H_b}{H_c^2} \cdot c_u \cdot c_i \cdot UI \cos\varphi \end{aligned} \tag{13}$$

The mean value of the electrical field along the longitudinal axis of a magnetoresistive stripe is thus proportional to the active power of the signal.

From (13), it can also be seen that setting an initial angle of $\vec{M}$ with a DC bias field H_b is indispensable – for $H_b = 0$ the mean value of E_x is also 0. The magnitude of the bias field has to be chosen carefully. Although the higher H_b, the higher the sensitivity of the convertor, one has to keep in mind that for $H_b = H_c$ the vector $\vec{M}$ is fully rotated into the H_b direction and does not react properly to the external field anymore. As well, $\vec{M}$ must not be rotated to the oposite direction from the x-axis for a proper function. The maximum applicable external field is thus $H_{ext,max} = H_c/2$ and the optimum biasing DC magnetic field is also $H_b = H_c/2$ (this means that the initial angle of magnetization is 30°), so that for maximum positive amplitude, the full rotation of $\vec{M}$ is achieved, whereas for the maximum negative amplitude $\vec{M}$ lies along the x-axis. Range of the convertor can be determined through the geometry and thus the strength of the shape anisotropy.

4 CONCLUSION

A theoretical model has been derived showing that a single magnetoresistive stripe can be used as an active power convertor for harmonic signals. Chosen approach does not neglect the uniaxial anisotropy of the stripe. On the contrary, the anisotropy is used in a beneficial way. One of the significant advantages of the proposed configuration, besides of simplicity, is supposed wide frequency range of such a converter. It can be expected that proposed converter can work properly for rather weak signals, moving the magnetization around the initial position determined by the bias field. The higher the angle of magnetization, the higher the effects associated with splitting of the stripe structure into multiple domains. Therefore, the theoretically possible rotation of magnetization to the orthogonal direction from the easy axis would very probably not yield good results.

REFERENCES

[1] CHASMAR, R.P. — COHEN, E. — HOLMES, D.P.: The design and performance of a Hall-effect multiplier, Proceedings of the IEE -

Part B: Electronic and Communication Engineering, Vol. 106, Iss. 16 (1959), 702-705

[2] MCGUIRE, T.R. — POTTER, R.I.: Anisotropic magnetoresistance in ferromagnetic 3d alloys, IEEE Transactions on Magnetics, Vol. Mag-11 (1975), No. 4, 1018–1038

[3] TUMANSKI, S: Thin film magnetoresistive sensors, Institute of Physics Publishing, 2001, ISBN 0 7503 0702 1

[4] VOUNTESMERI, V: Audio Frequency Magnetoresistive Watt-Converter, IEEE Transactions on Instrumentation and Measurement, Vol. 51, No. 1, Feb. 2002, p. 63-66

[5] FLUITMAN, J.H.: The influence of sample geometry on the magnetoresistance of Ni-Fe films. Thin Solid Films, Vol. 16 (1973), Iss. 3, 269–276

Received 8 September 2012

Michal Vopálenský (Ing, Bc, PhD), graduated from the Faculty of Electrical Engineering, Czech Technical University in Prague, in 2002, in measurement and instrumentation, received PhD in 2006 in measurement technology. With a scholarship for research activities in the field of anisotropic magnetoresistors from Secretary of Foreign Affairs of Government of Mexico, he stayed at the Universidad Nacional Autónoma de México in 2003. In 2006, he worked as a researcher in Tyndall National Institute, Ireland. During 2007 – 2011 he was employed as a specialist in Bosch Diesel, Jihlava, Czech Republic. Since 2011, he is with the Department of Electrical Engineering and Computer Science of the College of Polytechnics in Jihlava. His main research interests are sensors based on magnetoresistive effects.

[34] Vopalensky M., Ripka P., Kubik J., Tondra M.: Alternating biasing of SDT sensors. *Sensors and Actuators A, Vol. 110, Iss. 1-3 (2004), 182-186*

Available online at www.sciencedirect.com
SCIENCE DIRECT®
Sensors and Actuators A 110 (2004) 182–186
SENSORS AND ACTUATORS A PHYSICAL
www.elsevier.com/locate/sna

Alternating biasing of SDT sensors

Michal Vopálenský [a,*], Pavel Ripka [a,1], Jan Kubík [a,2], Mark Tondra [b,3]

[a] *Department of Measurement, Faculty of Electrical Engineering, Czech Technical University, Technicka 2, 166 27 Prague 6, Czech Republic*
[b] *NVE Corporation, 11409 Valley View Road, Eden Prairie, MN 55344-3617, USA*

Abstract

The spin dependent tunneling (SDT) effect has been observed in thin ferromagnetic multilayer structures. In general, two ferromagnetic layers are separated by a very thin non-conductive layer. In dependence on the angle between the magnetization of the upper and the lower ferromagnetic layer, electrons tunnel through the non-conductive barrier layer. We made experiments with an SDT sensor fabricated by NVE Corporation. Four elements in the bridge configuration are used in the sensor structure. One ferromagnetic layer of each element is pinned by an anti-ferromagnetic layer. The so-called orthogonal biasing can be applied in this sensor type. We also tried to study the possibilities of ac biasing techniques in the SDT sensors of this type.

Keywords: Magnetoresistive sensors; Orthogonal biasing; Spin dependent tunneling effect

1. Introduction

The basic description of the spin dependent tunneling (SDT) effect can be found in [1,2]. The SDT junctions have been designed and fabricated for the purposes of making linear solid state high-sensitivity magnetic sensors [3,4]. The SDT sensor we have worked with was manufactured at NVE Corp. The measurement bridge consists of four SDT elements. Ferromagnetic flux-concentrators are employed to achieve a bipolar response to the measured field. Thus two opposite elements of the bridge are exposed to the 10-times intensified field, whilst the other two bridge legs are effectively shielded. This design is shown schematically in Fig. 1.

One ferromagnetic layer in each element is pinned by means of an anti-ferromagnetic layer, so that its magnetization vector is not free to rotate. Such a structure is usually referred to as a “pinned sandwich” or “spin-valve”. Rotating the magnetization of the free layer to 90° with respect to the second layer magnetization direction, we can shift the operating point of the sensor to the area of the highest sensitivity of the characteristic [4]. This technique, usually called orthogonal biasing, is well known from the GMR technology [5,6]. It is usual to integrate the suitable biasing coil on-chip along with the bridge elements. Passing a current of a proper value through this coil, we can rotate the free-layer magnetization and thus we can change the properties of the sensor. The SDT structure and idealized resistance output are shown in Figs. 2 and 3.

2. ac biasing hypothesis

For high values of the biasing current, the characteristic of the SDT sensor becomes more linear and the hysteresis reduces. As the resistivity of the SDT element is dependent on the mutual angle of the magnetization vectors, and the sensitive axis of the biased sensor is parallel to the direction of the magnetization of the pinned layer, reversing the orientation of the orthogonal biasing field does not cause the reversing of the output characteristic in an ideal case. Even though we supposed that it would be interesting to study the behavior of the sensor with the periodical ac biasing. The hysteresis of the ferromagnetic material used in the SDT structure has a direct influence on the overall sensor hysteresis. When the magnetization of the free biased layer becomes inverted, the internal structure of the material is being re-ordered and thus the influence of the hysteretic behavior of the material is reduced. Since inverting the biasing field does not have any effect on the resistivity value, the output of the sensor stays dc even for the squarewave ac biasing in an ideal case. In fact, owing to non-symmetries in the sensor

* Corresponding author. Tel.: +420-224-353964; fax: +420-233-339929.
E-mail addresses: vopalem@fel.cvut.cz (M. Vopálenský), ripka@fel.cvut.cz (P. Ripka), kubikj@fel.cvut.cz (J. Kubík), markt@nve.com (M. Tondra).
[1] Tel.: +420-224-353945; fax: +420-233-339929.
[2] Tel.: +420-224-353964; fax: +420-233-339929.
[3] Tel.: 952-996-1615; fax: 952-996-1600.

0924-4247/$ – see front matter © 2003 Elsevier B.V. All rights reserved.
doi:10.1016/j.sna.2003.10.044

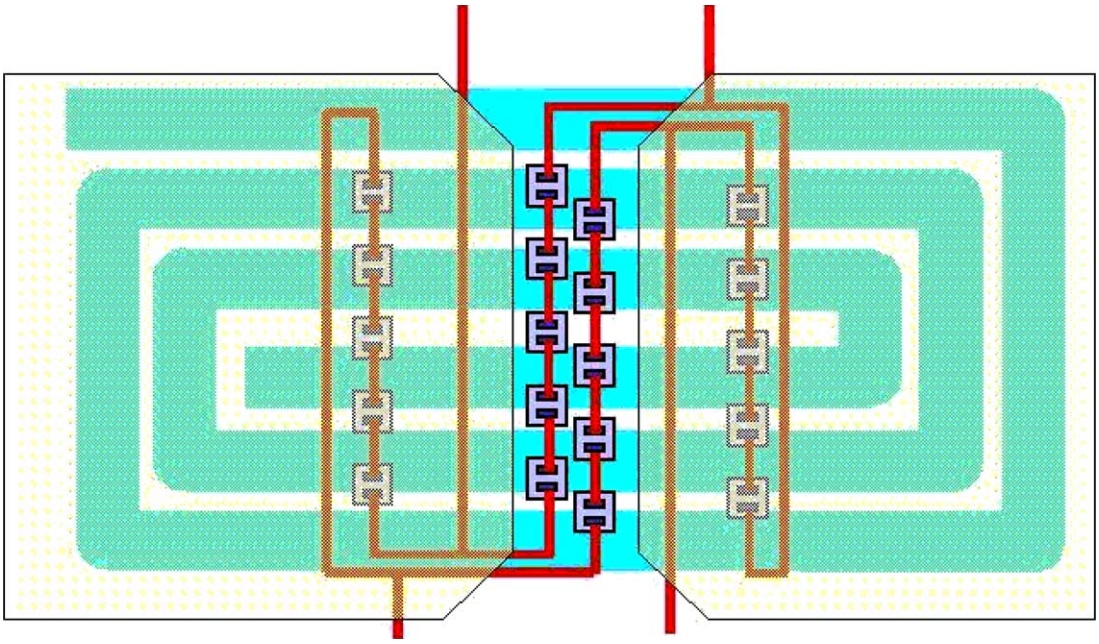

Fig. 1. Two legs of the SDT resistance bridge are in the gap between two flux concentrators, while two are under it. A planar coil, shown as a spiral over the bridge, generates the orthogonal biasing field.

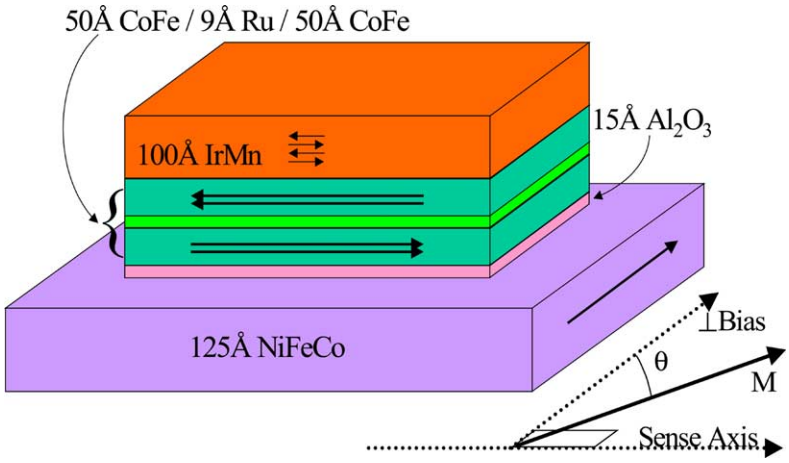

Fig. 2. The magnetic structure of a single tunnel junction, showing the orientation of the pinned and free layers when orthogonally biased.

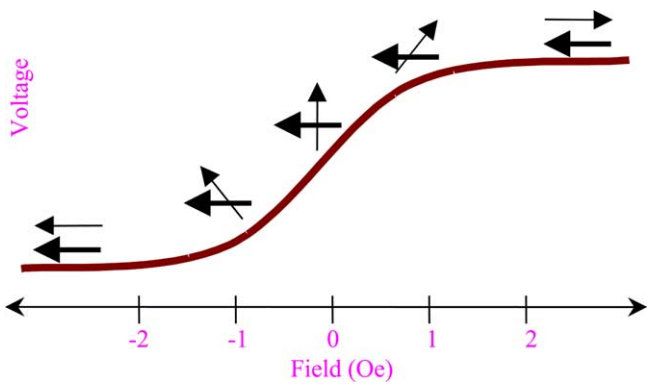

Fig. 3. Idealized SDT resistance versus field dependence.

structure, the output signal has a small ac component when the sensor is ac biased. Thus, it is useful to filter the output signal by a proper low-pass filter.

3. Measurement setup

The sensor employs flux concentrators to achieve the non-zero output and thus it works even without any biasing. Nevertheless, its behavior changes when the orthogonal biasing is used. The biasing reduces hysteresis of the sensor and even linearizes the characteristic in the middle part.

For the purpose of the measurement on the NVE SDT sensor, we used a universal evaluation board developed in our laboratory and an automatic computer-aided measurement

system [7]. Averaging from two samples was used in each measurement. The sensor was supplied by the on-board voltage source; the supplying voltage was 2 V.

Noise measurement of the dc and ac biased SDT sensor has been performed. During this measurement, the sensor was placed into a six-layer cylindrical permalloy magnetic shielding.

4. Measurement results

The first measurement was done without any biasing. The bias current was then increased to 20 mA, the maximum allowed value due to power dissipation limitations. The resulting characteristic is shown in Fig. 4. The signal was measured at the output of an instrumentation amplifier with a gain of 10. We can observe some facts from the characteristics. Firstly, the hysteresis is decreasing with the increasing value of the biasing current. Secondly, the linearity is increasing and the sensitivity is decreasing in the middle part with the increasing value of the biasing current, and thirdly, the voltage of the output, when the sensor is in saturation, is decreasing with the increasing bias. We can also see a big value of the offset of the sensor in Fig. 4. This fact is not surprising, due to the difficulties in fabricating the elements of the SDT bridge. The field offset is due to magnetic coupling between the sensing free layer and the pinned layer. The voltage offset is due to resistor mismatch, and can be trimmed in future designs.

The hysteresis of the characteristic is the lowest when 20 mA biasing current is used. The highest sensitivity is about 15 mV/(Am^{-1}) in the middle part of this characteristic, corresponding to 750 (mV/V)/ (kA/m) at the sensor output. The biasing current of 40 mA would probably be sufficient to fully eliminate the hysteresis. However, the present sensor design does not permit such a high current. We can notice that the reasonable linear operating range of this sensor for the maximum dc biasing current of 20 mA would be about 40–100 A m^{-1}. The hysteresis for the sensor going to the saturation is about 14% in this range. It would be lower if the sensor were operated just in this range and were not saturated. The linearity error is about 10% in this range.

In the case of the ac biasing, the sensor was supplied by a 2 V voltage source; the biasing coil current was about ±13.5 mA at the frequency of 1000 Hz. Besides this square-wave biasing measurement, we did a dc biasing measurement with the current of 13.5 mA. The results of the measurements are summarized in Fig. 5.

A very narrow linear range of the ac-biased SDT sensor can be seen, in which the sensitivity is very high (1750 (mV/V)/(kA/m). Whilst the sensitivity is almost of the same value both for the dc and ac biasing, the hysteresis decreases by the factor of five in the case of the ac squarewave biasing. Considering 0–100 A m^{-1} measurement range, the linearity error for the dc biasing is about 10% FS, reduced to 5% FS for the ac biasing.

The results of the dc biased sensor noise measurement are shown in the Fig. 6. The single sensor noise PSD value in the case of 13.5 mA dc biasing is 2 μV RMS $\sqrt{\text{Hz}}$ @ 1 Hz, corresponding to 600 μA m^{-1} (750 pT) RMS $\sqrt{\text{Hz}}$ @ 1 Hz in the most sensitive range. The noise rms value is about 2.7 mA m^{-1} (3.5 nT) in the 100 mHz to 10 Hz frequency

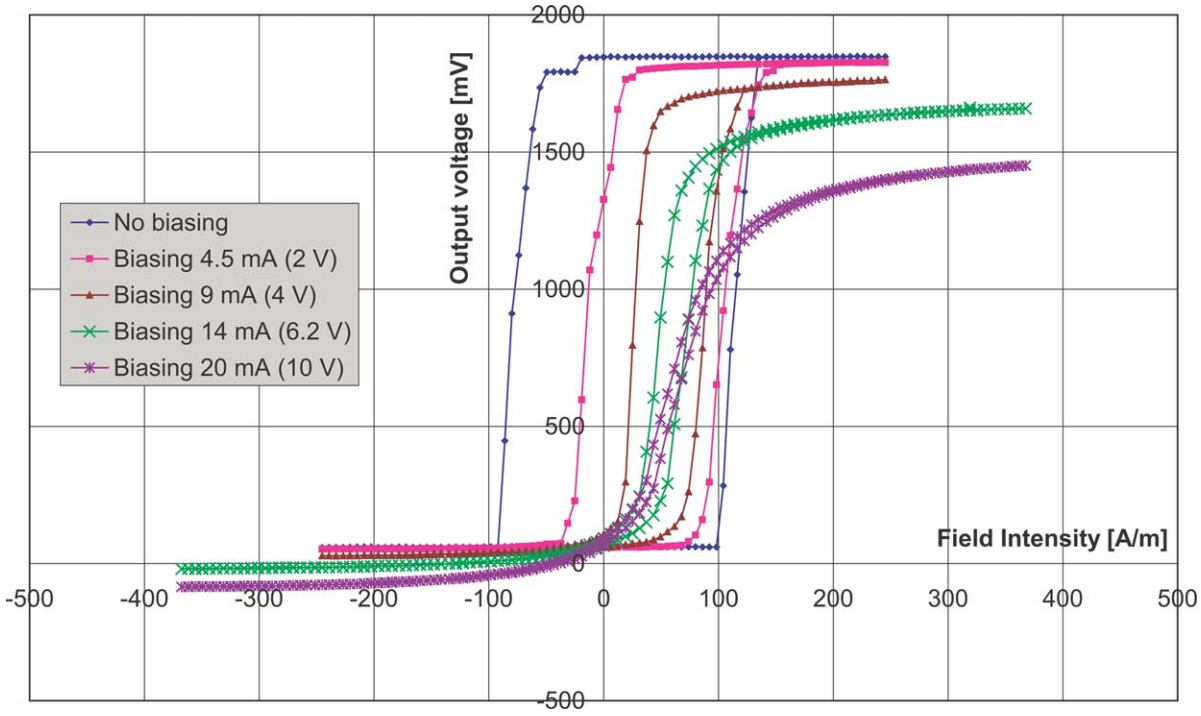

Fig. 4. Influence of the dc biasing field amplitude on the NVE SDT sensor characteristic.

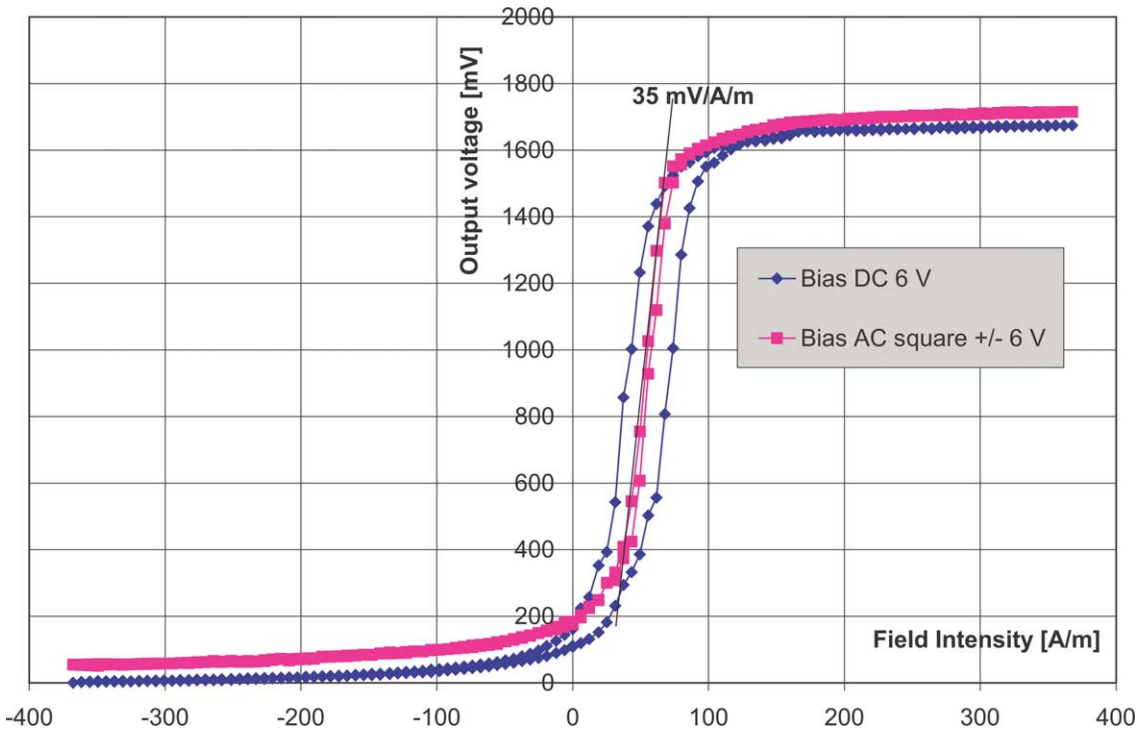

Fig. 5. Comparison of dc and ac biased NVE SDT sensor.

range, and the noise p–p value estimated from the lower diagram of Fig. 5 is about 13 mA m^{-1} (16 nT). Hence, the dc biased SDT sensor exhibits very good noise parameters.

In the case of ac square-wave biased SDT sensor, the single sensor noise PSD value is of 15 μV $\sqrt{Hz}$ @ 1 Hz, what corresponds to approx. 4 mA m^{-1} (5 nT) RMS $\sqrt{Hz}$ @ 1 Hz in the most sensitive range. The noise rms value is of 10 mA m^{-1} (12 nT) in the 100 mHz to 10 Hz frequency range, and the estimated noise p–p value here was about 40 mA m^{-1} (50 nT).

It can be seen that the linearity error and hysteresis of the SDT sensor can be significantly suppressed by means of the squarewave ac biasing. On the other hand, the noise parameters of the sensor have worsened in this case.

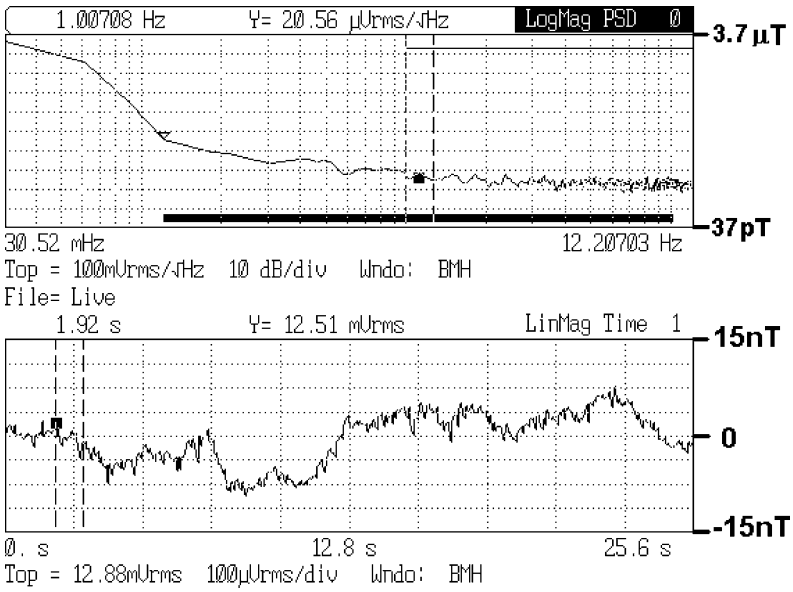

Fig. 6. The noise of the dc-biased NVE SDT sensor. (Upper trace) Noise PSD RMS value (scale log 10 dB div^{-1}), (lower trace) time record of the sensor output (scale line: 3.75 nT div^{-1}).

5. Conclusion

Our research has shown that alternating orthogonal biasing of an SDT sensor can make some improvements of its properties. The hysteresis is significantly reduced for the squarewave ac biasing in comparison to the dc biasing of the respective value. Also, the linearity error is smaller in the case of the ac biasing.

Owing to the small noise levels of the SDT sensors (single sensor noise PSD value $\sim 600\,\mu A\,m^{-1}$ (750 pT) RMS $\sqrt{Hz}$ @ 1 Hz for the dc biasing), a high sensitivity, and their rapid technological development [8], they are likely to find use in weak field measurements in the future.

References

[1] J.S. Moodera, L.R. Kinder, T.M. Wong, R. Meservey, Large magnetoresistance at room temperature in ferromagnetic thin film tunnel junctions, Phys. Rev. Lett. 74 (16) (1995) 3273–3276.
[2] T. Miyazaki, N. Tezuka, Giant magnetic tunneling effect in Fe/Al3O3/Fe junction, J. Magn. Magn. Mater. 139 (3) (1995) 231–234.
[3] M. Tondra, J.M. Daughton, D. Wang, R.S. Beech, A. Fink, J.A. Taylor, Picotesla field sensor design using spin-dependent tunneling devices, J. Appl. Phys. 83 (11) (1998) 6688–6690.
[4] M. Tondra, J.M. Daughton, C. Nordman, D. Wang, J. Taylor, Micromagnetic design of spin-dependent tunnel junctions for optimized sensor performance, J. Appl. Phys. 87 (9) (2000) 4679–4681.
[5] H. Hauser, M. Tondra, in: P. Ripka (Ed.), Magnetic Sensors and Magnetometers, first ed., Artech House Publishers, London, 2001, Chapter 4.2.2, pp. 152–162.
[6] S. Tumanski, Thin Film Magnetoresistive Sensors, first ed., Institute of Physics Publishing, Bristol, 2001, pp. 202–204.
[7] Jan Kubik, Michal Vopalensky, Automated MR sensor measurement, Poster 2002 International Student Conference, CTU-FEE, Prague, 2002, Section EI14.
[8] J.L. Prieto, N. Rouse, N.K. Todd, D. Morecroft, J. Wolfman, J.E. Evetts, M.G. Blamire, Integrated magnetic field sensor based on magnetoresistive spin valve structures, Sens. Actuators A: Phys. 94 (1–2) (2001) 64–68.

Biographies

Michal Vopálenský received an Ing. degree (equivalent to MSc) in 2002 at the Faculty of Electrical Engineering at the Czech Technical University in Prague, Czech Republic. Immediately he began to study for his PhD degree at the Department of Measurement at the mentioned faculty under the supervision of Prof. Pavel Ripka. During his Pre-Graduate study, he stayed for 6 weeks at the Milwaukee school of Engineering, Wisconsin, USA (2000) and for 4 months studying under the supervision of professor Hans Hauser at the Vienna University of Technology (2001). From February 2003, he was supported by the government of United States of Mexico to make a research on magnetoresistive materials at the National University of Mexico, Mexico City. At the Czech Technical University, he taught as a supervisor in the subjects of sensors and transducers, contactless measurements, electrical measurements and analog signal preprocessing. His research interests are magnetic sensors and magnetometers, especially the anisotropic magnetoresistive sensors, giant magnetoresistors and spin dependent tunneling sensors. At the time, he is an author or co-author of 18 papers.

Pavel Ripka received an Ing. degree in 1984, a CSc (equivalent to PhD) in 1989, Professor degree in 2001 at the Czech Technical University, Prague, Czech Republic. He works at the Department of Measurement, Faculty of Electrical Engineering, Czech Technical University as a lecturer, teaching courses in electrical measurements and instrumentation, engineering magnetism and sensors. His main research interests are magnetic measurements and magnetic sensors, especially fluxgate. A stay at the Danish Technical University (1991–1992) was a milestone is his scientific career. He is an author of more than 120 papers and five patents. He is a member of IEEE, Elektra society, Czech Metrological Society, Czech National IMEKO Committee and Eurosensors Steering Committee. He serves as an Associate Editor of the IEEE Sensors Journal. He was a General Chairman of Eurosensors 2002 Conference.

Jan Kubík received an Ing. degree (MSc equivalent) in March 2003. He is currently a PhD student under Prof. Pavel Ripka at the Faculty of Electrical Engineering of Czech Technical University in Prague. He spent altogether 4 months in 2001 and 2002 at the Power Electronics Research Center in Galway, Ireland, under the supervision of Prof. W.G. Hurley where he participated in magnetic sensors research project. His research interests include magnetic sensor (magnetoresistive and fluxgate) properties testing, precise applications of magnetic sensors and measurement systems development.

Mark Tondra Research Program Manager at NVE Corp. working with Czech Technical University in Prague on the development and testing of spin dependent tunneling sensors. He received a BS from the University of Wisconsin-Madison in 1989 and a PhD in physics from the University of Minnesota in 1996. At NVE, he is currently working on projects for the development of spin-dependent tunneling memory and magnetic field sensors, magnetic bead-based biological assays, magnetometers, and related electronics systems. His technical expertise includes magnetism, magnetoresistive thin film development, and fabrication process development.

[40] Hauser H., Fulmek P. L., Haumer P., Vopalensky M., Ripka P.: Flipping field and stability in anisotropic magnetoresistive sensors. *Sensors and Actuators A, Vol. 106, Iss. 1-3 (2003), 121-125*

Available online at www.sciencedirect.com
SCIENCE DIRECT®
Sensors and Actuators A 106 (2003) 121–125
SENSORS AND ACTUATORS A PHYSICAL
www.elsevier.com/locate/sna

Flipping field and stability in anisotropic magnetoresistive sensors

H. Hauser[a,d,*], P.L. Fulmek[a,b], P. Haumer[a], M. Vopalensky[c], P. Ripka[c]

[a] *Vienna University of Technology, Austria*
[b] *Christian Doppler Laboratory for Automotive Measurement Research, Austria*
[c] *Prague University of Technology, Prague, Czech Republic*
[d] *Siemens AG Erlangen, CTMM1, Germany*

Abstract

Switched-capacitor flipping circuits developed for Philips KMZ51 and KMZ52 anisotropic magnetoresistance (AMR) sensors give up to 2.8 A/1 kHz current peaks. Such unusually high current deeply saturates the sensor and thus removes hysteresis, reduces noise, and increases the resistance against field shocks. These necessary strong flipping fields are predicted by the energetic model (EM), applied to the magnetization reversal in thin films. The EM parameters have been correlated to microscopic variables, revealing the field dependence of the speed of magnetization reversal. This is responsible for the value of the critical switching field (and therefore for the stability of the AMR sensor) in the easy axis directions, depending on the saturating field amplitude.

Keywords: Anisotropic magnetoresistive sensors; Hysteresis model; Thin permalloy films; Direction dependence; Field reversal

1. Introduction

Magnetoresistive sensors, based on the anisotropic magnetoresistance (AMR) effect, are replacing Hall sensors in many industrial applications, as they are much more sensitive than any semiconductor sensor [1]. Philips KMZ sensors consist of patterned NiFe thin film structures in a Wheatstone bridge configuration equipped with Barber-pole structures for output linearization [2]. As periodic flipping by a perpendicular field improves stability and reduces hysteresis [3,4], the Philips KMZ51 and KMZ52 sensors have built-in flat flipping and feedback (compensation) coils so that they are ideally suited for magnetometers [2].

2. Experimental

We have built a simple single-axis magnetometer using a KMZ51 sensor. The sensor bridge is supplied by 3 mA current source to minimize the temperature coefficient of sensitivity. Switched-capacitor flipping circuits give up to 2.8 A/1 kHz current peaks. Such a unusually high current deeply saturates the sensor and thus removes hysteresis and increases the robustness against field shocks. The flipping pulse shape was optimized with respect to allowable heating of the sensor chip (50 mW absolute limit).

The flipping procedure optimizes the output signal/noise ratio. The reference pulses for the detector wait until the sensor output stabilizes after the flipping, avoiding the most noisy interval. The flipping current pulse is shown in Fig. 1. The current pulse peak value is 2.8 A, exceeding the manufacturer's recommended and maximum allowed values of 1 and 1.5 A, respectively. Due to the short pulse duration, the total power loss in the flipping circuit of the sensor is less than 10 mW.

The open-loop magnetometer linearity error is below 0.2% in the $\pm 200\,\mu$T range as shown in Fig. 2. As the Earth's field magnitude is usually about 50 μT, this range is sufficient for compass applications and monitoring of the Earth's field variations and anomalies. A further increase of the instrument range and a linearity of 0.04% was achieved using feedback compensation by the integrated coil. The most important advantage of using feedback compensation is that the temperature coefficient of the sensors' sensitivity is reduced from 0.25 to 0.01%/K, which is a typical temperature coefficient of the field factor of the compensation coil. The temperature coefficient of the sensor offset is about 10 nT/K.

The magnetometer noise has been measured both in frequency and time domain: the noise spectrum density was $30\,\mu\text{V}/\sqrt{\text{Hz}}$ at 1 Hz corresponding to $2\,\text{nT}/\sqrt{\text{Hz}}$ at 1 Hz, the rms level in the 100 mHz to 10 Hz frequency range was 7 nT and noise p–p value was approximately 15 nT.

* Corresponding author. Tel.: +43-1-58801-36614; fax: +43-1-58801-36695.
E-mail address: hans.hauser@tuwien.ac.at (H. Hauser).

0924-4247/$ – see front matter © 2003 Elsevier B.V. All rights reserved.
doi:10.1016/S0924-4247(03)00148-1

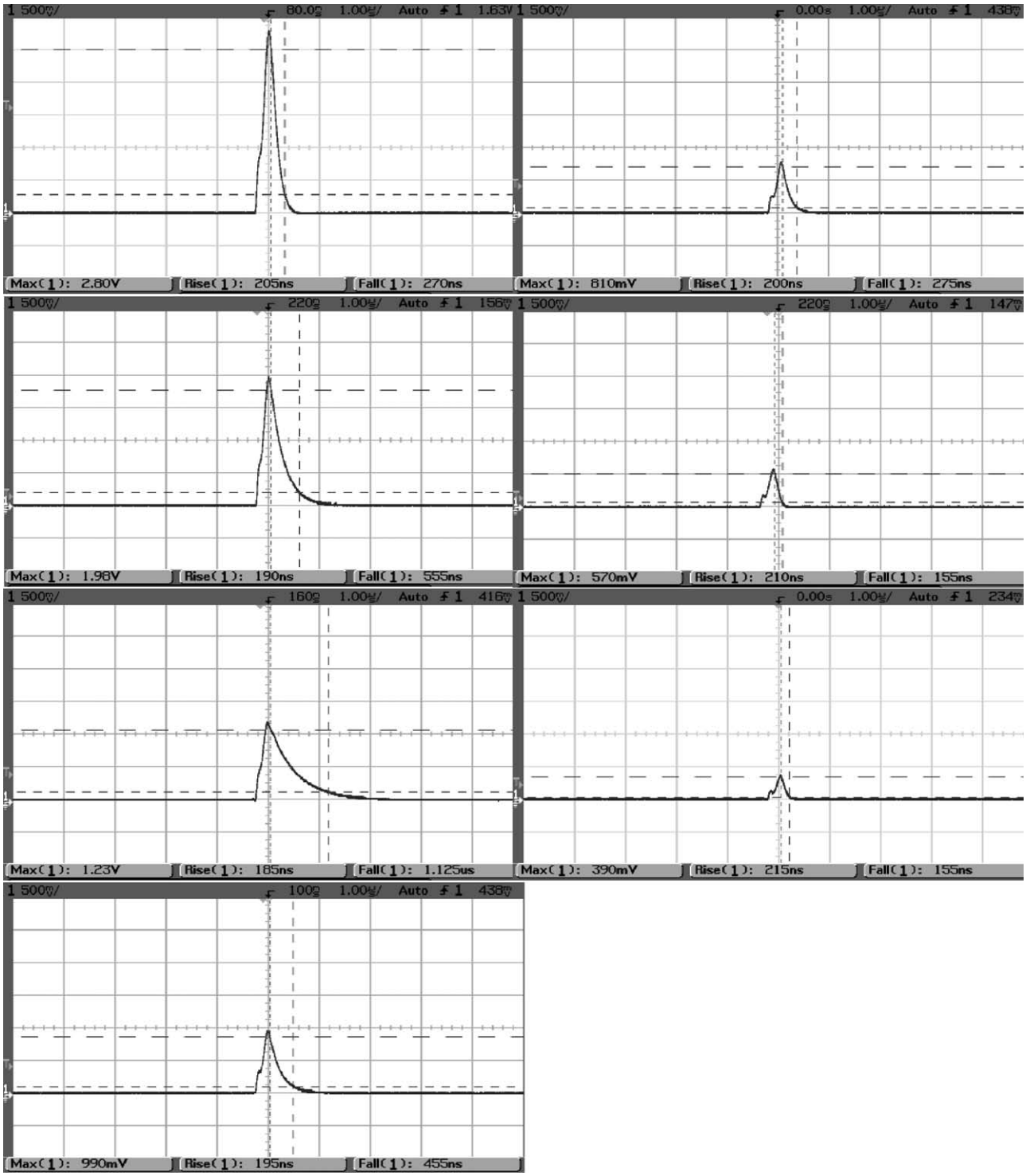

Fig. 1. Flipping current pulse (500 mA/division) vs. time (500 ns/division).

These values are only slightly higher than the sensor noise itself [2]. Fig. 3 shows the dependence of sensor stability and noise in dependence on the peak flipping current, exhibiting no significant increase of the performance beyond 2.8 A.

3. Energetic model

The need for strong flipping fields can be predicted by the energetic model (EM) [5], applied to magnetization reversal in thin films. Recently, the EM parameters have

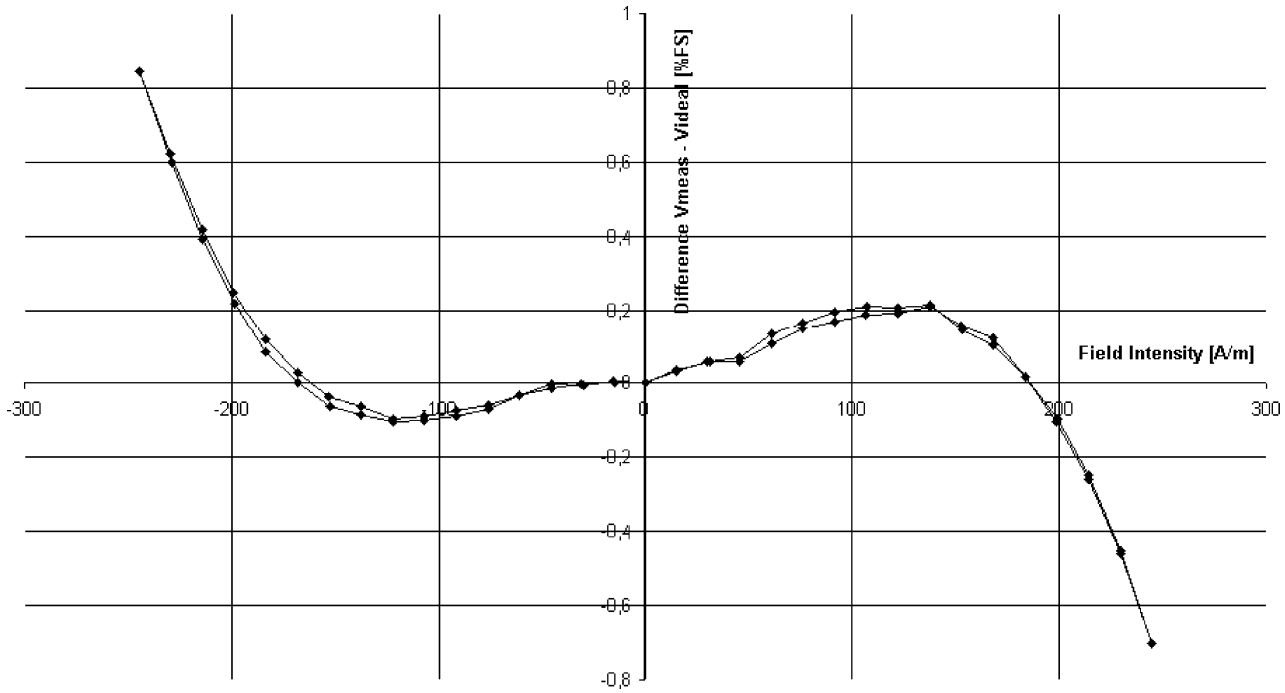

Fig. 2. Linearity error vs. B of the open-loop AMR magnetometer.

been correlated to microscopic variables, revealing the field dependence of the speed of magnetization reversal. This is responsible for the value of the critical switching field (and therefore for the stability of the sensor) in the easy axis directions, depending on the saturating field amplitude.

3.1. Hysteresis equations

The hysteresis of magnetization M depending on the applied field H is described by the following equations, where M_s is the spontaneous magnetization and using the geometrical demagnetizing factor N_d, reversible energy parameters g (related to anisotropy) and h (related to saturation field), irreversible energy parameters k (related to magnetization reversal losses) and q (related to pinning/anisotropy), and the microscopic constant c_r of reversal speed, where the sgn(x) function provides the correct four quadrant calculation (with the related magnetization $m = M/M_s$):

$$H = H_d + \mathrm{sgn}(m)H_R + \mathrm{sgn}(m - m_o)H_I. \quad (1)$$

The first term of Eq. (1) describes linear material behavior, using the demagnetizing field

$$H_d = -N_d M_s m, \quad (2)$$

the second term represents non-linear behavior using the reversible field

$$H_R = h[(1+m)^{1+m}(1-m)^{1-m})^{g/2} - 1], \quad (3)$$

including saturation at a field $H_s(M_s)$, and the third term describes hysteresis effects like initial susceptibility χ_0, remanence M_r, coercivity H_c, static losses, and accommodation, using the irreversible field

$$H_I = \left(\frac{k}{\mu_0 M_s} + c_r H_R\right)\left[1 - \kappa \exp\left(-\frac{q}{\kappa}|m - m_o|\right)\right]. \quad (4)$$

For the initial magnetization, beginning with $M = 0$, $H = 0$, we set $m_o = 0$ and $\kappa = 1$. The function κ describes the influence of the total magnetic state at points of magnetization reversal. Therefore, κ (old value κ_o) depends on the unit magnetization reversals $s = |m - m_o|$ up to this point of field reversal (m_o is the starting value of m at the last field reversal) with the simplification $e^{-q} \ll 1$:

$$\kappa = 2 - \kappa_o \exp\left[-\frac{q}{\kappa_o}|m - m_o|\right]. \quad (5)$$

The calculation always starts with the initial magnetization curve and m is increased stepwise (the stepwidth

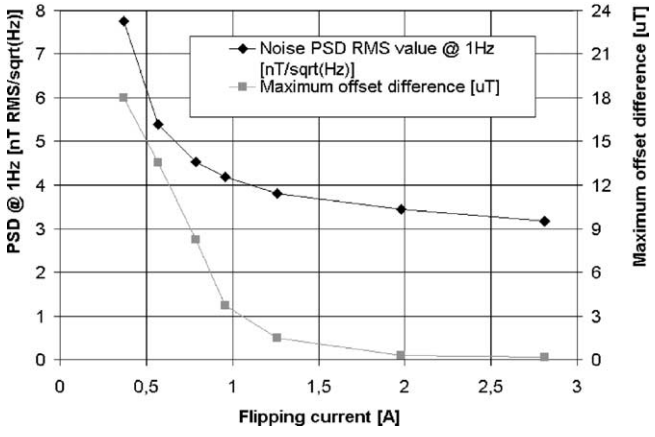

Fig. 3. Stability and noise of a KMZ sensor vs. flipping current amplitude.

determines the desired resolution of the calculation), which gives the corresponding field by Eq. (1). At a point of field reversal, κ is calculated by Eq. (5) and m_o is set to the actual value of m at this point. Then m is decreased stepwise until the next reversal point, etc.

3.2. Directional dependence

The directional dependence of the EM parameters is based on the law of approach to saturation [6] and the inner demagnetizing factor [7].

The behavior of $M(H)$ exhibits an instability at a critical field H_{cr}, where the magnetization switches from one easy direction anti-parallel to H into the easy direction parallel to H. This can be used for identification of c_r by H_{cr} and the magnetization $m_{cr}(H_{cr})$.

4. Calculations

The model parameters are identified with the magnetization curve of the sensor's permalloy film by measuring the output voltage versus applied field without compensation and flipping. The anisotropy field is determined to $H_k \approx H_{cr} = 940$ A/m and for Ni81/Fe19 permalloy we find $\mu_0 M_s = 1.01$ T. N_d is estimated to be zero and the other parameters g, h, k, and q are identified from magnetooptic Kerr-effect measurements of the hysteresis loops in the easy and hard axis directions of a thin permalloy film of similar geometry. The relevant values are hard axis coercivity $H_c = 20$ A/m, easy axis initial susceptibility $\chi_0 = 10$, reduced magnetization $m_m = 0.999$ at $H_m = 1500$ A/m, reduced remanence $m_r = 0.94 = m_g$ at $H_g = 1000$ A/m (magnetization and field at the knee of the hysteresis loop), and $c_r = 1.5$ which is mainly responsible for the difference between H_c and H_{cr} in the easy axis direction. Details of the identification procedure are described in [7].

Fig. 4 shows the calculated hysteresis loops of the permalloy film for different maximum fields. The peak magnetization has been increased for each branch and the corresponding field has been calculated by Eq. (1). The maximum field H_m of the diagram corresponds to a peak flipping current of 300 mA. But the maximum critical field $H_{cr} \approx 940$ A/m is obtained at about 2.8 A.

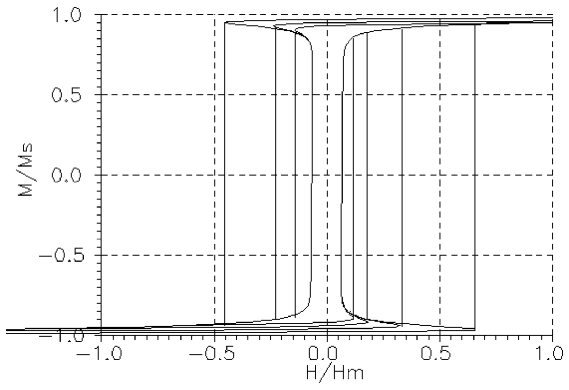

Fig. 4. Calculated easy axis hysteresis loops of a thin permalloy film: $H_m = 1500$ A/m, peak magnetizations m are 0.94, 0.95, 0.96, 0.97, 0.98, 0.99, and 1.0, respectively.

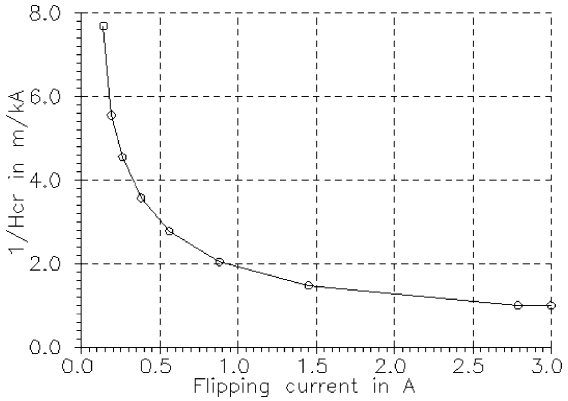

Fig. 5. $1/H_{cr}$ vs. flipping current, taken from Fig. 4.

Fig. 5 shows the dependence of H_{cr} on the flipping current amplitude in evaluation of Fig. 4. This plot can be compared to Fig. 3, showing a good correlation between noise and $1/H_{cr}$.

5. Discussion

Both noise and stability strongly depend on the uniformity of the AMR film magnetization. Due to the non-ellipsoidal geometry, the demagnetizing fields will cause small domain structures, especially in the corners of the film [8]. These domains will not perform a coherent rotation of magnetization in an applied field parallel to the hard axis direction. Moreover, they can be the nucleus of additional domain wall displacements.

Although contributing only little to the total magnetization, these regions can be saturated only with very strong fields: $m = 0.999$ at $H = 1500$ A/m, but total saturation is reached at $H_s = 14$ kA/m in our simulation. This explains the need of high current amplitudes. The duration of the pulse can be very short as long as eddy currents do not reduce the pulse field amplitude, thus providing a total loss power below the allowed limit.

The negative differential susceptibility regions depicted in Fig. 4 represent the field range, where the applied field could be reduced at still proceeding magnetization reversal (instability). The measured hysteresis loop can be obtained by drawing a straight line parallel to the M axis from the points where $dH/dM = 0$. The intersection of this line with the H-axis gives the measured easy axis "coercivity" (which is the critical field); it does not depend on the maximum field as strongly as shown in Fig. 4, which has been exaggerated to some extent in order to visualize the effect. But this does not affect the qualitative function shown in Fig. 5 and the conclusions.

6. Conclusions

The nominal critical field H_{cr} and the corresponding stability can be achieved only if the film is deeply saturated ($m_m = 1$). This is achieved by high but short flipping current pulses. In the case of lower maximum magnetization, H_{cr} is decreased, causing increased instability and noise.

These current amplitudes can be predicted by the EM, using M_s, N_d, and four parameters g, h, k, and q. Although these parameters allow the phenomenological simulation of magnetization curves, they can furthermore be related to the anisotropy energy by microscopic, dimensionless constants [7]. Thus, it is also possible to calculate the directional dependence of the hysteresis.

Acknowledgements

This work was carried out under the top priority *Sensors and Packaging* of the Faculty of Electrical Engineering and Information Technology at the Vienna University of Technology. The authors are indebted to Prof. Gerhard Fasching for making this work possible and to Thomas Zottl for technical assistance.

References

[1] P. Ripka (Ed.), Magnetic Sensors and Magnetometers, Artech, Boston, 2001.
[2] P. Ripka, J. Appl. Phys. 79 (1996) 5211.
[3] P. Ripka, G. Vertesy, J. Magn. Magn. Mater. 215–216 (2000) 795.
[4] Philips Semiconductors Data Handbook SC17: Semiconductor Sensors, Accessible at: http://www.semiconductors.philips.com.
[5] H. Hauser, J. Appl. Phys. 75 (1994) 2584.
[6] S. Chikazumi, Physics of Magnetism, Wiley, New York, 1964.
[7] H. Hauser, Magnetic hysteresis modeling for sensor applications, Sens. Actuators A 106 (2003) 84–90.
[8] J. McCord, A. Hubert, G. Schröpfer, U. Loreit, IEEE Trans. Magn. 32 (1996) 4806.

[41] Platil A., Vopálenský M., Ripka P., Kašpar P., Hauser H.: Improvement of AMR Magnetometer Precision. *Eurosensors XVI - Proceedings, Prague, 2002, 612-613*

Improvement of AMR Magnetometer Precision

A. Platil[1], M. Vopálenský[1], P. Ripka[1], P. Kašpar[1], H. Hauser[2]
[1]Czech Technical University, Technicka 2,
166 27, Prague 6, Czech Republic, platil@feld.cvut.cz
[2] TU Wien, Gusshausstrasse 27-29, Wien, Austria

SUMMARY

A magnetometer employing the Philips KMZ 51 AMR sensor has been developed. The achieved parameters (using flipping and feedback compensation) comprise linearity error of 0.04 % measured in the +/- 200 A/m range. The temperature coefficient of the sensor sensitivity has been reduced to 0.01 % / K. The temperature coefficient of the sensor offset is about 10 nT / K. The dependence of the sensor noise and offset stability on the flipping pulse amplitude was measured.

Keywords: magnetic sensors, AMR, magnetometers

Subject category: 4 - Magnetic sensors

INTRODUCTION

In many industrial application areas, the AMR (Anisotropic Magneto-Resistance) sensors [1] are increasingly replacing Hall sensors [2]. Modern AMR sensors (typically in the full Wheatstone - bridge configuration) use barber-pole and flipping techniques to improve their linearity, stability, hysteresis etc. The Philips KMZ51 and KMZ52 [3] sensors have built-in flat flipping and feedback (compensation) coils and thus they are ideally suited for magnetometers.

MAGNETOMETER DESIGN

A simple magnetometer was developed using KMZ51 sensor. The magnetoresistive bridge is supplied from a 3 mA current source so that the temperature coefficient of sensitivity is minimized. The switched-capacitor flipping circuit gives current peaks of up to 2.8 A @ 1 kHz. Thanks to a relatively high current, the sensor is deeply saturated and thus the influence of hysteresis is suppressed and the resistance against field shocks of any direction is improved. The flipping pulse shape was finely tuned using the energetic model applied to magnetization reversal in thin film [4] with respect to heating of the sensor chip.

The bridge output voltage is processed using a preamplifier and a synchronous detector. The controlling pulses (see Fig. 1) driving the synchronous detector are distributed in time in the manner that effectively suppresses the unwelcome transients from flipping [5]. (The post-flip settlement period is ignored and thus the noisiest interval in the signal is not detected.) The timing is controlled by a simple microprocessor.

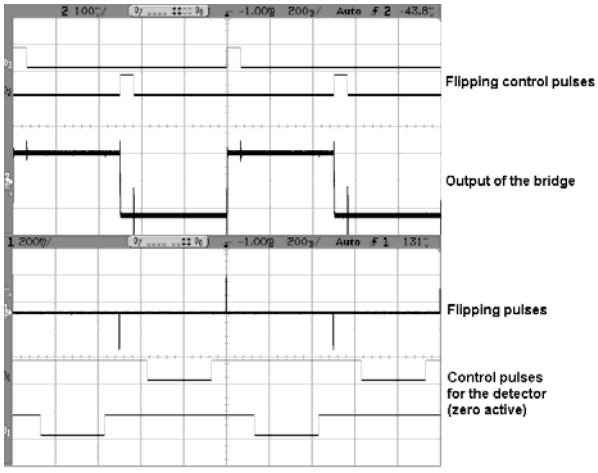

Fig. 1: *The flipping pulses (2.8 A peak value), the synchronous detector controlling pulses, and bridge voltage for the magnetic field 40 μT [6].*

ACHIEVED PARAMETERS

The hysteresis and linearity error of the sensor (without flipping or compensation) is approximately 0.4 % Full Scale (FS ~ +/- 200 A/m). With the flipping pulses of 2.8 A peak value, the hysteresis is reduced below 0.025 % FS, with the linearity error below 0.2 % FS. An improvement of the instrument range and linearity can be achieved using feedback compensation by the on-chip-integrated coil. In this case, a linearity error of 0.04 % was measured in the +/- 200 A/m range.

INFLUENCE OF THE FLIPPING

The influence of the flipping pulse amplitude on the noise parameters and on the offset stability was measured. The sensor was placed into a six-layer permalloy magnetic shielding, so that the influence of an external magnetic field was minimized. Firstly, the sensor noise has been measured. The sensor was

flipped manually (by a single pulse) with decreasing amplitude of the pulse. The noise was measured using Stanford Research SR770 FFT spectrum analyzer. For flipping pulse amplitude of 2.8 A, the noise PSD was 3.2 nT / √ Hz @ 1 Hz.

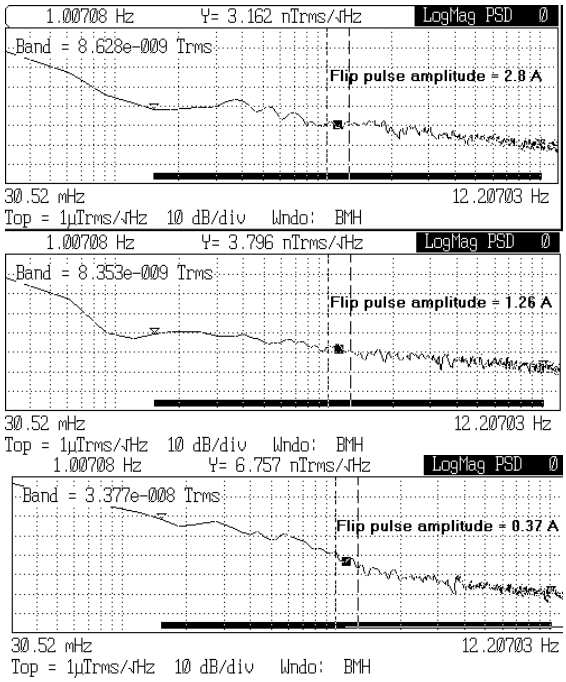

Fig. 2: *The noise spectra for 2.8 A, 1.26 A and 0.37 A flipping pulse amplitude.*

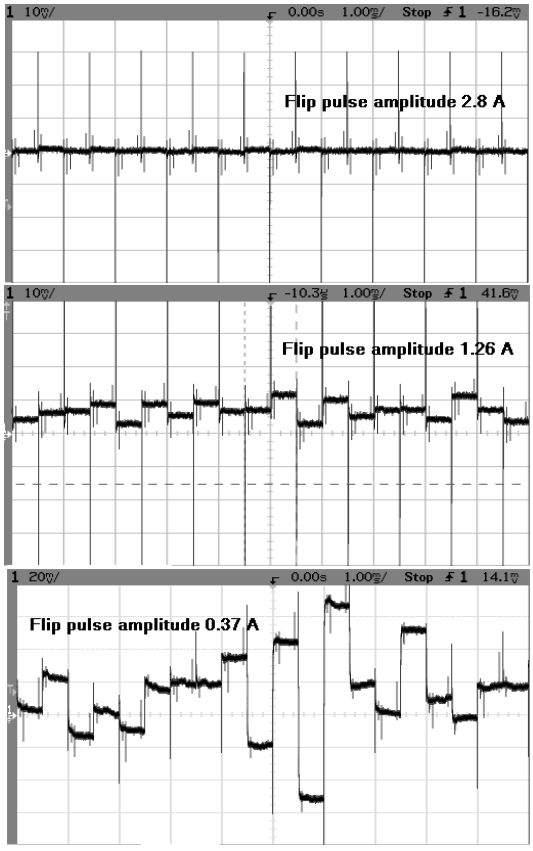

Fig. 3: *The offset variance for flipping pulse amplitude of 2.8 A, 1.26 A and 0.37 A (the scale is 10 mV, 10 mV, and 20 mV/div).*

The noise rms value was about 8.6 nT in the 100 mHz to 10 Hz frequency range and the noise peak to peak value was about 35 nT. For lower values of the flipping current peak, the noise increases as shown in Fig. 2.

It was observed that the offset of the sensor strongly depends on the flipping pulse peak value. If the pulse amplitude is not sufficient, the sensor output does not settle to the same value as that before the pulse. The variance of settled offset values between flipping pulses decreases with pulse amplitude as shown in Fig. 3 and 4.

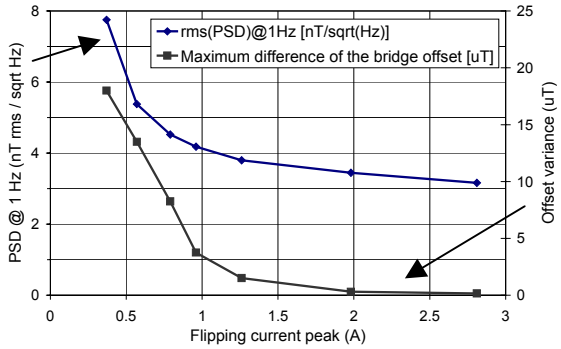

Fig. 4: *The dependence of noise level and offset variance on flipping pulse amplitude.*

CONCLUSION

The precision of an AMR magnetometer can be significantly improved by using optimized flipping pulses that remove perming and reduce hysteresis by a factor of 20. Preferable detection technique gates the sensor signal during and shortly after the flipping period. By ignoring these noisy intervals the sensor stability is improved over standard AMR magnetometers which either use flipping reversals with low repetition rate or symmetrical waveform and classical synchronous detection. The improved AMR magnetometer has 10 nT resolution and 100 nT precision, which is sufficient for many applications dominated by fluxgate sensors. A disadvantage of the described techniques is increased power consumption.

REFERENCES

[1] S. Tumanski: Thin film magnetoresistive sensors. IoP Publ. 2001, ISBN 0750307021.
[2] P. Ripka (ed.), Magnetic sensors and magnetometers, Artech H. 2001, ISBN 1580530575.
[3] Philips Semiconductors Handbook SC17: see http://www.semiconductors.philips.com
[4] H. Hauser: Energetic model of ferromagnetic hysteresis, *J. Appl. Phys.* 75 (1994) 2584.
[5] P.Ripka et.al.: AMR magnetometer. Proc. 15th Soft Magnetic Materials Conference, Bilbao 2001, pp. G-18. (Accepted for publ. in JMMM.)
[6] M. Vopálenský, P. Ripka, A. Platil: Precise magnetic sensors, Submitted to EMSA 2002, Athens

[42] Vopálenský M., Ripka P., Platil A.: Precise magnetic sensors. *Sensors and Actuators A, Vol. 106, Iss. 1–3 (2003), 38–42*

Available online at www.sciencedirect.com
SCIENCE DIRECT®
Sensors and Actuators A 106 (2003) 38–42
SENSORS AND ACTUATORS A PHYSICAL
www.elsevier.com/locate/sna

Precise magnetic sensors

Michal Vopálenský*, Pavel Ripka, Antonín Platil

Department of Measurement, Faculty of Electrical Engineering, Czech Technical University, Technicka 2, 166 27 Praha 6, Czech Republic

Abstract

Can magnetoresistors replace fluxgate sensors in precise applications such as navigation and detection of metal objects? Anisotropic Magnetoresistors (AMRs) and Giant Magnetoresistors (GMRs) can reach 10 nT resolution. It is possible to improve their stability by ac techniques, but the electronics becomes complex and consumes more power. If size is not limited, fluxgate sensors are still the winners.

Keywords: Magnetic sensors; Magnetoresistors; Magnetometers

1. Introduction

Stable and precise sensors are traditionally used for geophysical and space research magnetometers. The new military and industrial applications require precise vector magnetic field sensors, which are also rugged enough to work in hard environment, and which are resistant against temperature, mechanical and magnetic shocks, interferences, and field gradients. Precise magnetic sensors are also used for position trackers and biomagnetic measurements.

Fluxgates are the most suitable vector magnetic field sensors for applications requiring a resolution up to 0.1 nT and absolute precision of 1 nT (for station magnetometers) to 100 nT (for low-cost portable units). Only SQUIDs are more sensitive vector sensors [1]. Advances in Fluxgate technology are reviewed in [2].

Anisotropic Magnetoresistors (AMRs) and recently also Giant Magnetoresistors (GMRs) are the latest competitors of small-size fluxgate sensors. AMR bridges using barber-pole geometry are linear devices; their performance can be improved by periodical flipping. GMRs may be linearized by biasing techniques; moreover, it was recently shown that ac bias may decrease their offset, hysteresis and noise [3]. In general, commercial AMRs may have a resolution of 10 nT with sensor size of several millimeters, but their precision is limited by large temperature coefficient of sensitivity (typically 600 ppm/°C, compared to typically 50–30 ppm/°C for fluxgate), non-linearity and crossfield response. Fig. 1 shows relative temperature change of the sensitivity of low-cost fluxgate sensor produced in our laboratory. The temperature coefficient of sensitivity is 50 ppm/°C: the main source is temperature dilatation of the plastic bobbin of the feedback coil. This can be easily suppressed to 30 ppm/°C by using ceramic materials in mechanical design. As the temperature characteristics of precise fluxgate sensors are linear and show no significant hysteresis, the temperature coefficient of the sensitivity (tempco) can be compensated or numerically corrected with uncertainty of units of ppm, so that the corresponding error is much lower than temperature offset drift (typically 0.1 nT/°C).

Although magnetoresistors and fluxgates are based on completely different effects, it is necessary to periodically saturate their cores if one wants to remove perming (the offset caused by residual dc magnetization). As a result, the electronic circuits used are similar and there are no large differences in power consumption. A typical magnetometer with AMR sensor consists of the processing blocks as in Fig. 2.

In many applications the precise magnetometers work in the presence of the Earth's field (about 50 000 nT) and the measured field is in the order of 1–100 nT. In such a case the magnetometer absolute error is given by offset unstability, perming and crossfield errors of individual sensors and also by sensor head mechanical stability; sensor noise is often not critical [4].

The main drawback of fluxgate sensors is their large size: typical low-noise sensor has 20 mm diameter core. Micro-fluxgate sensors are still under development. Although they already reached nT resolution, their precision and stability is limited [5]. Magnetoresistors are the proper choice if sensor size below 5 mm is required.

* Corresponding author.
E-mail address: vopalem@fel.cvut.cz (M. Vopálenský).

0924-4247/$ – see front matter © 2003 Elsevier B.V. All rights reserved.
doi:10.1016/S0924-4247(03)00129-8

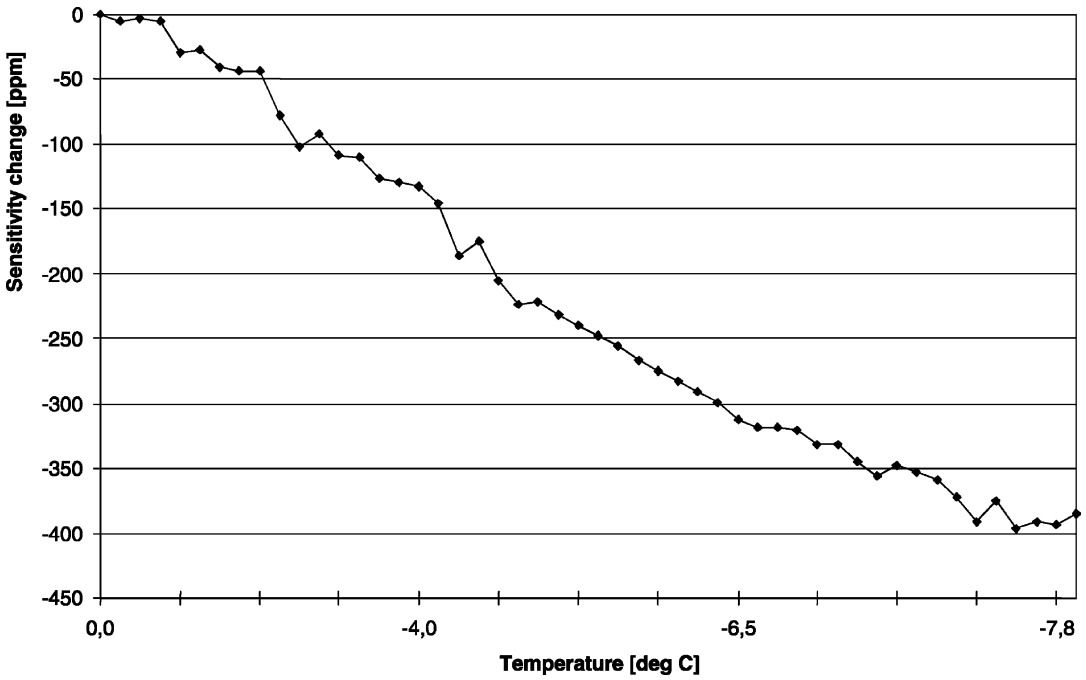

Fig. 1. Relative sensitivity change with temperature for low-cost fluxgate sensor produced by Czech Technical University.

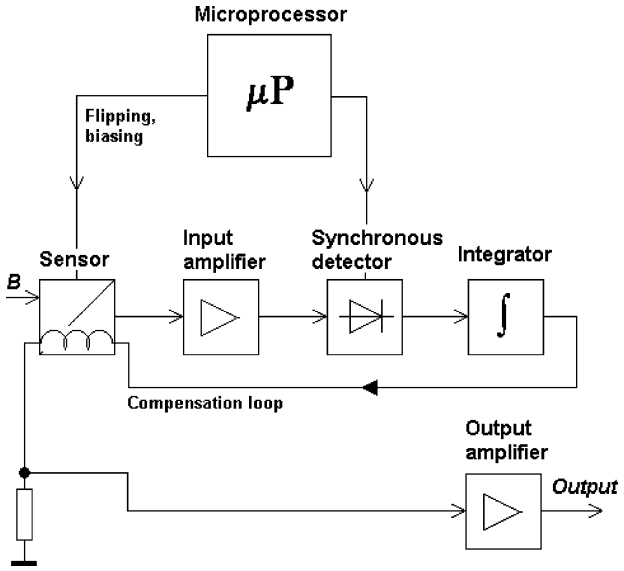

Fig. 2. A typical circuit design of a magnetometer with AMR sensor.

2. Anisotropic magnetoresistors

In the last decade, the utilization of the AMRs in the function of reading heads for hard disk drives has significantly boosted their development.

The resistivity of a Permalloy (Py) stripe depends on the angle between its magnetization and the current flowing through [1]. Since this basic arrangement would not give us the information about the orientation of the applied field, the so-called “Barber poles” design has been developed.

When four AMR elements are configured as a complementary full Wheatstone bridge, the change of the magnetization M direction causes reversion of the output characteristic. Actually, the M has two stable states parallel to the longitudinal direction of the Py strip. We can even switch, or “flip”, between those two stable states of the sensor. The typical value of the strip magnetization is about 300 A/m. When we create a field of greater intensity in the opposite direction, the magnetization vector M changes its direction and the sensor switches to the second stable state. This technique is referred to as “flipping”. When we use sensors with implemented Barber poles connected to a bridge, the periodical flipping causes the change in the output signal polarity, and the resulting ac output signal can be conveniently separated from the offset. The acting field in the “positive” direction (plus the offset) is measured in one half of the cycle, while this field in the “negative” direction (plus the offset) is measured in the second half of the cycle. This results in two different outputs positioned symmetrically around the offset value. After a high-pass filtering we can obtain the offset-free ac signal, which should be demodulated by a synchronous demodulator to recover the measured signal [6].

The synchronous detection would be possible even if the bridge were supplied with an alternating signal. However, the flipping technique has another advantages: suppression of the hysteresis and perming. The flipping frequency is not critical, but there are some parameters of the sensor that can determine its choice. The material does not change its properties in a zero time. The instabilities result in glitches and transients in the immediate time after the flipping pulse. Therefore, we developed the microprocessor-controlled

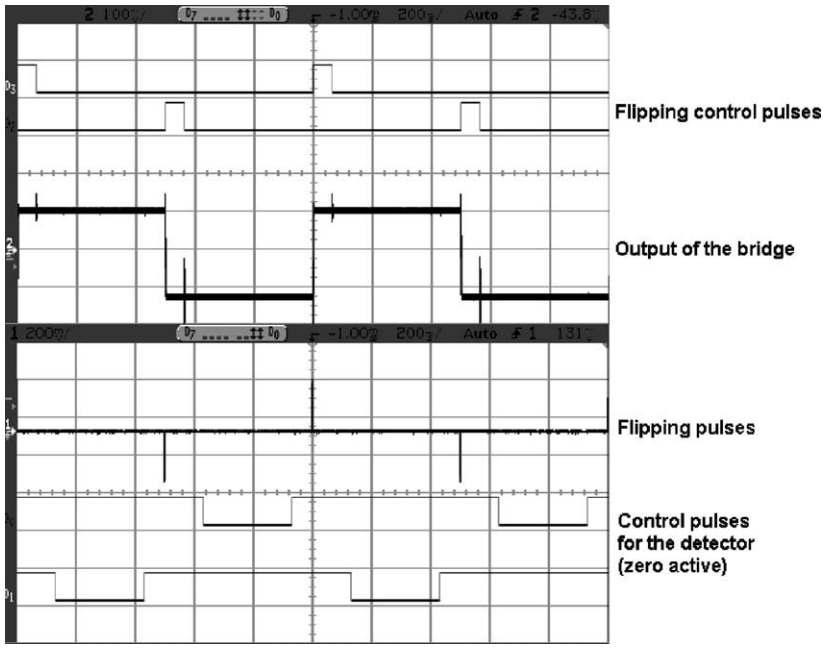

Fig. 3. Timing of the AMR flipping.

timing, which ignores the short areas after the flip and the synchronous detection is applied just to the stable areas of the output by means of a gated integrator (sample-hold circuit). The whole timing can be seen in Fig. 3.

To suppress the temperature sensitivity drift, the AMR sensors can be operated in the feedback compensation mode. For this purpose, another coil is integrated on chip, producing the field in the sensitive axis direction. Using proper electronic processing circuits, a negative feedback can be formed, which produces the field of the same amplitude but the opposite direction to the measured one in the compensation coil. Thus, the overall field acting to the sensor is zero and the sensor operates always near to the zero point, where the influence of the sensitivity drift is minimized.

3. Experiments with AMR

We performed experiments with the AMR sensor of the KMZ 51 type, produced by Philips company. We developed a universal evaluation board for the magnetoresistive sensors, which supports, among others, the KMZ 51 magnetoresistor. The flipping was performed by the switched capacitor, as recommended in [6]. The further processing of the output modulated square wave signal has been done by a gated integrator. In this procedure, the short unstable areas with transients immediately after the flipping pulses were ignored (see Fig. 3). The flipping frequency was of 1 kHz.

With this arrangement, we reached the linearity error lower than ±0.03% and the hysteresis about 0.03% in the range of ±200 μT in the feedback mode (see Fig. 4). For

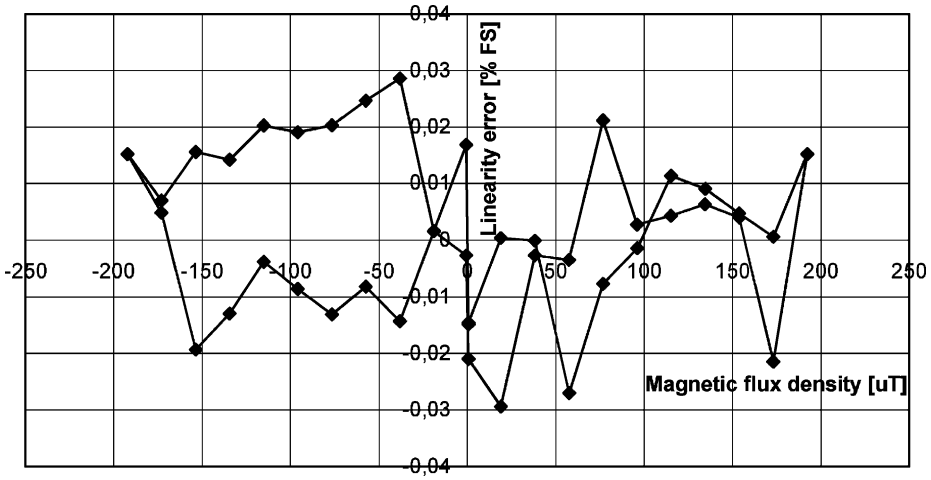

Fig. 4. Linearity error of the flipped and compensated KMZ 51 AMR sensor.

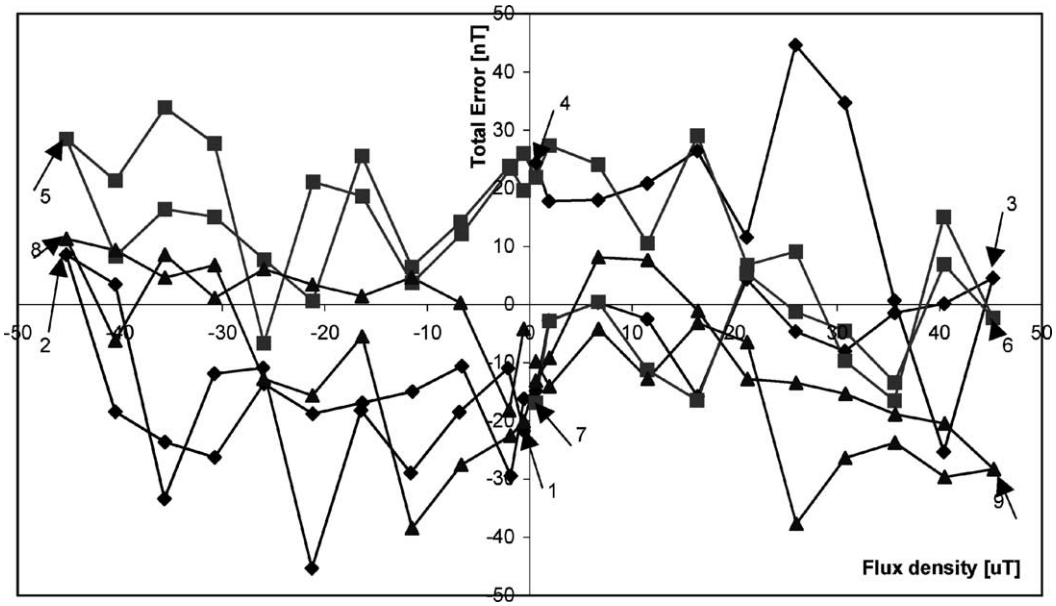

Fig. 5. Linearity error of the flipped and compensated KMZ 51 AMR magnetometer in the range used for compass applications.

comparison, the linearity error of the single sensor is about 0.3% and the hysteresis is almost of the same value in the range of ±200 μT. Using flipping without the feedback compensation, the hysteresis becomes reduced, but the linearity error stays almost unchanged. The sensitivity of the AMR sensor is about 16 mV/(V kA m) up to the field value of ±400 A/m. The important range for the compass application is ±60 μT, as this value is the value of the magnetic field of the Earth at poles. We have measured the behavior of our magnetometer in the range of ±45 μT and we figured out that the total error of the device lies in the range of ±50 nT (Fig. 5).

We have verified that the noise and offset stability of the sensor depend on the flipping pulse amplitude [7]. The higher is the amplitude of the flipping pulse, the smaller is the noise and the better is the offset stability. For the highest pulse amplitude of ±2.8 A, the noise PSD value has been of 3.2 nT/Hz$^{1/2}$ RMS at 1 Hz (Fig. 6). The noise rms value in this case is about 8.7 nT in the 100 mHz to 10 Hz frequency range and the noise p–p value is about 35 nT. For smaller amplitudes of the flipping pulse, the noise becomes higher; e.g. for 0.37 A the noise PSD value is of 6.8 nT/Hz$^{1/2}$ RMS at 1 Hz.

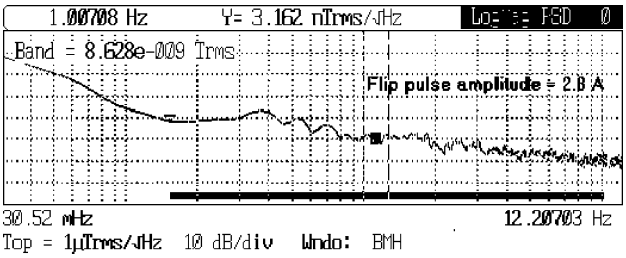

Fig. 6. Noise of the KMZ 51 sensor after flipping pulse of 2.8 A.

4. GMR and SDT magnetoresistors

The GMR effect arises mainly in thin ferromagnetic (FM) film multilayers [1,8].

To improve the sensor function, it is convenient to connect four GMR elements to the full Wheatstone bridge. However, as the GMR structures have unipolar response to the acting field, a special arrangement is needed to obtain a non-zero output. In addition, the output should vary for the opposite field direction. The behavior of this type in an unpinned sandwich or a multilayer is achieved by the parallel biasing, or sensitive axis biasing. This method is based on shifting the operating point of each leg of the measurement bridge to a suitable position on the characteristics, by means of a proper field applied in the parallel direction to the sensitive axis of the sensor [8].

Using the parallel biasing, we can operate each magnetoresistor of the bridge in a very advantageous mode of function, being at the maximum slope of its R versus H characteristic. In this point the sensitivity is the highest. The necessary biasing field can be produced by a well-designed on-chip flat coil. When we reverse the biasing current and thus the biasing field, also the R versus H characteristic of the bridge becomes inverted.

5. Experiments with GMR

We worked with the GMR sensor from the American company NVE Corp. (formerly Non-Volatile Electronics), whose internal structure is unpinned sandwich. The sensor has integrated a biasing coil, allowing the parallel biased mode of the sensor function. Differently from [3], we used the square wave signal at 1 kHz as the biasing signal. The configuration of the detection circuit was the same as in

the experiment with the AMR sensor, since we have used the same instrument. However, the timing of GMR biasing current should be different: while AMR flipping pulses are short and come before the measuring interval, GMR biasing current is either dc or square wave, and it should be on during the whole measuring time.

Firstly, we investigated the influence of the dc biasing field value to the characteristic of the sensor. The higher is the dc bias, the better is the linearity of the sensor and the smaller is the hysteresis. However, the ac square wave biasing at 1 kHz significantly improves the properties of the sensor. The maximum linearity error in the case of dc biasing is about 3%, and the hysteresis is considerably high, approx. 2% in the range of ±300 A/m. The output of the ac biased GMR sensor exhibits slightly better linearity and significantly smaller hysteresis. The maximum linearity error is about 2% and the hysteresis is reduced under 0.5% in the range of ±300 A/m in the case of square wave ac biasing.

For the noise measurement, the sensor was placed into the same shielding as in the case of AMR. The ac biased GMR sensor noise PSD value is of 37 nT/Hz$^{1/2}$ RMS at 1 Hz, the noise rms value is about 100 nT in the 100 mHz to 10 Hz frequency range and the noise p–p value is about 450 nT. Detailed results were presented in [9].

6. Experiments with SDT

Spin Dependent Tunneling (SDT) devices can exhibit a 20% magnetoresistance at room temperature, low hysteresis when the orthogonal biasing mode is applied [8], and signal-to-noise ratio of 1:1 at 1 pT [10].

The NVE SDT sensors with a pinned FM layer utilize the technique of the orthogonal biasing of the free layer to improve their properties [8]. This technique allows us to recognize the orientation of the measured field and, additionally, the characteristic of the sensor is linearized in the vicinity of the point of 90° and the sensitivity is the maximum at this point. An orthogonal biasing coil is integrated on the chip with the SDT junctions. Connecting four SDT junctions to the full bridge configuration, so-called flux concentrators, shielding two SDT elements and concentrating the field acting to the other two ones, are often used [8].

Although inverting the orthogonal biasing field does not cause the inverting of the output characteristic, we verified that the square wave biasing can lower the hysteresis and improve the linearity of the SDT sensor. We suppose the reason is that the material structure is being periodically recovered to a defined state. The ac biased SDT sensors exhibit a very large sensitivity, being of 1750 mV/(V kA m), in a narrow linear range (40–80 A/m).

The square wave ac biasing has been used in measurements of the SDT and GMR sensors from the NVE Corp. The hysteresis of these sensors can be highly suppressed by square wave ac biasing (GMR—2% by dc biasing, 0.5% by ac biasing in the range of ±300 A/m; SDT—60% by dc biasing, 12% by ac biasing in the range of ±100 A/m).

The issue of the SDT sensors and more detailed results were presented in [11].

7. Conclusion

The best linearity and hysteresis properties in a weak field range have been achieved with the flipped KMZ 51 AMR sensor operated in the compensation feedback mode (linearity error $< \pm 0.03\%$, hysteresis $\sim 0.03\%$ in the range of $\pm 200\,\mu$T). Typical offset drift of AMR sensors is 10 nT/K, sensitivity tempco is 0.25 and 0.01%/K for uncompensated and compensated sensors, respectively.

Even though the mentioned results are significantly worse compared to standard fluxgates, AMRs may serve in many applications previously dominated by fluxgates. Typical example is a compass: if 0.5° precision is sufficient, AMR is the proper choice.

GMR and SDT sensors offer higher sensitivity and, in the case of SDT, also lower noise than AMR. Unfortunately they currently cannot be used for precise applications because of their high non-linearity and hysteresis.

Acknowledgements

Thanks to Jan Kubik, who designed measurement system used for calibrations.

References

[1] P. Ripka (Ed.), Magnetic Sensors and Magnetometer, Artech House Publishers, 2001, ISBN 1-58053-057-5.
[2] P. Ripka, Advances in Fluxgate Sensors, Invited lecture to EMSA 2002, Athens (S1_INV in the Book of Abstracts).
[3] P. Ripka, M. Tondra, J. Stokes, R. Beech, AC-driven AMR and GMR magnetoresistors, Sens. Actuators A 76 (1999) 227–232.
[4] P. Ripka, W. Billingsley, Crossfield effect at fluxgate, Sens. Actuators A 81 (2000) 176–179.
[5] P. Ripka, New Directions in Fluxgate Sensors, J. Magn. Magn. Mater. 215–216 (2000) 735–739.
[6] Datasheet—Magnetic Field Sensors—General. Philips Semiconductors, http://www.semiconductors.philips.com.
[7] H. Hauser, P.L. Fulmek, P. Haumer, M. Vopalensky, P. Ripka, Prediction of flipping fields in AMR sensors, in: Proceedings of the 46th Annual Conference on Magnetism and Magnetic Materials, Seattle, USA 2001, p. 292 (Abstracts).
[8] S. Tumanski, Thin Film Magnetoresistive Sensors, Institute of Physics Publishing, 2001, ISBN 0 7503 0702 1.
[9] M. Vopalensky, P. Ripka, J. Kubik, M. Tondra, Improved GMR sensor biasing design, Eurosensors XVI, 15–18 September 2002, Prague, Section TP24, Book of Abstracts, p. 343–344.
[10] M. Tondra, J.M. Daughton, D. Wang, R.S. Beech, A. Fink, J.A. Taylor, Picotesla field sensor design using spin-dependent tunneling devices, J. Appl. Phys. 83 (11) (1998) 6688–6690.
[11] M. Vopalensky, P. Ripka, J. Kubik, M. Tondra, Alternating biasing of SDT sensors, in: Eurosensors XVI, 15–18 September 2002, Prague, Section W1A3, Book of Abstracts p. 511–512.

[43] Ripka P., Vopálenský M., Platil A., Döscher M., Lenssen K. M. H., Hauser H.: AMR magnetometer. *Journal of Magnetism and Magnetic Materials, Vol. 254 (2003), 639–641*

ELSEVIER

Journal of Magnetism and Magnetic Materials 254–255 (2003) 639–641

journal of magnetism and magnetic materials

www.elsevier.com/locate/jmmm

AMR magnetometer

P. Ripka[a,b,*], M. Vopálenský[a,c], A. Platil[a], M. Döscher[d], K.-M.H. Lenssen[e], H. Hauser[c]

[a] *Department of Measurement, Faculty of Electrical Engineering, Czech Technical University, Technicka 2, Praha 6 16627, Czech Republic*

[b] *Marie Curie fellow at the National University of Ireland, Galway, Ireland*

[c] *Institute of Industrial Electronics and Material Science, Vienna University of Technology, A-1040 Wien, Gußhausstraße 27-29/366, Austria*

[d] *Philips Semiconductors, P.O. Box 54 02 40, Hamburg D-22502, Germany*

[e] *Philips Research Laboratories, Prof. Holstlaan 4, Eindhoven NL-5656 AA, The Netherlands*

Abstract

Simple anisotropic magnetoresistance magnetometer with improved parameters was developed. New flipping circuits deliver optimized current pulse with 2.8 A amplitude. New type of signal processing uses switched integrator to avoid the most noisy time intervals. The achieved linearity is 0.2% in the $\pm 200\,\mu T$ range without feedback and 0.04% using integrated feedback coil. The magnetometer noise at 1 Hz is $2\,nT/Hz^{1/2}$, uncompensated temperature coefficient of sensitivity is $-0.25\%/K$ without the feedback and $0.01\%/K$ with feedback. Temperature offset drift is typically 10 nT/K.

Keywords: Magnetic sensors; Magnetoresistors; AMR; Magnetometry

Magnetoresistive sensors, based on the anisotropic magnetoresistance effect (AMR), are replacing Hall sensors in many industrial applications, as they are much more sensitive than any semiconductor sensor [1]. Philips KMZ sensors consist of patterned NiFe thin-film structures in a Wheatstone bridge configuration equipped with Barber-pole structures for output linearization [2]. As periodical flipping by a field perpendicular to the sensing direction improves stability and reduces hysteresis [3,4], the Philips KMZ51 and KMZ52 sensors have built-in flat flipping and feedback (compensation) coils so that they are ideally suited for magnetometers.

We have built a simple single-axis magnetometer using a KMZ51 sensor. The sensor bridge is supplied by 3 mA current source to minimize the temperature coefficient of sensitivity. Developed switched-capacitor flipping circuits give up to 2.8 A/1 kHz current peaks even from a ± 6 V voltage source. Such unusually high current deeply saturates the sensor and thus removes hysteresis and increases the resistance against field shocks of any direction. The flipping pulse shape was optimized with respect to allowable heating of the sensor chip.

These necessary strong flipping fields can be predicted by the energetic model (EM) [5], applied to the magnetization reversal in thin films. Recently, the EM parameters have been correlated to microscopical variables, revealing the field dependence of the magnetization reversal velocity. This is responsible for the value of the critical switching field (and therefore for the stability of the sensor) in the easy axis directions, depending on the saturating field amplitude. Simulations confirm that the stable response can be achieved only if the film is fully saturated by the flipping field.

The flipping current pulse train is shown in Fig. 1 (top trace). The reference pulses for the detector wait until

*Corresponding author. Department of Measurement, Faculty of Electrical Engineering, Czech Technical University, Technicka 2, Praha 6 16627, Czech Republic. Tel.: +420-2-2435-3945; fax: +420-2-3333-9929.

E-mail address: ripka@feld.cvut.cz (P. Ripka).

0304-8853/03/$ - see front matter © 2002 Elsevier Science B.V. All rights reserved.
PII: S0304-8853(02)00927-7

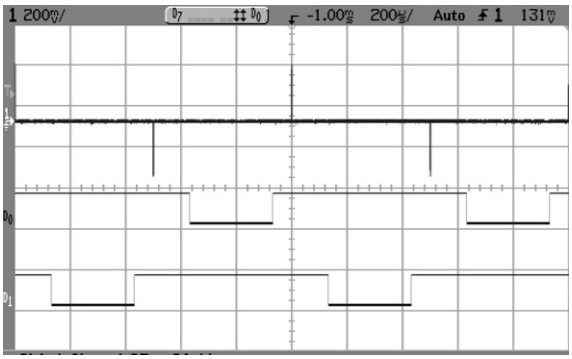

Fig. 1. Flipping current (top trace, 1 A/div), detector reference signals (middle and bottom traces, active logical low).

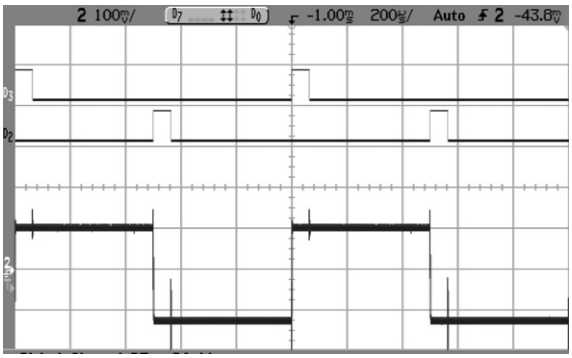

Fig. 2. Flipping control (upper and middle traces), bridge output for the measured field of 40 μT (lower trace, amplified by 10).

the sensor output stabilizes after the flipping, avoiding the most noisy interval (Fig. 1, middle and bottom traces). The bridge output is first amplified by an instrumentation amplifier and processed by a differential switching integrator. The sensor bridge output (after the instrumentation amplifier with a gain of 10) for the measured field of 40 μT (vertical component of the Earth's field) is shown in Fig. 2. The short peaks are coupled from the digital control signals. The flipping current pulse is shown in Fig. 3. The current pulse peak value is 2.8 A, exceeding the manufacturer's recommended and maximum allowed values of 1 and 1.5 A, respectively.

The open-loop magnetometer linearity error is below 0.2% in the ±200 A/m range as shown in Fig. 4. As the Earth's field magnitude is usually about 50 μT, this range is sufficient for compass applications and monitoring of the Earth's field variations and anomalies. Further increase of the instrument range and linearity of 0.04% was achieved using feedback compensation by the integrated coil. The most important advantage of using feedback compensation is that the temperature

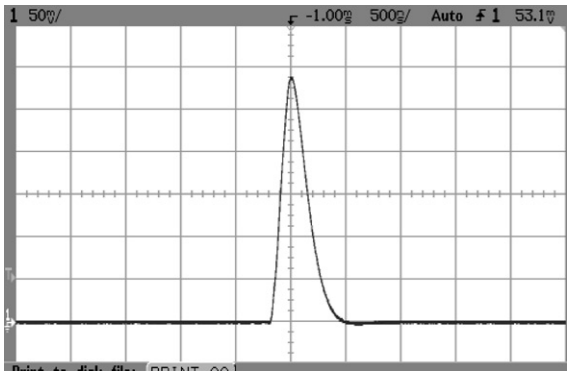

Fig. 3. Flipping pulse in detail, 500 mA/div.

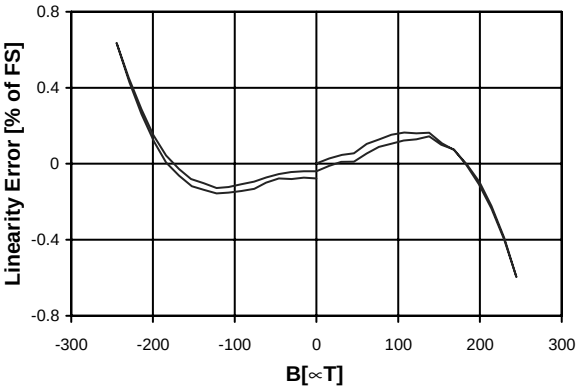

Fig. 4. Linearity of the open-loop AMR magnetometer.

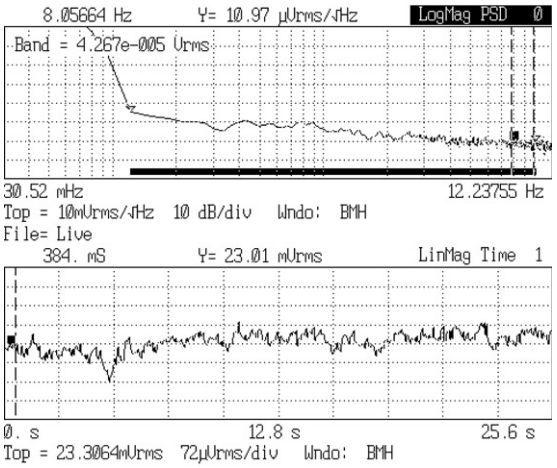

Fig. 5. Noise of the open-loop AMR magnetometer: power spectrum density and time plot (5 nT/div).

coefficient of sensors sensitivity is reduced from 0.25%/K to 0.01%/K, which is a typical temperature coefficient of the field factor of the compensation coil. The

temperature coefficient of the sensor offset is about 10 nT/K.

The magnetometer noise is shown in Fig. 5 both in frequency and time domain: the noise spectrum density was 30 $\mu V/Hz^{1/2}$ at 1 Hz corresponding to 2 $nT/Hz^{1/2}$ at 1 Hz, the rms level in the 100 mHz to 10 Hz frequency range was 7 nT and noise p–p value was approximately 15 nT. These values are only slightly higher than the sensor noise itself.

We demonstrated that magnetometer using AMR sensors can achieve low noise and high stability if the flipping pulses guarantee deep saturation of the sensor film. Further noise reduction is achieved by avoiding transient period *s* from the output signal by improved design of the switching detector (integrator) circuits and their timing.

This research has been supported by a Marie Curie fellowship of the European Community programme Human potential under Contract Number HPMF-CT-2000-00695.

M. Vopalensky was partly supported by Grant No. 1905 from FRVS and by Socrates/Erasmus fellowship.

A. Platil was supported by Ministry of Education of the Czech Republic under No. J04/98:212300016.

References

[1] P. Ripka (Ed.), Magnetic Sensors and Magnetometers, Artech, Boston, London, 2001.
[2] Philips Semiconductors Data Handbook SC17: Semiconductor Sensors. Accessible under: http://www.semiconductors.philips.com
[3] P. Ripka, J. Appl. Phys. 79 (8) (1996) 5211.
[4] P. Ripka, G. Vertesy, J. Magn. Magn. Mater. 215–216 (2000) 795.
[5] H. Hauser, J. Appl. Phys. 75 (1994) 2584.

[44] Vopalensky M., Platil A.: Temperature Drift of Offset and Sensitivity in Full-Bridge Magnetoresistive Sensors. *IEEE Transactions on Magnetics, Vol. 49, Iss. 1 (2013), 136-139*

Temperature Drift of Offset and Sensitivity in Full-Bridge Magnetoresistive Sensors

Michal Vopalensky[1] and Antonin Platil[2]

[1]Deptartment of Electrical Engineering and Computer Science, College of Polytechnics Jihlava, 58601 Jihlava, Czech Republic
[2]Faculty of Electrical Engineering, Czech Technical University in Prague, 16601 Prague, Czech Republic

A typical commercially available magnetoresistive sensor, and particularly an anisotropic magnetoresistive sensor, employs a full bridge of the Wheatstone type formed by two complementary magnetoresistive elements in each branch. This configuration provides linearized response and enlarged sensitivity compared to any other configuration made up of the same elements. Since in a large scale production it is practically impossible to adjust the zero-field resistances of all the four elements to an exactly identical value, there is always some zero-field offset present at the bridge output diagonal even when the sensor is placed in the zero magnetic field. The sensitivity of the sensor, i.e., the ratio of the output voltage change to the change of the measured field H, is associated with the sensitivity of the individual elements. The change of the output voltage is determined by the change of the resistance ΔR of the individual elements. Both the offset and the sensitivity of a full-bridge magnetoresistive sensor is dependent on the zero-field resistances R_{i} of the elements. However, as in most metallic material, the resistivity of a magnetoresistive element is influenced by temperature. Hence, both the offset and the sensitivity of a real magnetoresistive sensor is temperature dependent. It can be shown that, theoretically speaking, the offset is temperature independent when the bridge is supplied with a constant voltage (but the sensitivity in that case is temperature dependent), and the sensitivity is temperature independent when the bridge is supplied with a constant current (but the offset in that case is temperature dependent). This hypothesis has been verified on KMZ52 sensor (albeit in small temperature range—about 25 °C–45 °C).

***Index Terms*—Anisotropic magnetoresistence (AMR), bridge circuits, magnetoresistive devices.**

I. Introduction

MAGNETORESISTIVE Sensors often employ four magnetoresistive elements configured into a full bridge of the Wheatstone type [1]–[4]. Each element has its basic value of R, which changes by ΔR when exposed to a magnetic field. The change in resistance is usually opposite in two adjacent bridge elements.

The resistance R of each element is associated with the resistivity ρ through the following equation:

$$R = \rho \frac{l}{A} \tag{1}$$

where l is the length of the element and A is its cross-section area.

The resistivity of an anisotropic magnetoresistor (AMR) depends on the angle of magnetization, which in turn is determined by the external magnetic field [4], [5]. In a typical sensor with elements linearized with barber-poles, the resistivity of the material along the longitudinal axis of the magnetoresistive stripe is given by the formula

$$\rho_{\mathrm{m}} = \frac{\rho_{\parallel} + \rho_{\perp}}{2} \pm \Delta\rho \frac{H_{\mathrm{meas}}}{H_{\mathrm{a}}}. \tag{2}$$

Here,

ρ_{m}	is the measured resistivity;
$\rho_{\parallel}$ and $\rho_{\perp}$	is the resistivity in the direction parallel and orthogonal to the magnetization, respectively;
$\Delta_{\rho} = \rho_{\parallel} - \rho_{\perp}$	is the difference between parallel and orthogonal resistivity (material-specific);
H_{meas}	is the measured field applied in the appropriate direction;
H_{a}	is the characteristic field of uniaxial anisotropy of the element (combination of induced and shape anisotropy).

The "±" sign represents the fact that the same external field leads to increase in resistivity in one element and decrease of resistivity in the adjacent one.

Combining (1) and (2), the resistance is given as

$$R = \frac{\rho_{\parallel}+\rho_{\perp}}{2} \cdot \frac{l}{A} \pm \Delta\rho \frac{H_{\mathrm{meas}}}{H_{\mathrm{a}}} \cdot \frac{l}{A} = \frac{R_{\parallel}+R_{\perp}}{2} \pm \Delta R \frac{H_{\mathrm{meas}}}{H_{\mathrm{a}}}. \tag{3}$$

The meaning of the quantities in (3) is obvious.

II. Temperature Dependence of Resistivity

The dependence of resistivity on temperature in metallic compounds may be rather a complicated function. However, it is often described as a polynomial approximation of the first order, neglecting the higher order terms, giving

$$\rho(t) = \rho_0(1 + \alpha.\Delta t). \tag{4}$$

Here,

$\rho_0[\Omega \cdot \mathrm{m}]$	is the resistivity at reference temperature t_0;
$\alpha[^{\circ}\mathrm{C}^{-1}]$	is the temperature coefficient of resistivity;
$\Delta t = t - t_0$	is the difference between the given temperature and the reference temperature.

In the magnetoresistive sensor, the resistivity changes with the magnetic field, as described in (2). The change of resistivity with temperature is caused by different physical phenomenon than the change due to the magnetic field. The minimum resistivity, which can be measured in the magnetoresistive material,

Manuscript received July 11, 2012; revised September 05, 2012; accepted September 14, 2012. Date of current version December 19, 2012. Corresponding author: A. Platil (e-mail: platil@fel.cvut.cz).

Color versions of one or more of the figures in this paper are available online at http://ieeexplore.ieee.org.

Digital Object Identifier 10.1109/TMAG.2012.2220535

is the resistivity $\rho_\perp$, which is measured in the direction orthogonal to the direction of magnetization. This resistivity will be considered as a background resistivity, which is influenced by the temperature and by the acting field independently. For completeness, it has to be mentioned that in fact also the anisotropy field H_a and magnetoresistivity term $\Delta\rho$ are affected by the temperature [3], but these effects will not be considered in the further text. The temperature-induced effects on geometry of the sensor will also be neglected.

Let it be assumed that the temperature dependence of $\rho_\perp$ is

$$\rho_\perp(t) = \rho_{\perp,0}(1 + \alpha.\Delta t) \tag{5}$$

where $\rho_{\perp,0}$ is the resistivity in the orthogonal direction to the magnetization at reference temperature.

Consequently, knowing that $\rho_\parallel = \rho_\perp + \Delta\rho$, (2) can be written in the following form:

$$\rho_\mathrm{m} = \frac{2\rho_{\perp,0}(1 + \alpha.\Delta t) + \Delta\rho}{2} \pm \Delta\rho\frac{H_\mathrm{meas}}{H_\mathrm{a}} \tag{6}$$

and finally after a short modification

$$\rho_\mathrm{m} = \frac{\rho_{\perp,0} + \rho_{\parallel,0}}{2} + \rho_{\perp,0}\cdot\alpha\cdot\Delta t \pm \Delta\rho\frac{H_\mathrm{meas}}{H_\mathrm{a}}. \tag{7}$$

Since

$$\rho_{\perp,0} = \frac{\rho_{\perp,0} + \rho_{\parallel,0}}{2} - \frac{\Delta\rho}{2} \tag{8}$$

and $\Delta\rho$ is in order of units of percent of $(\rho_{\perp,0}+\rho_{\parallel,0})/2$ in AMR magnetoresistive materials, the member $-(\Delta_\rho/2)\cdot\alpha\cdot\Delta t$ can be neglected and (7) takes the form

$$\rho_\mathrm{m} = \frac{\rho_{\perp,0} + \rho_{\parallel,0}}{2}\cdot(1 + \alpha\cdot\Delta t) \pm \Delta\rho\frac{H_\mathrm{meas}}{H_\mathrm{a}}. \tag{9}$$

Writing (9) in resistances rather than in resistivities

$$R(t, H_\mathrm{meas}) = \frac{R_{\parallel,0} + R_{\perp,0}}{2}\cdot(1+\alpha\cdot\Delta t) \pm \Delta R\frac{H_\mathrm{meas}}{H_\mathrm{a}}. \tag{10}$$

Introducing $R_0 = (R_{\parallel,0} + R_{\perp,0})/2$ and normalized "sensitivity" (or ratio of relative change of resistance) $s = \Delta R/(R_0\cdot H_\mathrm{a})$, (10) can be written as

$$R(t, H_\mathrm{meas}) = R_0\cdot(1 + \alpha\cdot\Delta t \pm s\cdot H_\mathrm{meas}). \tag{11}$$

III. Offset and Sensitivity of a Full Bridge

The available literature on bridge circuits [6]–[9] does not relate well to the nature of our specific problem and thus we made own derivations.

The output voltage V_out of a general bridge made up of the resistances $R_1, \ldots, R_4$, as in Fig. 1 (left), is given by

$$V_\mathrm{out} = V_\mathrm{supp}\left(\frac{R_2}{R_1 + R_2} - \frac{R_4}{R_3 + R_4}\right) \tag{12}$$

in the case of constant voltage supply V_supp, and

$$V_\mathrm{out} = I_\mathrm{supp}\left(\frac{R_2(R_3 + R_4) - R_4(R_1 + R_2)}{R_1 + R_2 + R_3 + R_4}\right) \tag{13}$$

in the case of constant current supply I_supp.

In the absence of the external field, the branches of the measurement bridge $R_1, \ldots, R_4$ of the sensor have the initial resistances $R_{1,0}, \ldots, R_{4,0}$. In an ideal case, these four resistances

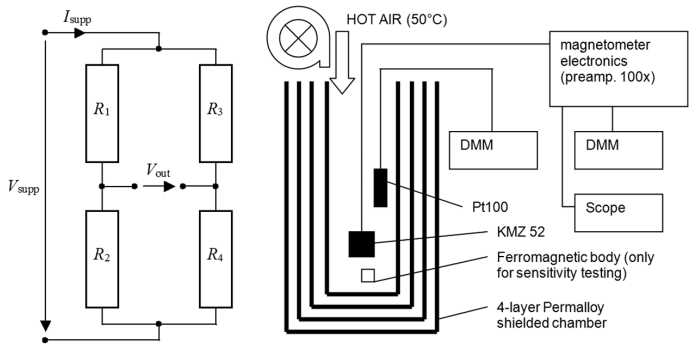

Fig. 1. Left: full bridge arrangement of AMR sensor like KMZ52. Right: the measurement setup schematical drawing.

are identical and the output of the bridge is zero. In a real case, however, the resistances are not identical, leading to an offset even in the zero field, both in the case of constant voltage and constant current supply.

Substituting R_0 in (11) with $R_{1,0}, \ldots, R_{4,0}$, leaving $H_\mathrm{meas} = 0$ and putting the resulting resistances $R_1, \ldots, R_4$ in their full temperature-dependent form (11) into (12), it can be derived using standard mathematical modifications that the temperature dependent terms cancel out in the case of constant voltage supply, so that the offset $V_\mathrm{off,V}$ of a constant voltage supplied bridge is independent of temperature. However, putting the same $R_1, \ldots, R_4$ formulas into (13), it can be derived that in the case of the constant current supply, the offset $V_\mathrm{off,I}$ is temperature dependent with the same coefficient, as is the resistance of the elements

$$V_\mathrm{off,I}(t) = V_\mathrm{off,0,I}(1 + \alpha\cdot\Delta t). \tag{14}$$

In (14), $V_\mathrm{off,0,I}$ is the offset voltage of the constant current supplied bridge at reference temperature.

The sensitivity S of the bridge is the ratio of the change of output voltage to the change of the measured field, $S = \Delta V_\mathrm{out}/\Delta H_\mathrm{meas}$. For infinitesimal changes around $H_\mathrm{meas} = 0$, the sensitivity can be calculated as the derivative of the function $V_\mathrm{out} = f(H_\mathrm{meas})$. Using (11) and keeping in mind that the sign of the H_meas term is "+" for R_2, R_3, and "−" for R_1, R_4, one gets general formulae for all the four bridge resistances. Using these $R_1, \ldots, R_4$ terms in their full form in (12) and (13) provides general formulae for the bridge output as the functions of both temperature and magnetic field [10]. The derivative of the output voltage function, i.e., the sensitivity S_V in the case of constant voltage supply is then

$$S_\mathrm{V}(t) = 2V_\mathrm{supp}\cdot s\cdot\frac{1}{1 + \alpha\cdot\Delta t} \times\frac{R_1R_2R_3^2 + R_1R_2R_4^2 + R_3R_4R_1^2 + R_3R_4R_2^2 + 4R_1R_2R_3R_4}{(R_1 + R_2)^2(R_3 + R_4)^2}. \tag{15}$$

The sensitivity S_I in the case of the constant current supply is given in (16), shown at the bottom of the next page. The temperature-related term in (15) is in denominator, but for small $\alpha\cdot\Delta t$ (about 0.052 in our case), it can be written as $(1 + \alpha\cdot\Delta t)^{-1} \approx (1-\alpha\cdot\Delta t)$. Thus, the sensitivity of a bridge supplied with a constant voltage is decreasing when temperature is increasing, with the same temperature coefficient α as that of the resistance of

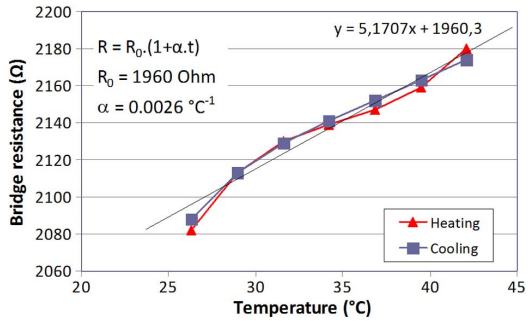

Fig. 2. Bridge resistance as a function of temperature. The thermal coefficient of resistance is approximately $0.0026\,^{\circ}\mathrm{C}^{-1}$.

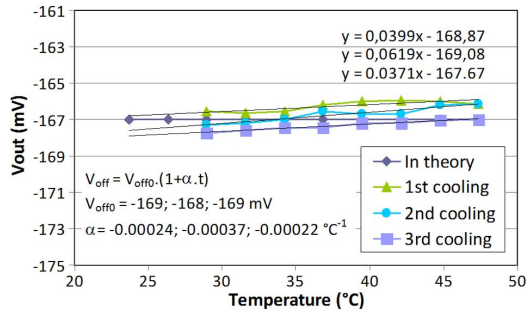

Fig. 3. Constant voltage supplied bridge offset (100x amplified) as a function of temperature. The thermal coefficient of offset voltage is approximately $-0.00024\,^{\circ}\mathrm{C}^{-1}$, one order of magnitude lower than thermal coefficient of resistance (in theory, exactly zero).

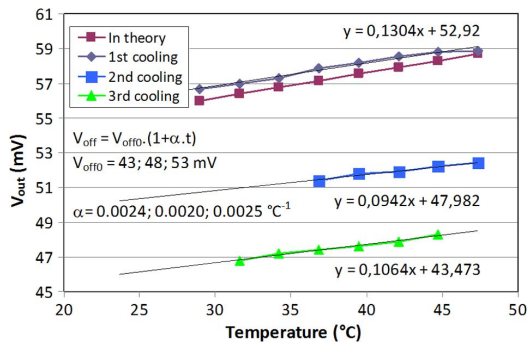

Fig. 4. Constant current supplied bridge offset (100x amplified) as a function of temperature. The thermal coefficient of offset voltage is approximately $0.0024\,^{\circ}\mathrm{C}^{-1}$, roughly the same as thermal coefficient of resistance.

bridge elements. The sensitivity of a bridge supplied with constant current is theoretically temperature independent.

IV. Experimental Verification

For the verification of the outlined hypothesis, KMZ52 sensor was used. During all the measurements in setup (Fig. 1, right), the sensor was placed in a heated magnetic shielded chamber with dc attenuation of approximately 75 dB @ 100μT (i.e., the Earth's field is attenuated $5600\times$ to about 10 nT residual level). The ambient air temperature inside the chamber was measured with a Pt100 thermometer, the output voltage of the bridge was measured with an Agilent 34401A multimeter after amplification $100\times$ provided by a precise instrumentation amplifier. Influence of the offset voltage and bias current of the instrumentation amplifier has been neglected due to their values (output offset voltage maximum is 30 μV with the temperature drift of $0.5\,\mu\mathrm{V}/^{\circ}\mathrm{C}$, input bias current maximum is 50 pA). Each heating cycle was 15 min, spontaneous cooling was 40 min. Only one of the internal KMZ52 bridges was used in the experiment. Flipping was employed when measuring the sensitivity, as described later, compensation terminals were not used.

The temperature coefficient α of the bridge resistance (assumed equal to each element's resistance) can be determined by measuring the resistance along the diagonal of the bridge, when sensor is placed in a zero magnetic field, under variable temperature. The results of the measurement can be seen in Fig. 2, the respective α can be estimated to approximately $0.0026\,^{\circ}\mathrm{C}^{-1}$ (compare [3] and [11]).

For the measurement of offset temperature dependence, the bridge was supplied with either a constant voltage of 7.6 V or a constant current of 3 mA. The dependence of offset voltage in the case of *constant voltage supply* can be seen in Fig. 3. It has been measured in three temperature cycles. The temperature coefficient of the offset drift in individual cycles is $-0.00024\,^{\circ}\mathrm{C}^{-1}$, $-0.00037\,^{\circ}\mathrm{C}^{-1}$, and $-0.00024\,^{\circ}\mathrm{C}^{-1}$. Hence, the temperature coefficient is negative and by one order of magnitude lower than the temperature coefficient of the resistance of a single element. The dependence of offset voltage in the case of *constant current supply* can be seen in Fig. 4. Again, three temperature cycles were made, giving the temperature coefficient values of $0.0024\,^{\circ}\mathrm{C}^{-1}$, $0.0020\,^{\circ}\mathrm{C}^{-1}$, and $0.0025\,^{\circ}\mathrm{C}^{-1}$, roughly the same as that of resistance.

For the measurement of sensitivity, the sensor was again placed into the magnetic shielding, but a small piece of ferromagnetic material was placed near to the sensor to provoke a response in output voltage. The output voltage can have two values symmetrical around the value of offset, depending on the position of magnetization, which can be over-switched by flipping (set/reset) pulses. By evaluating the difference of the output voltage in the two states of magnetization, the influence of the offset drift is eliminated. The sensitivity can be expressed as $\Delta V_{\mathrm{out}}/\Delta H_{\mathrm{meas}}$, so if the ΔH_{meas} remains constant (within tens of nT), the temperature dependence of sensitivity is the same as the temperature dependence of ΔV_{out}.

The temperature dependence of the output voltage measured in the above described way with the *constant voltage supply* can be seen in Fig. 5. A series of temperature cycles has been performed, giving the minimum temperature coefficient of sensitivity $\alpha = -0.0023\,^{\circ}\mathrm{C}^{-1}$, similar in magnitude to the coefficient of resistance (sensitivity is decreasing with temperature).

In the case of *constant current supplied bridge* the resulting sensitivity behavior is shown in Fig. 6. According to the above declared hypothesis, the sensitivity should be independent of

$$S_{\mathrm{I}}(t) = I_{\mathrm{supp}} \cdot s \cdot \frac{R_1R_4^2 + R_4R_1^2 + R_2R_3^2 + R_3R_2^2 + 3R_1R_2R_3 + 3R_1R_2R_4 + 3R_2R_3R_4 + 3R_1R_3R_4}{(R_1 + R_2 + R_3 + R_4)^2} \tag{16}$$

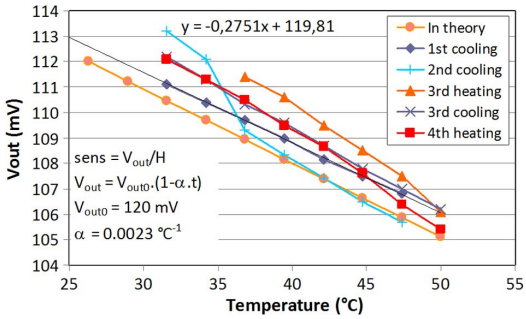

Fig. 5. Constant voltage supplied bridge sensitivity measured as output voltage (100x amplified) for constant field H shown as a function of temperature. The thermal coefficient of sensitivity is approximately. 0.0023 $^{\circ}\mathrm{C}^{-1}$ (decreasing), roughly the same as thermal coefficient of resistance.

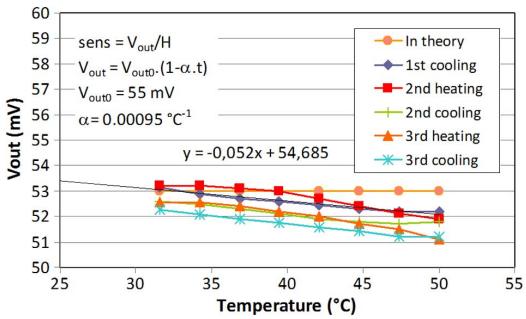

Fig. 6. Constant current supplied bridge sensitivity measured as output voltage (100x amplified) for constant field H shown as a function of temperature. The thermal coefficient of sensitivity is approximately 0.001 $^{\circ}\mathrm{C}^{-1}$ (decreasing), approximately half of the thermal coefficient of resistance (in theory, exactly zero).

temperature. However, there is still a strong temperature dependence of the sensitivity, with the coefficient of approximately $-0.001\ ^{\circ}\mathrm{C}^{-1}$.

V. Conclusion

A model of the temperature behavior of the resistances of anisotropic magnetoresistive elements has been developed. Based on this model, theoretical temperature dependences of the offset and sensitivity in full-bridge anisotropic magnetoresistors have been derived. Theoretically, for a *constant voltage supplied bridge* the offset temperature drift is zero, however, sensitivity in this case decreases with the temperature coefficient equal in magnitude to the temperature coefficient of resistance of each bridge element. Conversely, in the case of a *constant current supplied bridge*, the offset theoretically increases with temperature with the coefficient equal to the temperature coefficient of resistance of each element, and the sensitivity is independent of temperature.

This hypothesis has been verified on the KMZ52 sensor, albeit in small temperature range (25 °C to 45 °C), using setup shown in Fig. 1 (right). The temperature coefficient of the resistance of bridge elements has been found to be approximately $0.0026^{\circ}\ \mathrm{C}^{-1}$. In the case of *constant voltage supply*, the offset temperature drift, contrary to the hyphotesis, has a nonzero coefficient of approximately $-0.0003\ ^{\circ}\mathrm{C}^{-1}$, which is still almost by an order of magnitude lower than the temperature coefficient of resistance of the bridge elements. The sensitivity in this case showed the temperature coefficient of $-0.0023\ ^{\circ}\mathrm{C}^{-1}$, corresponding very well to the hypothesis. In the case of a *constant current supply*, the offset changed with a temperature coefficient of approximately $0.0025\ ^{\circ}\mathrm{C}^{-1}$, again fitting very well the hypothesis. However, the sensitivity decreased in this case with a coefficient of approximately $-0.001\ ^{\circ}\mathrm{C}^{-1}$. Although this value is not zero, it is much better than the temperature coefficient of resistance of bridge elements. The discrepancy between measured data and the hypothesis is caused probably by neglecting the temperature dependence of the characteristic field of anisotropy and temperature induced changes of the geometrical parameters of the sensor elements.

When designing a magnetometer with anisotropic magnetoresistors, periodical flipping (set/reset pulses) and synchronous detection is usually employed. In that case, the dc offset of the bridge is effectively eliminated by the appropriate processing of the output signal [3]. Therefore, offset temperature drift does not represent a big problem. The change in sensitivity, however, can cause troubles, as it is not possible to easily distinguish between response to a change in measured field and the effect of temperature dependence of sensitivity. From this point of view, it is highly desirable to suppress the temperature changes of sensitivity up to the maximum possible degree. For this reason, using of a (fixed) constant current source (a well known technique) for supplying full-bridge magnetoresistive sensors is recommendable. This may provide simpler solution than e.g. one described in [12], where additional temperature sensor is employed.

References

[1] Philips KMZ 51 AMR sensor datasheet., (Jul. 10, 2012) [Online]. Available: http://www.datasheetcatalog.org/datasheet/philips/KMZ51_3.pdf

[2] Honeywell HMC1001 datasheet., (Jul. 10, 2012) [Online]. Available: http://www51.honeywell.com/aero/common/documents/myaerospacecatalog-documents/Missiles-Munitions/HMC_1001-1002-1021-1022_Data_Sheet.pdf

[3] S. Tumanski, *Thin Film Magnetoresistive Sensors*. Philadelphia, PA: Inst. Phys., 2001, 0-7503-0702-1.

[4] H. Hauser and M. Tondra, "Magnetoresistors," in *Magnetic Sensors and Magnetometers*, P. Ripka, Ed. Norwood, MA: Artech House, 2001, 1-58053-057-5.

[5] T. R. McGuire and R. I. Potter, "Anisotropic magnetoresistance in ferromagnetic 3-D alloys," *IEEE Trans. Magn.*, vol. MAG-11, no. 4, pp. 1018–1038, Jul. 1975.

[6] G. Weiss, "Wheatstone bridge sensitivity," *IEEE Trans. Instrum. Meas.*, vol. IM-18, no. 1, pp. 2–6, Mar. 1969.

[7] J. E. Maisel, "Optimization of the Wheatstone bridge sensitivity," *IEEE Trans. Instrum. Meas.*, vol. IM-26, no. 1, pp. 17–21, 1977.

[8] E. Takagishi, "On the balance of an AC wheatstone bridge," *IEEE Trans. Instrum. Meas.*, vol. IM-29, no. 2, pp. 131–136, 1980.

[9] K. Stankovic, M. Vujisic, D. Kovacevic, and P. Osmokrovic, "Statistical analysis of the characteristics of some basic mass-produced passive electrical circuits used in measurements," *Measurement*, vol. 44, pp. 1713–1722, 2011.

[10] M. Vopalensky, "Magnetoresisitive sensor and applications of anisotropic magnetoresistors," Ph.D. dissertation, Dept. Meas., Czech Technical Univ. Prague, Prague, Czech Republic, 2006, unpublished.

[11] G. Counil *et al.*, "Temperature dependences of the resistivity and the ferromagnetic resonance linewidth in permalloy thin films," *IEEE Trans. Magn.*, vol. 42, no. 10, pp. 3323–3325, Oct. 2006.

[12] D. Ramirez Munoz *et al.*, "Temperature compensation of Wheatstone bridge magnetoresistive sensors based on generalized impedance converter with input reference current," *Rev. Sci. Instrum.*, vol. 77, p. 105102, 2006.

[48] Platil A., Kubík J., Vopálenský M., Ripka P.: Precise AMR Magnetometer for Compass**.** *IEEE SENSORS 2003, p. 472-476, Toronto 2003, ISBN 0-7803-8134-3*

Precise AMR magnetometer for compass

A. Platil, J. Kubik*, M. Vopalensky*,+, P. Ripka**

* Czech Technical University, Faculty of Electrical Engineering, Technicka 2, 166 27 Prague, Czech Republic, platil@feld.cvut.cz

+Universidad Autónoma Nacional de México, Ciudad Universitaria, México, D.F.

ABSTRACT

AMR sensors gain growing popularity in linear applications such as compassing [1, 2]. We discuss techniques, how to achieve precision required for 0.2 deg azimuth error in wide temperature range. While linearity of 80 ppm FS and sensitivity tempco of 20 ppm/K can be achieved by using feedback compensation, offset drift and crossfield error can be lowered to nT level by periodical flipping.

1. INTRODUCTION

Navigation systems usually comprise a triplet of magnetic sensors with inclinometers as an "electronically gimbaled" electronic compass, traditionally of fluxgate type. The AMR sensors are smaller, but less precise than fluxgate. Various techniques like AC operation can improve the parameters [3, 4, 5, 6].

The parameters achieved [7] for a Philips KMZ51 [8] sensor were 0.2 % linearity without feedback (0.04 % using integrated feedback coil). The magnetometer noise at 1Hz was 2 nT/sqrtHz (compare fluxgate noise of 10 pT/sqrtHz [9]), uncompensated temperature coefficient of sensitivity was 0.25 %/K without the feedback and 0.01 %/K with feedback. Temperature offset drift was typically 10 nT/K. Similar values were measured for Honeywell AMR sensors. Latest results [10] indicate that linearity of 80 ppm in +/- 300 μT range, offset temperature stability of approximately 2 nT/K and sensitivity temperature.coefficient of 20 ppm/K can be reached by optimization of the circuits. For compass applications, this theoretically represents a limit of 0.2 deg precision.

2. MEASUREMENT SETUP AND RESULTS

Zero stability measurement:

Long-term offset stability was measured for the flipped and compensated sensor (i.e. for the whole magnetometer) at constant temperature. The sensor was placed into the cylindrical four-layer permalloy magnetic shielding with the attenuation of the DC field of 75 dB (measured for the Earth-field). The temperature in the measurement room changed between 23°C and 25°C within 48 hours, and during this time the output offset (recomputed to the magnetic field) changed between 0nT and 60 nT. Offset stability under varying temperature was measured using an 8 layer cylindrical permalloy magnetic shielding with internal thermostat. In this case, we measured also the offset stability of the unflipped and uncompensated sensor. The temperature varied within the interval of –20°C to 65°C (-4°F to 149°F), the offset changed correspondingly from +3600 nT to –4000 nT around initial value at 23°C (36500 nT –the sensor was not flipped nor compensated). See Fig. 1 illustrating the temperature behaviour of unflipped and uncompensated sensor. From this, we can calculate the temperature coefficient of the offset as approx. –90 nT/K.

The same measurement arrangement was used for measuring of the long-term offset stability in the case of flipped and compensated KMZ51 sensor. In the range of the temperatures from –18°C to 58°C, the offset changed between –100nT to +60nT. However, there is not a simple characteristic of the output change, corresponding to the temperature change. Nevertheless, we can compute the temperature coefficient from the above given values as approx. 2.1 nT/K, what is 5 times better than referred in [7]. The offset behavior in this case is illustrated in Fig. 2.

Temperature dependence of the sensitivity:

For the measurement of the temperature sensitivity dependence, the sensor was placed into Helmholtz coils with temperature-controlled chamber. Unfortunately, in this case the minimal temperature reached was only -2°C. The sensitivity behavior for the unflipped and uncompensated sensor was checked. The sensitivities were computed from two samples taken in mg. fields of the opposite polarity, both in the middle of the range of +/- 300μT, i.e. at +150μT and -150μT. The initial sensitivity at the temperature of 24°C was approx. 7.636 mV/μT. For the temperature range of –1°C to 63°C, the sensitivity changes from 7.715mV/μT to 7.439mV/μT – see Fig. 3. From these values, we can determine the sensitivity temperature coefficient as approx. – 585 ppm/K (again 5 times better than referred in [7]).

In the case of flipped and compensated sensor, it is not easy to determine the direct influence of the temperature to the sensitivity. As the basic temperature dependence is already compensated, other second-order effects play dominant role. Nevertheless, in the range of temperatures from –2°C to 60°C, the sensitivity changed from 15.199mV/μT to 15.180mV/μT. This corresponds to 20ppm/K (once more, 5 times better than referred in [7]). In the Fig. 4, you can see that there is no significant change of the sensitivity during the cooling process. After heating, the sensitivity changes, but it does not return to the initial value.

0-7803-8133-5/03/$17.00 ©2003 IEEE

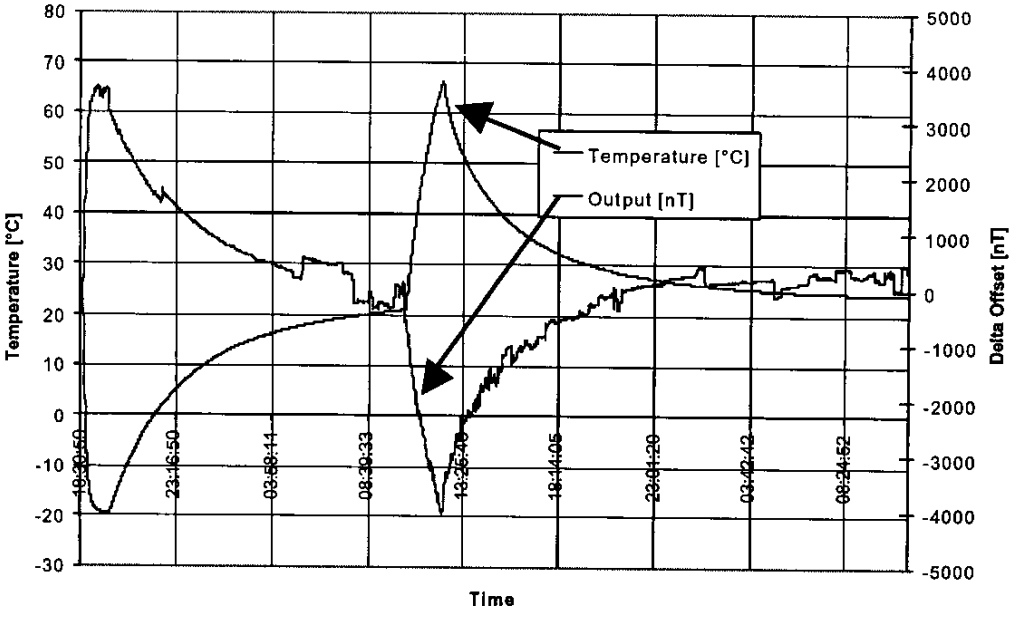

Figure 1 – The offset behavior of the unflipped and uncompensated KMZ51 AMR sensor under varying temperature

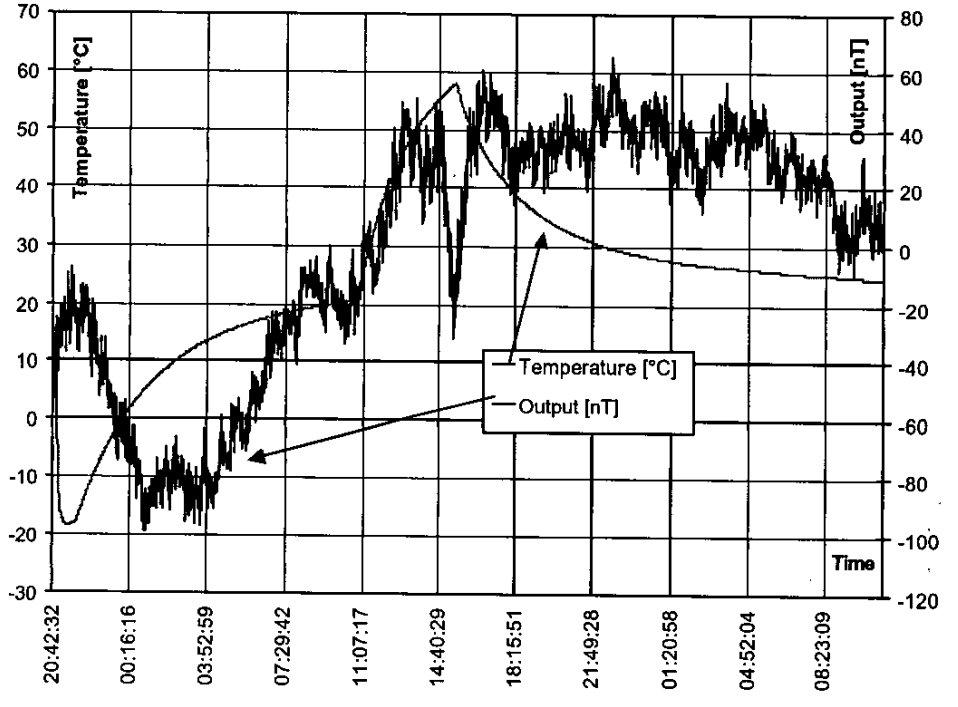

Figure 2 - The offset behavior of the flipped and compensated KMZ51 AMR sensor under varying temperature

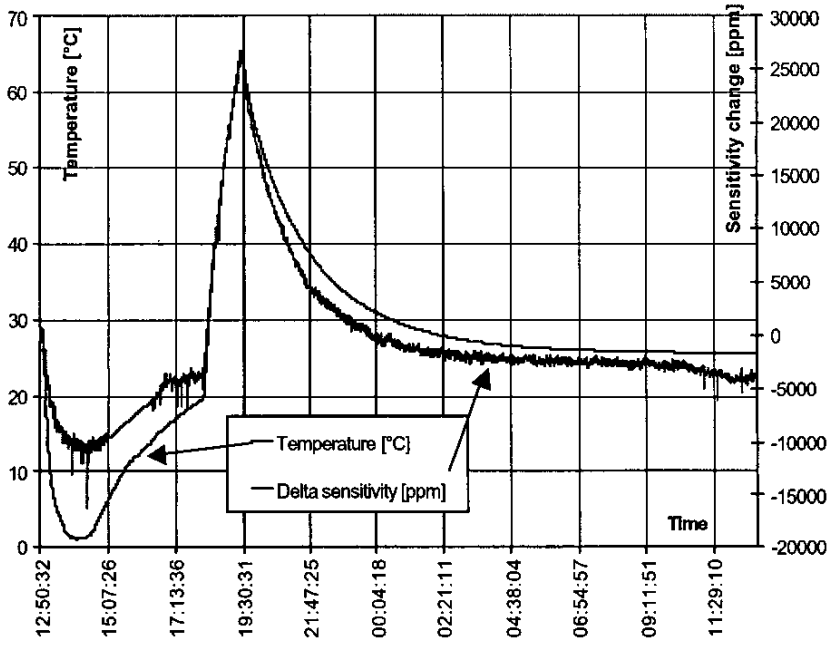

Figure 3 - The temperature dependence of sensitivity for the unflipped and uncompensated KMZ51 AMR sensor

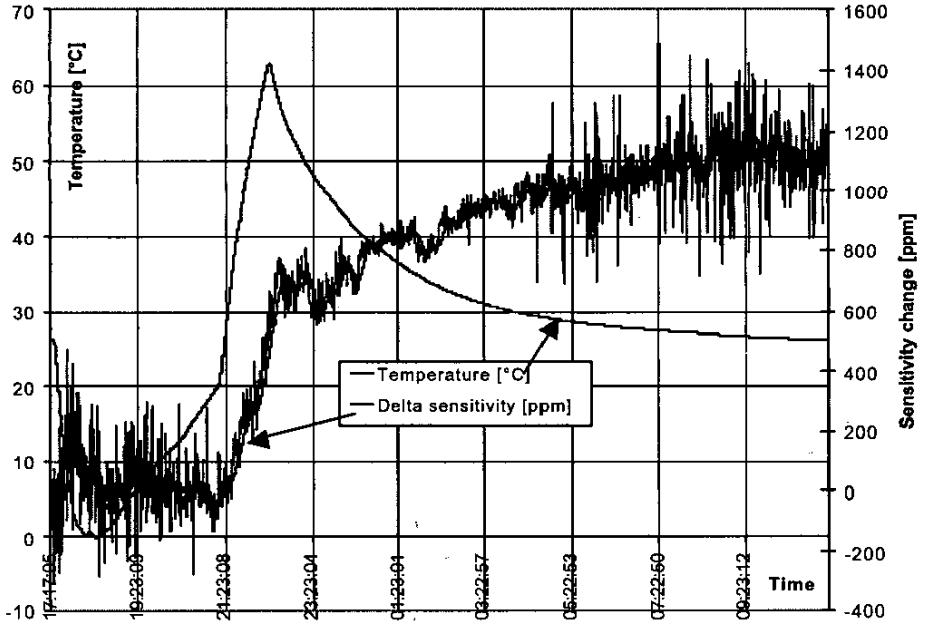

Figure 4 - The temperature dependence of sensitivity for the flipped and compensated KMZ51 AMR sensor

Crossfield effect

Crossfield effect is unwanted sensitivity to magnetic field in axis perpendicular to the normal sensing direction. This sensitivity has non-linear character, so that it cannot be corrected simply by shifting the sensitivity axis. In another words, there is no insensitive direction in the sensor plane. Crossfield is much stronger at AMRs than at fluxgates [11].

The sensor reading can be calculated (after [12]) as:

$$B_{rdg} = c\frac{B_x}{B_S + B_y} \qquad (1)$$

where the reading depends not only on the field in the main sensitive axis B_x , but also on the perpendicular field B_y. The anisotropy characteristic field B_S is a parameter of the sensor characterizing its crossfield sensitivity. It is worth noting that over the years, the advances in AMR sensor technology reduced the crossfield sensitivity by an order of magnitude.

The crossfield effect should be compensated both in the routine measurement and in the calibration procedure. The error due to uncompensated crossfield may result in 2.4 deg. errors in azimuth (according to Bs value of 0.8 mT [12] specified for Honeywell sensors). In the Fig. 5, there is shown a simulation of the error of azimuth caused by uncompensated crossfield for true azimuth varying from 0 to 360 deg. The compass is in horizontal position.

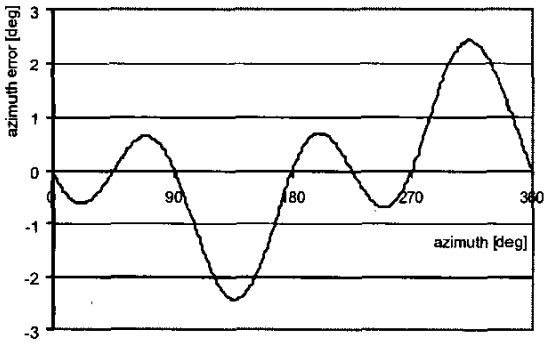

Figure 5 – Azimuth error caused by uncompensated crossfield

While the procedure for numerical correction [12] of the crossfield is known, the practical limitation lies in the knowledge of B_S, which is used in the calculation. The 5% error in the B_S value may cause +/-0.25 deg. error in azimuth. The value specified by the manufacturer is B_S = 0.8 mT (i.e. 8 Gauss) for Honeywell HMC1001 and 1002 sensors. However, there are sparse data on the batch-to-batch variation or the temperature dependence of that value. We have developed a calibration procedure to identify the B_S value. For 2-axis Honeywell HMC1002 sensor, the found values were B_{SX} = 0.7967 mT for one sensitive axis and B_{SY} = 0.7882 mT for the other sensitive axis. (For Philips KMZ51 sensor, the B_S value is approx. 940 A/m, i.e. 1.18 mT [5].)

Crossfield and perpendicularity errors are tangled so that none of the corrections can be done independently from the other.

Non-orthogonalities, individual sensitivities, and offsets of the three sensors can be found by "scalar field calibration" [13]. If the ideal 3-axis sensor is rotated in homogenous field, the calculated total field value should be constant. Variations of this value are due to non-orthogonality of individual sensors, differences in their sensitivities and offsets. These errors can be compensated by coefficients found in iterative numerical process. The residual error is due to sensors non-linearity and crossfield error.

The Fig. 6 shows behavior of 3-axis AMR magnetometer (Honeywell HMR2300) in scalar field calibration. The initial variation of the total field (during random rotation in the homogenous field) is 4000 nT RMS. The correct value was 48515 nT (measured by proton magnetometer). After performing iterative search of correction constants for sensitivities, offsets and orthogonalities, the variation was decreased to 35 nT RMS – see Fig. 7.

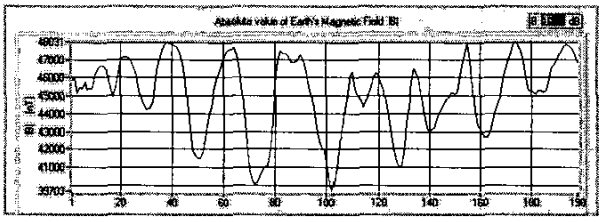

Figure 6 – AMR scalar field calibration – total field variation due to crossfield and non-orthogonality before calibration is 4 000 nT RMS.

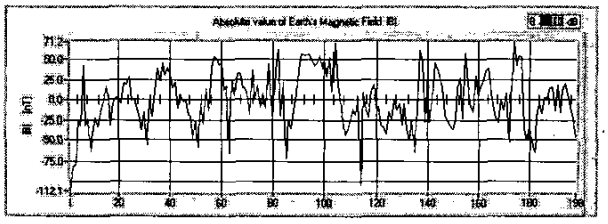

Figure 7 – After calibration, the total field variation around correct value is 35 nT RMS

Gimbaling of the compass

In order to achieve correct compass reading, it must be carefully gimbaled in horizontal position – otherwise the vertical component of the Earth's magnetic field influences the compass. For classical compasses, it is done in viscous liquid bath or in mechanical gimbals. For electronic compasses, this can be done

mathematically, using information from inclinometers. The pitch and roll of the compass must be taken into account, otherwise errors are introduced to the azimuth reading. For example, as a rule of thumb valid for central Europe, uncompensated roll of 1 deg may cause max. azimuth error of more than 2deg. Fig. 8 shows the simulation of azimuth error caused by uncompensated roll (0, 1, 2, and 5 degs) for true azimuth varying from 0 to 360 degs.

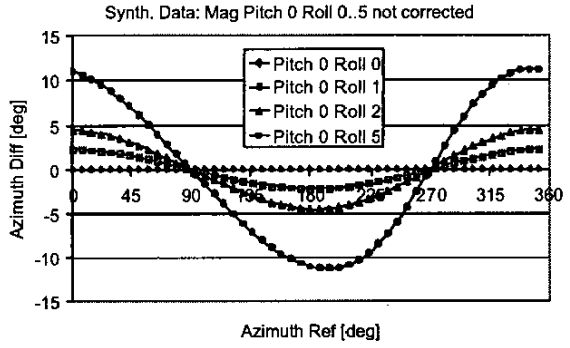

Figure 8 – Azimuth error caused by uncompensated roll

3. SUMMARY

We have demonstrated that flipping and feedback techniques can improve the parameters of AMR sensors. Achievable parameters with optimized electronics comprise linearity of 80 ppm in +/- 300 μT range, offset temperature stability of approximately 2 nT/K and sensitivity temperature coefficient of 20 ppm/K. The simulations show the importance of mathematical compensation of crossfield sensitivity that can cause errors of 2.4 degrees of azimuth (considering anisotropy characteristic field of 0.8 mT for Honeywell HMC1001 sensors). Also the horizontal position of the compass must be secured or mathematically compensated – typically, deviation from horizontality of 1 deg can result in 2 degs azimuth error (for geomagnetic field in central Europe).

Acknowledgements:

Michal Vopalensky was supported by the Secretaria de Relaciones Exteriores de Gobierno de Mexico in his study at Universidad Nacional Autonoma de Mexico.

4. REFERENCES

[1] S. Tumaski: Thin Film Magnetoresistive Sensors, IoP Publishing, ISBN 0-7503-0702-1

[2] P. Ripka (ed.): Magnetic Sensors and Magnetometers, Artech, Boston, ISBN 1-58053-057-5, 2001.

[3] P. Ripka: AC - excited magnetoresistive sensor, J. Appl. Phys. 79 (8), 1996, pp. 5211-5213.

[4] Ripka, M. Tondra, J. Stokes, and R. Beech: AC - driven AMR and GMR magnetoresistors, Sensors & Actuators A, Vol. 76 (1999), pp. 227-232.

[5] H. Hauser, P.L. Fulmek, P. Haumer, M. Vopalensky, P. Ripka, Flipping field and stability in anisotropic magnetoresistive sensors Sensors & Actuators A, 106 (2003), 34-37, pp 121-125.

[6] M. Vopalensky, P. Ripka, A. Platil: Precise Magnetic Sensors, Sensors & Actuators A 106 (2003), 38-42.

[7] P. Ripka, M. Vopálenský, A. Platil, M. Döscher, K. -M. H. Lenssen and H. Hauser: AMR magnetometer. Journal of Magnetism and Magnetic Materials 254-255 (2003), pp. 639-641

[8] Datasheet Magnetic Field Sensors - General. Philips Semiconductors, http://www.semiconductors.philips.com

[9] P. Ripka: Noise and Stability of Magnetic Sensors, J. Magn. Magn. Mat. 157/158 (1996), pp. 424-427.

[10] M. Vopalensky, A. Tipek, P. Ripka: Influence of the flipping and feedback techniques on the temperature behavior of anisotropic magnetoresistors. VI Latin Amer. Workshop on Mag, Mg. Mat., Chihuahua. (submitted paper)

[11] P.Ripka, W. Billingsley: Crossfield effect at fluxgate, Sensors & Actuators A 81 (2000), 176-179.

[12] B. Pant, M. Caruso: Magnetic Sensors Cross-axis effect, Honeywell Application note AN-205

[13] J. M. G. Merayo, P. Brauer, F. Primdahl, J. R. Petersen and O. V. Nielsen: Scalar calibration of vector magnetometers, Meas. Sci. Technol. 11 (2000) 120–132.

[55] Vopalensky M., Ripka P., Kubik J., Tondra M.: Improved GMR sensor biasing design. *Sensors and Actuators A, Vol. 110, Iss. 1-3 (2004), 254-258*

Available online at www.sciencedirect.com
SCIENCE DIRECT®
Sensors and Actuators A 110 (2004) 254–258
SENSORS AND ACTUATORS A PHYSICAL
www.elsevier.com/locate/sna

Improved GMR sensor biasing design

Michal Vopálenský [a,*], Pavel Ripka [a], Jan Kubík [a], Mark Tondra [b]

[a] *Department of Measurement, Faculty of Electrical Engineering, Czech Technical University, Technicka 2, 166 27 Prague 6, Czech Republic*
[b] *NVE Corporation, 11409 Valley View Road, Eden Prairie, MN 55344-3617, USA*

Received 1 November 2002; received in revised form 5 September 2003; accepted 10 September 2003

Abstract

Sensors based on the giant magnetoresistance (GMR) effect have been used for years as the reading heads in the hard-disk technology. However, just a simple on/off detection function has been required in that application. Various techniques have been developed to make the GMRs suitable for a linear measurement of a magnetic field. Using a proper technique, we can achieve an alternating output signal of the sensor, that can be convenient for further signal processing. This paper deals with the method of alternating sensitive-axis field biasing and its influence on the sensor properties. We show that a squarewave biasing is preferred over the sinewave one, as it results in a higher sensor sensitivity and lower noise. With optimized reading circuits, we achieved a sensitivity of 20 mV/V/kA/m, a hysteresis of 0.5% in the ±300 A/m range and a noise PSD value of 30 mA/m RMS /$\sqrt{\text{Hz}}$ at 1 Hz.

Keywords: Magnetoresistive sensors; Biasing techniques; Giant magnetoresistance

1. Introduction

The giant magnetoresistance (GMR) sensors used as reading heads in hard-disk technology do not need to measure precisely a linear magnetic field, as the function required of them in these applications is just an on/off detection. Because of their convenient properties, such as high sensitivity and low cost, there have been some attempts to adapt the GMRs to the linear magnetic field magnitude measurement. For this purpose, various methods such as sensitive-axis biasing, orthogonal biasing, flux concentrators, and feedback compensation have been developed [1–3]. The sensitive-axis biasing technique in the unpinned GMR structures by an additional field consists of shifting the operating point of the sensor on its characteristic. The results of some experiments with field alternating biasing and respective signal processing have been reported in [4].

GMR sensors for linear measurement usually contain a full bridge of the Wheatstone type consisting of four complementary magnetoresistive elements in their internal structure. It is desirable to make the output characteristic of the whole sensor bipolar. The characteristic of a simple bridge element of the GMR "unpinned sandwich" structure, however, is unipolar. Creating a field of a proper value parallel to the sensitive axis, we can shift the operating point of each element to the linear part of its characteristic. This technique is called biasing in the sensitive-axis direction. Biasing the neighboring elements of the bridge to the opposite sides (having opposite slopes) of the characteristics, we can achieve bipolar output [5].

2. Measurement setup

The biasing field of a desired value is usually provided by an integrated on-chip flat coil. Reversing the polarity of the so-called field bias current, flowing through the biasing coil, we can easily reverse the output characteristic of the sensor. Thus supplying the biasing coil by an alternating current we can obtain an alternating output signal.

To recover the dc or low-frequency signal corresponding to the measured field value, synchronous detection has to be used. Periodical reversing of the biasing field orientation results in significant reduction of the output hysteresis. In [4], the biasing coil was supplied by a sinewave signal, and the Stanford Research Systems lock-in amplifier SR 830 was used to process the output signal. However, in our experiments, a squarewave 1000 Hz biasing signal was used, and a gated-integrator was the signal reconstruction circuit. The measurement setup can be seen in Fig. 1.

* Corresponding author. Tel.: +420-2-2435-3964; fax: +420-2-3333-9929.
E-mail address: vopalem@fel.cvut.cz (M. Vopálenský).

0924-4247/$ – see front matter © 2003 Elsevier B.V. All rights reserved.
doi:10.1016/j.sna.2003.09.036

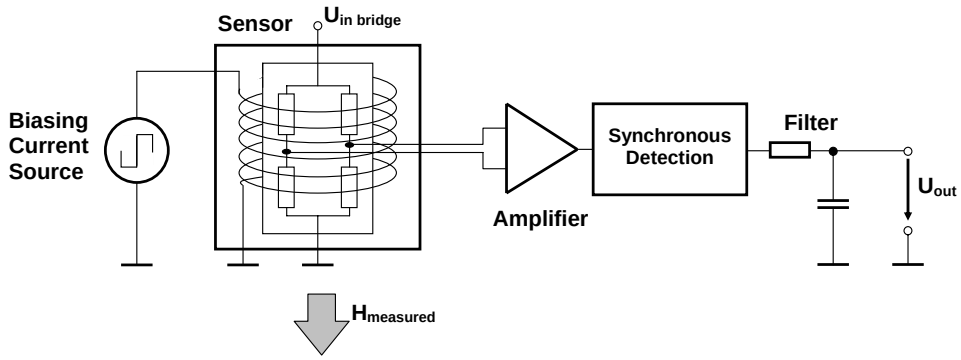

Fig. 1. Setup for the ac-biased GMR sensor measurement.

3. Measurement results

We used a laboratory supply source to create the dc bias field in the biasing coil. The characteristic becomes reversed for the inverted polarity of the biasing current. Thus we have made two measurements for each current value. The GMR sensor bridge (prototype provided by NVE) was supplied with a dc current source of 3 mA. As the bridge resistance is about 1060 Ω, the voltage across the bridge was about 3.16 V. The sensor was placed into Helmholtz coils, and an automatic computer-aided system [6] was used to control the coil current and to measure the output voltage value of the device. In this experiment, we measured the output voltage of the instrumentation amplifier with a gain of 10. Two samples were averaged.

One can see the comparison of the characteristics for ±8 and ±12 mA dc field biasing current in Fig. 2. The sensitivity is approximately 17 mV/V/kA/m in the case of 12 mA biasing current, which is a little less than for 8 mA biasing current. Nevertheless, the linearity range is wider and the hysteresis reduces to the half value in the same range for 12 mA biasing current. Considering the range of ±700 A/m to be the full scale, the hysteresis value is about 3% of the FS.

For the purpose of investigating ac field biasing possibilities for the magnetoresistive sensors, we developed a special evaluation board in our laboratory. The GMR sensor bridge was supplied by an 8 V dc voltage source in this case. Special timing of the synchronous detection was applied. As the sensor material properties are not stable immediately after the field biasing current changes its polarity, we decided to ignore the output for a short period of the time after the change of the bias field polarity (see Fig. 3). In Fig. 3, the zero-level active pulses controlling the synchronous detector are shown. The transients after reversing the characteristic of the sensor do not have any influence on the output, since just the stable, settled parts of the output signal are being selected.

In Fig. 4, one can compare the characteristics of the +9 and −9 mA dc field-biased GMR sensor to the characteristic of the same sensor being biased by an alternating squared field produced by a current with an amplitude of ±9 mA at a frequency of 1000 Hz. We measured in the range of ±300 A/m. There was an amplifier with a gain of 2 at the output of the synchronous detector and therefore the characteristic for the ac biasing is two times bigger than the characteristics for the dc biasing. However, the real sensitivity

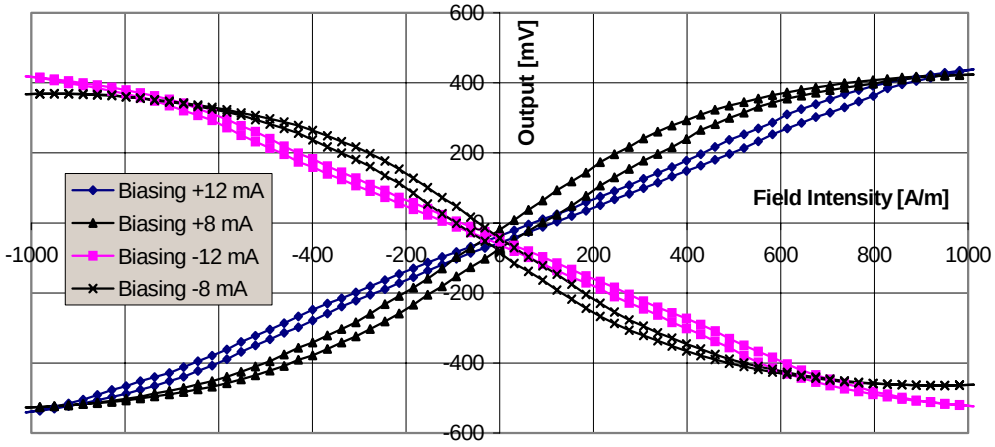

Fig. 2. The characteristics of sensitive-axis dc-biased GMR sensor.

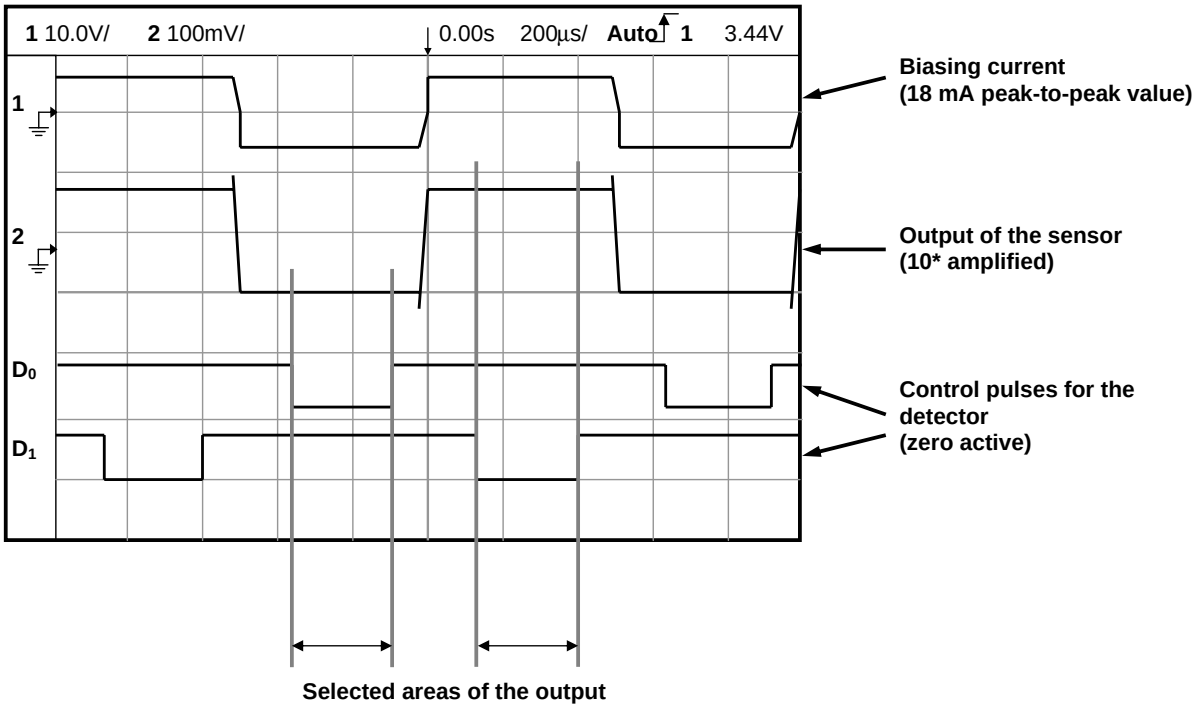

Fig. 3. The timing of the ac-biased GMR measurement.

of the sensor is about 20 mV/V/kA/m in both cases. One observes significantly suppressed hysteresis in the case of the ac biasing. Also, the linearity is slightly better than in the case of dc biasing. The detailed graphs showing the error in the case of dc and ac field biasing can be found in the Fig. 5. We suppose that the linearity could be improved using the feedback compensation of the sensor.

A measurement of the noise parameters of the NVE GMR sensor has been done. In [7], one can see that the noise power spectral density of a GMR sensor of the investigated type is of the character of $1/f$. The sensor was placed into a six-layer permalloy magnetic shielding. The supplying voltage of the bridge was of 8 V during these experiments. Fig. 6 shows the noise properties of the dc field-biased sensor and an example of the sensor output time plot. The biasing current was 9 mA. The gain of the instrumentation amplifier processing the sensor output signal was 10. The marker in the upper trace in Fig. 6 is placed at 1 Hz. The noise PSD value of the sensor output was approximately 2.5 µV RMS/$\sqrt{\text{Hz}}$ at 1 Hz, corresponding to approximately 16 mA/A RMS/$\sqrt{\text{Hz}}$ at 1 Hz, when we consider the measured sensitivity of 20 mV/V/kA/m. This noise value is much

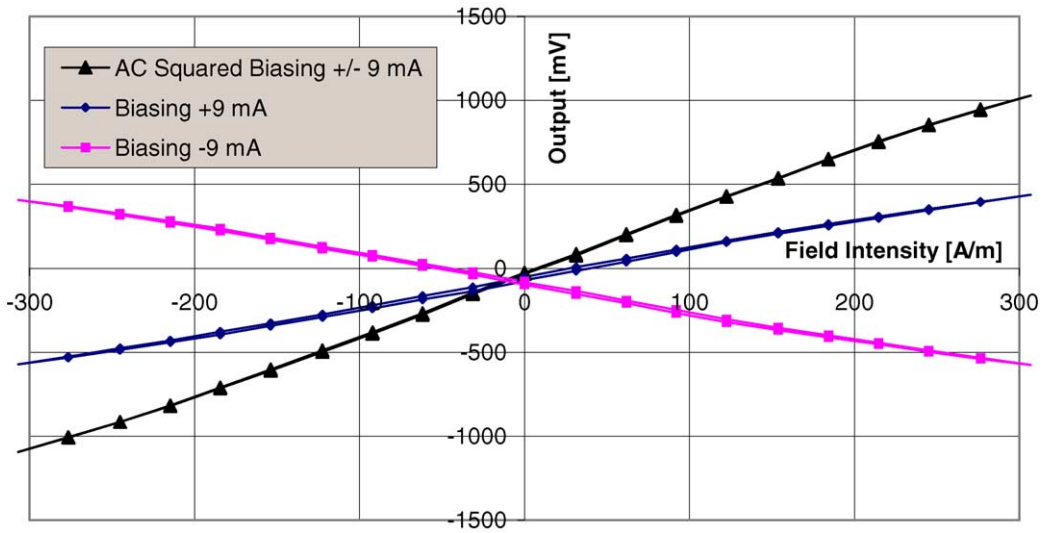

Fig. 4. The characteristics of the dc/ac sensitive-axis-biased NVE GMR sensor.

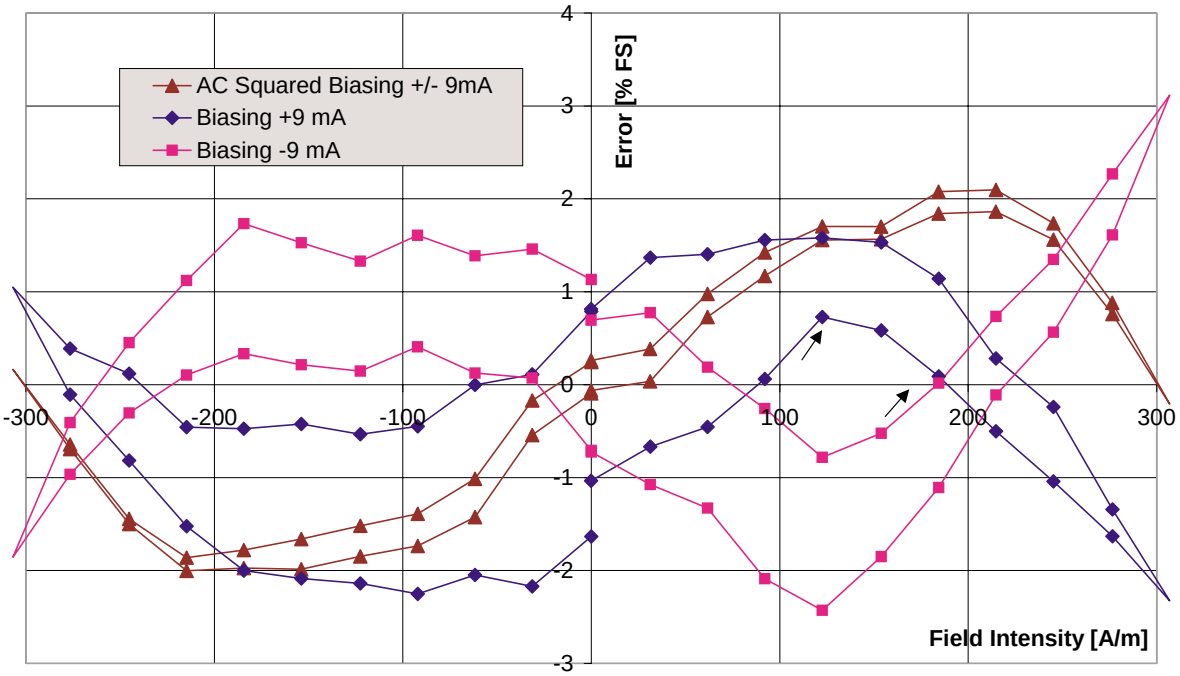

Fig. 5. The linearity and hysteresis of the sensitive-axis-biased NVE GMR sensor.

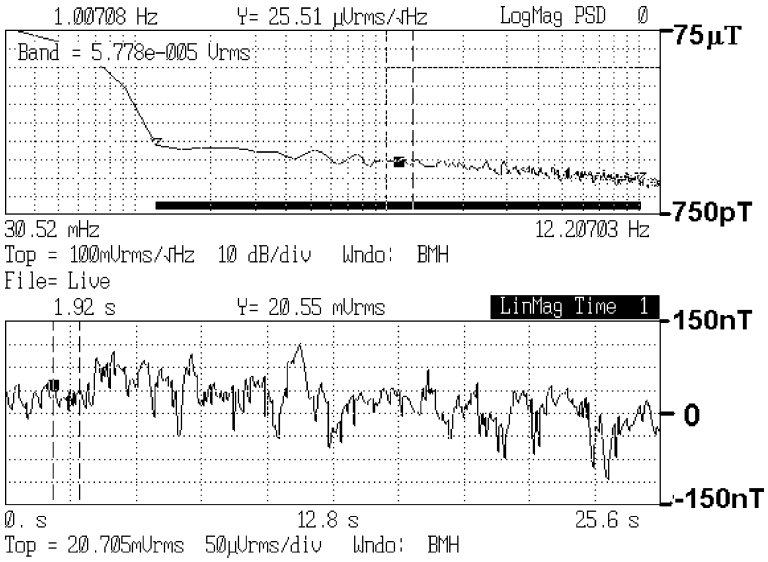

Fig. 6. The noise PSD RMS value of the dc-biased NVE GMR sensor. Upper trace—noise PSD RMS value (scale: log, 10 dB per division), lower trace—time record of the sensor output (scale: linear, 30 mA/m per division).

smaller than that referred to in [4]. The noise RMS value is about 35 mA/m in the 100 mHz to 10 Hz frequency range and the noise *p–p* value estimated from the lower diagram is about 180 mA/m.

When the sensor was biased by the alternating field produced in the biasing coil by a squarewave current of ±9 mA, the noise was measured after the synchronous detector. The single sensor output noise PSD value is about 5 µV RMS/$\sqrt{\text{Hz}}$ at 1 Hz, corresponding to approximately 28 mA/m RMS/$\sqrt{\text{Hz}}$ at 1 Hz. The noise RMS value in the case of ac biasing is about 80 mA/m in the 100 mHz to 10 Hz frequency range and the noise *p–p* value is about 360 mA/m.

4. Conclusion

The method used for biasing the sensor and processing the output signal results in significant improvements of the sensor behavior (see Fig. 5). The sensitivity was

about 20 mV/V/kA/m in the both cases. The waveforms in Fig. 5 demonstrate the difference between the measured and ideal characteristics. The linearity error both in the case of dc and squarewave ac ±9 mA field biasing is about 3% of FS in the respective ±300 A/m range. However, the hysteresis in the case of ac biasing was reduced to 0.5% of the FS, compared to 2% FS for the dc biasing.

The noise PSD value in the case of 9 mA dc field biasing was approximately 16 mA/m RMS/$\sqrt{\text{Hz}}$ at 1 Hz. Nevertheless, the noise has increased in the case of alternating biasing as described above. Our further research will focus on this problem.

References

[1] M. Tondra, in: P. Ripka (Ed.), Magnetic Sensors and Magnetometers, Artech House Publishers, London, first ed., 2001, Chapter 4.2.3, pp. 163–165
[2] General GMR Information. Nonvolatile Electronics, http://www.nve.com/technical/GMR/
[3] J.M. Daughton, Weakly coupled GMR sandwiches, IEEE Trans. Magn. 30 (2) (1994) 364.
[4] P. Ripka, M. Tondra, J. Stokes, R. Beech, AC-driven AMR and GMR magnetoresistors, Sens. Actuators, A 76 (1999) 225–230.
[5] S. Tumanski, Thin Film Magnetoresistive Sensors, Institute of Physics Publishing, Bristol, first ed., 2001, p. 291.
[6] J. Kubik, M. Vopalensky, Automated MR sensor measurement, Poster 2002 International Student Conference, CTU-FEE Prague 2002, Section EI14.
[7] A.F.Md. Nor, E.W. Hill, Noise power spectral density in single-strip NiFeCo–Cu GMR sensors, IEEE Trans. Magn. 38 (5) (2002) 2697–2699.

Biographies

Michal Vopálenský Received an Ing. degree (equivalent to MSc) in 2002 from the Faculty of Electrical Engineering at the Czech Technical University in Prague, Czech Republic. Immediately, he began to study for his PhD degree at the Department of Measurement at the mentioned faculty under the supervision of Prof. Pavel Ripka. During his pre-graduate study, he stayed for 6 weeks at the Milwaukee School of Engineering, Wisconsin, USA (2000) and for 4 months studying under the supervision of Prof. Hans Hauser at the Vienna University of Technology (2001). From February 2003, he was supported by the Government of United States of Mexico to make a research on magnetoresistive materials at the National University of Mexico, Mexico City. At the Czech Technical University, he taught as a supervisor in the subjects of sensors and transducers, contactless measurements, electrical measurements and analog signal preprocessing. His research interests are magnetic sensors and magnetometers, especially the anisotropic magnetoresistive sensors, giant magnetoresistors and spin-dependent tunneling sensors. At the time, he is an author or co-author of 17 papers. Tel.: +420-2-2435-3964; fax: +420-2-3333-9929. Email: vopalem@fel.cvut.cz.

Pavel Ripka Received an Ing. degree in 1984, a CSc (equivalent to PhD) in 1989, Prof. degree in 2001 from the Czech Technical University, Prague, Czech Republic. He works at the Department of Measurement, Faculty of Electrical Engineering, Czech Technical University as a lecturer, teaching courses in electrical measurements and instrumentation, engineering magnetism and sensors. His main research interests are magnetic measurements and magnetic sensors, especially fluxgate. A stay at the Danish Technical University (1991–1992) was a milestone is his scientific career. He is an author of >120 papers and five patents. He is a member of Elektra society, Czech Metrological Society, Czech National IMEKO Committee and Eurosensors Steering Committee. He was a General Chairman of Eurosensors 2002 Conference. Tel.: +420-2-2435-3945; fax: +420-2-3333-9929. E-mail: ripka@fel.cvut.cz

Jan Kubik Received an Ing. degree (MSc equivalent) in March 2003. He is currently a PhD student under Prof. Pavel Ripka at the Faculty of Electrical Engineering of Czech Technical University in Prague. He spent altogether 4 months in 2001 and 2002 at the Power Electronics Research Center in Galway, Ireland, under the supervision of Prof. W.G. Hurley where he participated in magnetic sensors research project. His research interests include magnetic sensor (magnetoresistive and fluxgate) properties testing, precise applications of magnetic sensors and measurement systems development. Tel.: +420-2-2435-3964; fax: +420-2-3333-9929. E-mail: kubikj@fel.cvut.cz

Mark Tondra Research Program Manager at NVE Corp. working with CVUT on the development and testing of spin-dependent tunneling sensors. He received a BS from the University of Wisconsin, Madison in 1989 and a PhD in Physics from the University of Minnesota in 1996. At NVE, he is currently working on projects for the development of spin-dependent tunneling memory and magnetic field sensors, magnetic bead-based biological assays, magnetometers, and related electronics systems. His technical expertise includes magnetism, magnetoresistive thin film development, and fabrication process development. Tel.: +1-952-996-1615; fax: +1-952-996-1600. E-mail: markt@nve.com.

[62] Vopálenský M., Mlejnek P., Ripka P.: AMR current measurement device. *Sensors and Actuators A, Vol. 141, Iss. 2 (2008), 649-653*

Available online at www.sciencedirect.com
ScienceDirect
Sensors and Actuators A 141 (2008) 649–653
SENSORS AND ACTUATORS A PHYSICAL
www.elsevier.com/locate/sna

AMR current measurement device

Pavel Mlejnek *, Michal Vopálenský, Pavel Ripka

Czech Technical University, Faculty of Electrical Engineering, Department of Measurement, Technicka 2, 166 27, Prague 6, Czech Republic

Received 20 April 2007; received in revised form 18 July 2007; accepted 3 October 2007
Available online 16 October 2007

Abstract

Many devices for contactless current measurement employ a magnetic circuit (flux concentrator) formed by a ferromagnetic ring (or yoke) with the sensor (typically Hall element) placed in the air gap. Thus the impact of the ambient magnetic fields (i.e. other than caused by the measured current) is highly reduced and the sensitivity of the device is increased. However, the linearity of such measurement can be affected by the non-linear behavior of the magnetic material of the yoke. A device for the contactless current measurement with anisotropic magnetoresistive sensors (AMR) has been developed. As the AMRs are much more sensitive than classically used Hall sensors, no magnetic concentrator is needed. The realized device reaches so far the linearity error of ±0.05% in the current range of ±8 A, i.e. the absolute resolution is 4 mA.

Keywords: Anisotropic magnetoresistive sensors; Contactless current measurement; Magnetic sensors applications

1. Introduction

Often used configuration of contactless current measurement devices comprise magnetic flux concentrators (yokes) in the form of a ring around the hole, where the examined wire is led through. Into an air gap formed in the ring, a magnetic field sensor with the sensitive axis perpendicular to the cross-section of the ring is placed. The Hall sensors are typical components used for this purpose [1]. Using of the magnetic field concentrator has some indisputable advantages—the magnetic field is highly concentrated in the air gap so that less sensitivity of the sensor is sufficient to a proper function, the error due to the un-centered position of the examined wire in the hole is suppressed because of the concentration effect; the impact of eventual un-clamped (out-of-hole) currents and/or another ambient magnetic fields (e.g. the magnetic field of Earth) on the sensor output is highly reduced for a similar reason. Nevertheless, there are a couple of disadvantages of such measurement setup: the response can be influenced by the nonlinear behavior of the magnetic material of the yoke (hysteresis, saturation, . . .), so that a special care must be taken choosing the material for the concentrator.

Anisotropic magnetoresistive sensors (AMR) have recently proven their suitability in various areas of the industry. They are much more sensitive than the Hall sensors and using of proper improvement techniques helps to reduce some undesired effects as the non-linearity, hysteresis and temperature dependences [2,3]. These properties make the AMRs suitable for the current measurements in the configuration of a rose-like array of AMRs surrounding the hole for the measured wire symmetrically, even without the need of the ring concentrators.

2. Brief theoretical considerations

The detailed analysis of the influences of non-linear behavior, non-identical sensitivities, non-identical compensating coil factors of the sensors etc. will be the subject of another intended paper. Nevertheless, let us make a brief analysis of the influence of one evident big error source—the displacement of the examined wire. In the following, we will consider the sensors to be strictly vectorial, reacting only to the magnetic field component parallel to their sensitivity axes. In addition, the sensitivities s will be considered to be identical for all the sensors as well as the compensating coils current-to-field converting factors f. The sensors are placed in an ideal symmetry and equidistance around the measurement hole so that their centers lie all on one concentric circle, dividing it in eight equal arcs. The sensitive axis of

* Corresponding author. Tel.: +42 2 2435 3964; fax: +42 2 3333 9929.
E-mail addresses: mlejnp1@fel.cvut.cz (P. Mlejnek), vopalem@centrum.cz (M. Vopálenský), ripka@fel.cvut.cz (P. Ripka).

0924-4247/$ – see front matter © 2007 Elsevier B.V. All rights reserved.
doi:10.1016/j.sna.2007.10.016

each sensor is tangent to the circle in this point. It can be shown that the error of the measurement caused by the displacement of the wire is the same for uncompensated and/or compensated sensors (even if not each sensor individually) for *strictly linear sensors*.

Sensor i responses to the respective field $H_{||,i}$ by a voltage

$$U_{\text{out},i} = sH_{||,i} \tag{1}$$

According to the Ampere's law, the magnetic field in the distance r from a straight current line in a homogeneous space is

$$H = \frac{I}{2\pi r} \tag{2}$$

In other words, the lines of constant field H are concentric circles with the center in the current line and the magnitude of H is decreasing with r. The most natural is to calibrate the measurement probe for wire led through the center of the hole and orthogonal to the sensors plane. Let the hole diameter be of 10 mm and sensor circumference 25.4 mm. For the centered position of the wire, the summed output voltage U_{tot} of the device is

$$U_{\text{tot}} = nU_{\text{out},i} = nsH_{||} = ns\frac{I}{2\pi r} \tag{3}$$

here n is the number of the sensors in the sensor array, and the meaning of the other quantities is explained above.

Hence the current can be calculated as

$$I_{\text{measured}} = \frac{2\pi r}{ns}U_{\text{tot}} = kU_{\text{tot}} \tag{4}$$

and k (A/V) is the transfer constant of the device calibrated for the central wire position.

When the wire is not centered, the outputs of all the sensors are not identical, and neither the sum of them is equal to that for the centered wire at the same current value. However, the current is calculated using the same k, i.e. the calculated current value is not correct. Let us define the relative error of the measurement as

$$\delta I = \left|\frac{I_{\text{measured}} - I_{\text{correct}}}{I_{\text{correct}}}\right| = \left|\frac{kU_{\text{tot}} - I_{\text{correct}}}{I_{\text{correct}}}\right| \tag{5}$$

Of course, the error decreases dramatically with the increasing number of sensors. From the Maxwells' equation or Ampere's law it is obvious that the measurement reading would be independent of the wire position for infinite number of sensors. The theoretical possibility of using one single sensor for the current measurement is conditioned by strictly assured fixed distance between the wire and the sensor. As the magnetic field depends hyperbolically on the distance from the wire, the error of the determination of current increases dramatically when the wire approaches the sensor. The maximum error occurs for minimum distance possible. For example in our case $r = 12.7$ mm, $(\Delta r)_{\max} = 5$ mm (the maximum displacement from the central position) and the corresponding $\delta I_{\max} = 65\%$.

Little more optimistic results we obtain using two sensors. Supposing the wire moves only on the line between the both sensors, the increase of the field at one sensor is bound with the decrease at the second one. However, because of the hyperbolic dependence of the field on distance, the increase of the field in the first sensor is not compensated by the same decrease in the second one. Let Δr be the displacement of the wire from the central position. Then, summing the both sensor outputs together, we obtain

$$U_{\text{tot}} = U_{\text{out},1} + U_{\text{out},2} = s\frac{I_{\text{correct}}}{2\pi(r - \Delta r)} + s\frac{I_{\text{correct}}}{2\pi(r + \Delta r)} = s\frac{I_{\text{correct}} r}{\pi(r^2 - \Delta^2 r)} \tag{6}$$

For the central position of the wire

$$k = \frac{\pi r}{s}, \tag{7}$$

and substituting to (4)

$$I_{\text{measured}} = I_{\text{correct}}\frac{r^2}{r^2 - \Delta^2 r} \tag{8}$$

From (5), the relative error as a function of the displacement Δr is

$$\delta I = \frac{\Delta^2 r}{r^2 - \Delta^2 r} \tag{9}$$

The maximum error occurs for maximum possible displacement. In our case $r = 12.7$ mm, $(\Delta r)_{\max} = 5$ mm and the corresponding $\delta I_{\max} = 18\%$.

Similar analyses could be done for another number of sensors, taking into account that for non-concentric wire the direction of the field in the position of a concrete sensor need not be parallel to the sensor sensitive axis and therefore the corresponding component has to be calculated.

In Table 1, the maximum relative errors for different numbers of sensors are listed for our dimensions. The theoretical relative error as a function of the angle when the current wire moves around the edge of the hole can be seen in Fig. 1. Note that y-axis is in logarithmic scale.

Table 1
The dependence of the maximum relative error of the current determination due to uncentered position of the wire on the number of sensors

Number of sensors	$\|\delta\|$ (%)
1	65
2	18.3
4	2.46
8	0.0578
16	0.0000333

Diameter of the hole 10 mm, diameter of the sensor array 25.4 mm (1 in.).

3. Measurement setup

Eight AMR sensors of KMZ51 type [4] (Philips product) are placed in a radial symmetry around the hole for the examined wire, so that the sensitive axes of the sensors are tangential to a circumference concentric with the hole. The hole has the diameter of 10 mm, the centers of sensors lay on a circle of

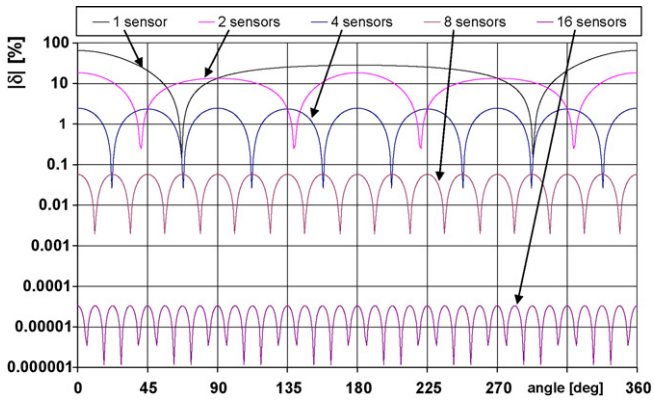

Fig. 1. The theoretical dependence of the relative error of the current determination, when the wire rotates around the measurement hole for various numbers of sensors. Diameter of the hole 10 mm, diameter of the sensor array 25.4 mm (1 in.).

the diameter of 25.4 mm (1 in.). Together with the sensors, the flipping capacitors and transistors are integrated at one board, forming the measurement probe of the device, as seen in Fig. 2. The sensors are flipped periodically at 1 kHz. Strong current pulses (>2 A) are needed in order that the flipping works properly [5] and the supply voltage of the device does not allow that such large pulses flow through all the eight flipping coils connected in series. Therefore the eight sensors are divided to two sections of four sensors connected in series, and each section of four has its own flipping capacitor controlled by its own transistor. For a similar reason, the compensating coils form two sections of four coils connected in series, but these two sections are parallel with the same source of the compensation current. The outputs of the individual sensors are led through a multiwire cable to the signal processing board, where they are 100× amplified by precise instrumentation amplifiers INA 131 [6] and then summed together (although exist better methods of signal processing than just averaging [7]). We have to notice that due to possible offsets

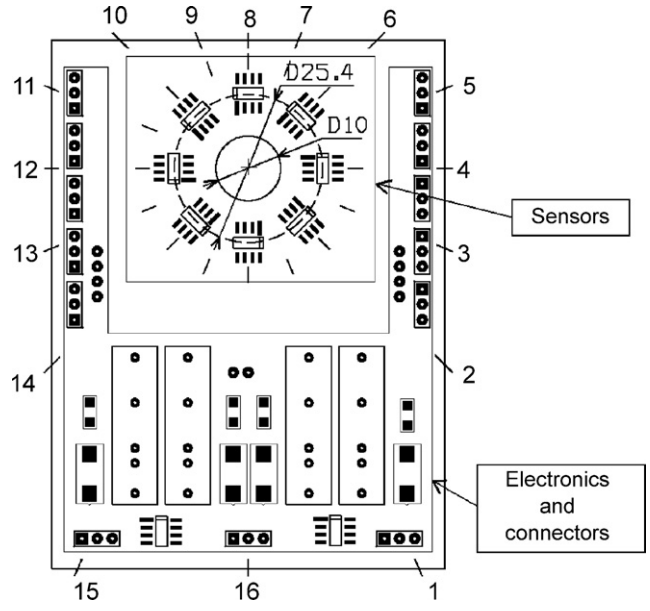

Fig. 2. The measurement probe layout.

of the sensor bridges, it is reasonable to block the dc component of the outputs of individual sensors after amplification by capacitors of a proper value (660 nF in our device) before the summing circuit. It is important to sum the individual bridge outputs with *correct polarity*. The rest of the processing chain is based on our previous experiences from the magnetometer development [2,3] and it is designed in a "traditional" manner. Resulting summed signal is squarewave at the flipping frequency and its amplitude is proportional to the sum of the magnetic fields acting at the positions of individual sensors, or, better, to the components of the field parallel to the sensitive axes. The signal is demodulated by slightly modified synchronous detector that ignores unstable parts (transients) of the waveform occurring at the sharp edges of the signal [2]. Demodulated quasi-dc signal is integrated and the output of the integrator is used as the compensation current for the sensors, producing in the sensor a magnetic field of the same magnitude but the opposite polarity to the external acting field, by means of the compensation coil. Thus the sensor bridge is operating always in zero operation point, working as a zero-indicator, a fact that results in a large suppression of the impact of the (temperature or cross-axis field) dependence of the sensitivity on the measurement. The voltage drop on a precise resistor connected in series within the compensation current loop represents the output of the device, being proportional to the compensating current and thus also to the measured magnetic field caused by the measured current flowing through the hole of the probe.

4. Measurement results

The most interesting parameters are the linearity, resolution, sensitivity and measurement range for a well-centered wire. Respecting the recommended linear range of the KMZ51 sensors [4] being of ±200 A/m, the maximum measured current can approach 16 A with or without the compensation. Of course, compensation mode has significant advantages. The linearity was measured in the range of ±8 A, since for higher currents the output amplifier of the device is saturated. The results are shown in Fig. 3. The linearity error is ±0.05% of ±8 A (considered as Full Scale), i.e. ±4 mA. The −3 dB bandwidth of

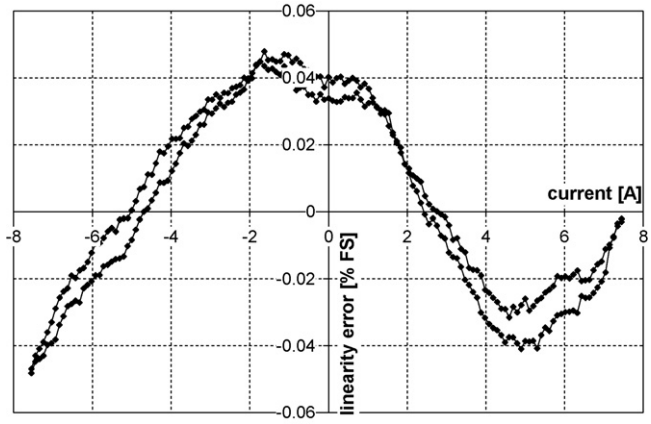

Fig. 3. The linearity error for centered wire and compensated sensor.

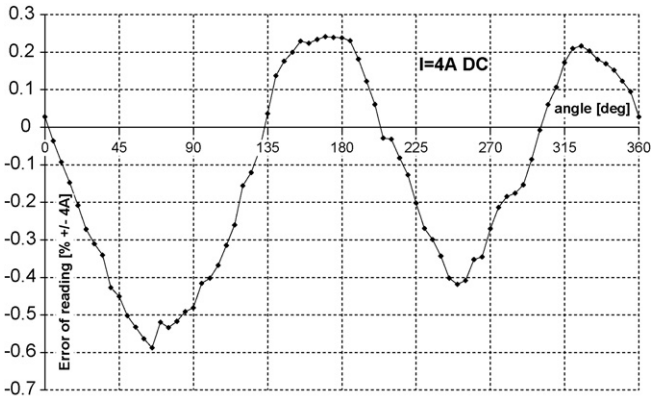

Fig. 4. Output reading of the device, when the wire rotates around the measurement hole. Diameter of the hole 10 mm, diameter of the sensor array 25.4 mm (1 in.).

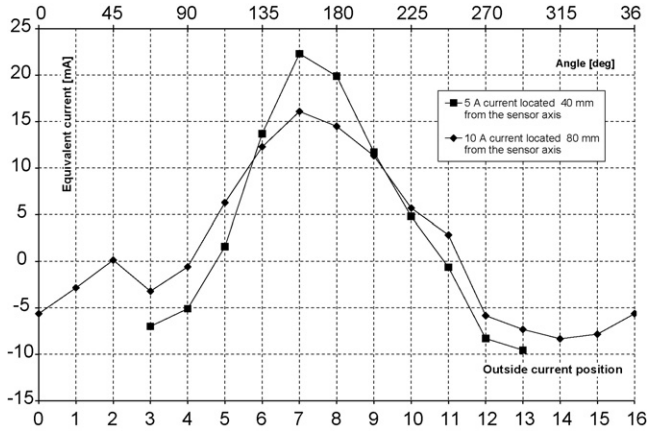

Fig. 5. The influence of an outer wire carrying the current of 4 A and placed to the positions by Fig. 1 on the output of the device. Diameter of the hole 10 mm, diameter of the sensor array 25.4 mm (1 in.).

this measurement is approx. 60 Hz @ 1 A, but probably it can be enhanced by minor changes in the circuitry. The influence of the wire displacement is illustrated in Fig. 4. The measurement was performed with a constant DC current of 4 A and the wire moved around the edge of the measurement hole. From Fig. 4, the error due to non-concentric wire seems to be very high (±0.5%) compared to the theoretically expected value (approx. ±0.06%). This error is caused mainly by the different sensitivities and compensation coil factors of the sensors, as well as by overall asymmetries in the probe layout. The influence of the outer "un-clamped" current is shown in Fig. 5. There was no current led through the measurement hole and thus the absolute values of the reading error recalculated to the "equivalent current" through the calibrated sensitivity for centered wire are indicated.

5. Conclusion

We showed the suitability of the commercial anisotropic magnetoresistors for the contactless current measurement application. The sensitivity of the sensors allows that no flux concentrator is needed. The error caused by the un-centered wire position decreases rapidly with the number of the sensors used in the rose-like array. The used configuration with eight KMZ51 sensors, array diameter of 25.4 mm and the hole diameter 10 mm theoretically allow measurement of the currents up to 20 A in the centered wire. We measured up to 8 A and the error reached ±0.05% of ±8 A, which is considerably better result than the previous work published in [8]. The error of the current determination caused by uncentered wire is of ±0.5%, which is much worse than promises the numerical simulation, and it is caused by differences between the sensitivities and feedback coil factors of individual sensors. An external current of 5 A in the distance 40 mm from the sensor array center causes an additional absolute error of max. 25 mA. Detailed analyses of the non-identical behavior of individual sensors used in the array will be a subject of another paper.

References

[1] K. Iwansson, G. Sinapius, W. Hoornaert (Eds.), Measuring Current, Voltage and Power, first ed., Elsevier, Amsterdam, 1999, p. 41.
[2] P. Ripka, M. Vopálenský, A. Platil, M. Döscher, K.-M.H. Lenssen, H. Hauser, AMR magnetometer, J. Magnetism Magnetic Mater. 254–255 (2003) 639–641.
[3] M. Vopálenský, P. Ripka, A. Platil, Precise magnetic sensors, Sens. Actuators A106 (2003) 38–42.
[4] KMZ51 Magnetic field sensor, Datasheet, accessible at http://www.semiconductors.philips.com/acrobat/datasheets/KMZ51_3.pdf.
[5] H. Hauser, P.L. Fulmek, P. Haumer, M. Vopalensky, P. Ripka, Flipping field and stability in anisotropic magnetoresistive sensors, Sens. Actuators A106 (2003) 121–125.
[6] INA131 Precision G=100 Instrumentation Amplifier, Datasheet, accessible at http://focus.ti.com/lit/ds/symlink/ina131.pdf.
[7] R. Bazzocchi, L. Di Rienzo, Interference rejection algorithm for current measurement using magnetic sensor arrays, Sens. Actuators 85 (2000) 38–41.
[8] P. Ripka, P. Kejík, P. Kašpar, K. Draxler, Precise DC current sensors, in: IEEE Instrumentation and Measurement Conference, Brussels, Belgium, June 4–6, 1996, pp. 1479–1483.

Biographies

Pavel Mlejnek graduated from the Faculty of Electrical Engineering at the Czech Technical University in Prague with an Ing. degree (MSc equivalent) at the Department of Measurement in 2005. The subject of his diploma thesis was "Contactless current measurement device with the anisotropic magnetoresistive sensors". Currently a PhD student in the Laboratory of Magnetic Measurements, Department of Measurement, CTU-FEE in Prague. His research interests are current sensors resistant to external interference (dc tolerant current transformers, Rogowski coils).

Michal Vopálenský received an Ing. degree (eq. to MSc) in 2002 and PhD in 2006 from the Faculty of Electrical Engineering at the Czech Technical University in Prague, Czech Republic. During his study, he stayed for 6 weeks at the Milwaukee school of Engineering, Wisconsin, USA (2000) and for 4 months at the Vienna University of Technology (2001). In 2003, he was with National University of Mexico, Mexico City, supported with a scholarship from Government of Mexico for making research on magnetoresistive materials. From March 2006 to March 2007, he worked as a researcher on a magnetoresistive sensors oriented project at Tyndall National Institute, Ireland. His research interests are Magnetic Sensors and Magnetometers, especially the Anisotropic Magnetoresistive Sensors, Giant Magnetoresistors and Spin Dependent Tunneling Sensors. At the time, he is an author or co-author of about 30 scientific papers.

Pavel Ripka received an Ing. degree in 1984, a CSc (equivalent to PhD) in1989 and Prof. degree in 2001 at the Czech Technical University, Prague, Czech Republic. He works at the Department of Measurement, Faculty of Electrical

Engineering, Czech Technical University as a full professor, teaching courses in electrical measurements and instrumentation, engineering magnetism and sensors. He also worked as visiting scientist at Danish Technical University (1990–1993), National University of Ireland (2001) and in the Institute for the Protection and the Security of the Citizen, European Commission Joint Research Centre in Italy (2005/2006). His main research interests are magnetic measurements and magnetic sensors, especially fluxgate. He is an author of >50 SCI journal papers and five patents. He is a member of IEEE, Elektra Society, Czech Metrological Society, Czech National IMEKO Committee and Eurosensors Steering Committee. He served as an associate editor of the *IEEE Sensors Journal*. He was a General Chairman of Eurosensors 2002 conference.

[65] Vopálenský M., Platil A., Kašpar P.: Wattmeter with AMR sensor. *Sensors and Actuators A, Vol. 123-124 (2005), 303-307*

Available online at www.sciencedirect.com
SCIENCE DIRECT®
Sensors and Actuators A 123–124 (2005) 303–307
SENSORS AND ACTUATORS A PHYSICAL
www.elsevier.com/locate/sna

Wattmeter with AMR sensor

Michal Vopálenský *, Antonín Platil [1], Petr Kašpar [2]

Czech Technical University, Faculty of Electrical Engineering, Department of Measurement, Technicka 2, 166 27 Prague 6, Czech Republic

Received 13 September 2004; received in revised form 24 January 2005; accepted 4 March 2005
Available online 19 April 2005

Abstract

Analog multipliers comprising the Hall sensors have been used in electronic design, typically in powermeters. This article summarizes the results of experiments performed with a commercially available anisotropic magnetoresistive (AMR) sensor, used for the same purpose. The on-chip compensation coil can be successfully used in the function of the "current clamps" of the wattmeter. Periodical re-magnetizing (flipping) of the sensor structure performed by the flipping coil can improve the device parameters. This paper is not a description of a functioning, practice-ready device. It reports an experiment showing the feasibility of AMRs in the area of power measurements.

Keywords: Analog multipliers; Electronic powermeters; Electronic wattmeters; Anisotropic magnetoresistive sensors

1. Introduction

The need for measurement of the active electric power led to the development of various types of powermeters. The basic, classical electromechanical gauges using electrodynamic measurement system are still used, in spite of their drawbacks. The dynamical response of them is limited, since they employ coils of considerable inductance. Recently, the bandwidth of powermeters became a crucial parameter due to the need of the measurement of general, rather non-harmonic signals with a high content of the higher harmonic frequencies. By that time, two basic approaches arose:

(1) separate real-time sampling and A/D conversion of the current $i(t)$ and voltage $u(t)$, followed by fully digital processing of acquired data;
(2) using of an appropriate electronic multiplier, where the two signals proportional to the voltage and current, respectively, are multiplied in real-time. Thus, the output of such a transducer is the instantaneous power of the signal defined as

$$p(t) = i(t)u(t) \tag{1}$$

For the harmonic signals described as

$$\begin{aligned} i(t) &= I_{\mathrm{m}} \sin \omega t \\ u(t) &= U_{\mathrm{m}} \sin(\omega t + \phi) \end{aligned} \tag{2}$$

where I_{m} and U_{m} are the amplitudes of the current and voltage, respectively, the mean value of (1) over one period, called the *active power*, can be expressed by a well-known formula

$$P = \frac{1}{T}\int_T u(t)i(t)\,\mathrm{d}t = UI\cos\phi \tag{3}$$

Here, $U = U_{\mathrm{m}}/\sqrt{2}$ and $I = I_m/\sqrt{2}$ are the root mean square (RMS) values of $u(t)$ and $i(t)$, respectively.

Power transducers with the Hall sensors [1,2] as multiplying elements gained a huge importance in the field of the described 'direct' power measurement. The basic problems are caused by their insufficient sensitivity, resulting in the need of ferromagnetic yokes to concentrate the magnetic flux into the sensor area.

More advantageous anisotropic magnetoresistive (AMR) sensors can replace the Hall sensors [3–5].

* Corresponding author. Tel.: +42 2 2435 3964; fax: +42 2 3333 9929.
E-mail addresses: vopalem@fel.cvut.cz (M. Vopálenský), platil@fel.cvut.cz (A. Platil), kaspar@fel.cvut.cz (P. Kašpar).
[1] Tel.: +42 2 2435 3964; fax: +42 2 3333 9929.
[2] Tel.: +42 2 2435 2188; fax: +42 2 3333 9929.

0924-4247/$ – see front matter © 2005 Elsevier B.V. All rights reserved.
doi:10.1016/j.sna.2005.03.033

2. Measurement setup

The basic idea of the AMR used in the function of an analog multiplier is very simple: the Wheatstone bridge of the AMR sensor is supplied by a signal, which is proportional to the voltage of the measured signal. At the same time, current proportional to the current of the measured signal is led through a coil, generating magnetic field which is the Wheatstone bridge exposed to. The output (diagonal) voltage of the bridge is (linearly) dependent on the acting magnetic field, and at the same time, it is linearly dependent on the supplying voltage. As a direct consequence of these two facts, the output is dependent on the multiple of the two signals. There are various ways how to design the proper coil creating the magnetic field. Usually, this coil is external, wound around the sensor [3]. In a commercial AMR, in our case the KMZ51 [6], usually a flat coil is integrated, dedicated to the compensation of the bridge when measuring the magnetic field. However, we can employ this internal coil for the excitation of the bridge, gaining some important advantages: highly enlarged sensitivity (because of the proximity of the coil to the bridge), well-defined direction of the field (minimizing thus the cross-axis fields [7]), and simple realization. Moreover, the inductance of this planar coil is negligible compared to its resistance (∼180 Ω) up to 100 kHz (measured with the HP 4263B RLC bridge). On the other hand, when using the internal coil for generating of the field, we have to consider the maximum allowed dc compensation current (in our case, 15 mA) as the upper RMS limit of the ac current led through. Additional problems may arise because of the proximity of the coil to the magnetoresistive bridge—15 mA flowing through 180 Ω resistance of the coil may cause temperature increase inside the sensor, accompanied by unavoidable change of the bridge resistances.

The overall arrangement of the measurement setup is illustrated in Fig. 1. The voltage and current signals are provided by two locked HP 33120 generators. We used the sine waveform for the testing. It is very important to determine properly the mutual phase shift between the two signals. For this purpose, we used an oscilloscope in the *xy*-mode, trying to obtain a straight line on the screen, when the shift between the signals is 0°. This procedure provides a very well-defined basic point for the phase shift determination. Bifilarly wound resistance standard (ethalon) 100 Ω was used as the sensing element for the current measurement, having the temperature coefficient of 10^{-3} Ω/K. The voltages across the bridge and on the current sensing resistance were measured by HP 34401 multimeters (RMS measurement) and monitored by Agilent 54624 four-channel oscilloscope. The magnetoresistive material was re-magnetized, or flipped, before each reading by a strong 2.8 A pulse to get the ferromagnetic material to a defined initial state. The optimum flipping performance is provided by well-designed flipping circuits (see [8]). The output signal of the bridge is 100× amplified by a precise instrumentation amplifier INA129 [9] and then filtered by a passive low-pass filter with the corner frequency $f_c \approx 5$ Hz, to

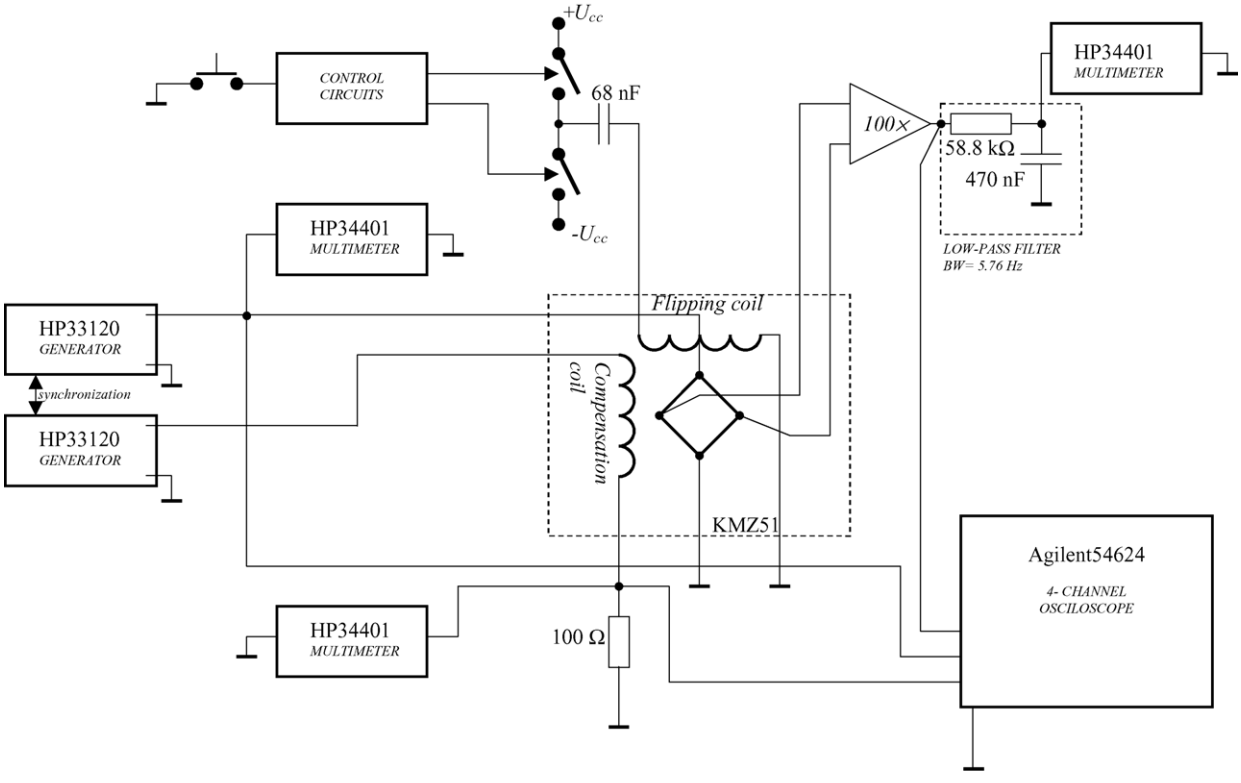

Fig. 1. The measurement setup.

obtain the *mean value* of the signal. Another HP 34401 was used to measure the mean value of the output signal after the filter. The influence of the output offset of the instrumentation amplifier was eliminated subtracting its value (measured as 1.5 mV when the both inputs were grounded) from each reading. Knowing the RMS values of the voltage and current and the phase shift between the two signals, the active power can be calculated after (3). The dc offsets in both the voltage and current input signal have to be reduced the best possible way because they would cause an undesirable additional dc component of the output waveform. The output before filtering is a sinewave signal at a double frequency of the input signals and its dc component is proportional to the active power. The offset of the measuring bridge can be eliminated from the result subtracting the dc values obtained for the same input signals and two opposite flipping directions.

During the measurement, the sensor was placed into a four-layer permalloy cylindrical magnetic shielding to eliminate the influence of disturbing external magnetic fields (dc attenuation of the shield ∼ 75 dB at 100 mT).

3. Measurement results

It is a little difficult to characterize a multiplier or wattmeter by a single parameter, or even set of parameters or a 2D-diagram, as it has more than one input each having its own frequency characteristics, it behaves differently for various phase shifts between the input signals, etc. Respecting the producer recommended values of the dc input voltage and current, being of 9 V dc and 15 mA dc, we decided to measure up to 5 V RMS across the bridge and 10 mA RMS through the compensation coil. These values were chosen in order that neither the amplitude values of the ac signals exceed the maximum recommended values for dc. As the minimum values adjustable at the generators correspond to 34 mV RMS and 0.107 mA RMS, the dynamic range of our measurement setup is approximately two decades in both the voltage and current inputs. In terms of the power, chosen ranges of voltage and current mean the power range from approximately 3.6 μW to 50 mW for zero phase shift of the signals, i.e. more than four decades (factor 1.4×10^4).

3.1. Phase shift dependence

The zero phase shift was adjusted as described above and the phase shift function of the generators was used to adjust another values. The dependence of the mean value of the output on the phase shift between the input signals for the smallest (34 mV, 0.107 mA), medium (300 mV, 1 mA) and large (4 V, 10 mA) input signals at the frequency of 100 Hz was measured. The results of the last two cited measurements can be seen in Fig. 2. The relative error calculated as

$$\delta = \frac{\text{correct value} - \text{measured value}}{\text{correct value}} \times 100\%$$

in the range of ±70° is below 0.1% in most cases. Due to its definition, the relative error increases dramatically when the phase shift approaches 90°. For the smallest input signals measured, the dependence of the error is not displayed, because it reaches up to 20% of the correct value in the range of ±70°; however, this considerable error may be caused by the low resolution of the measurement of such small values (the maximum active power for $\varphi = 0°$ is less than 3.7 μW,

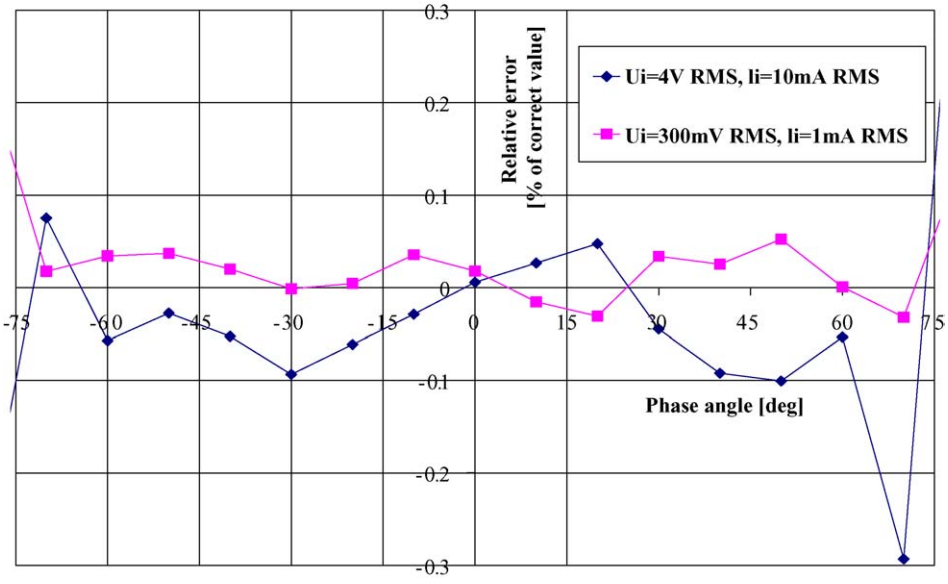

Fig. 2. Relative error of the indicated value as a dependence of the input signals phase shift at 100 Hz.

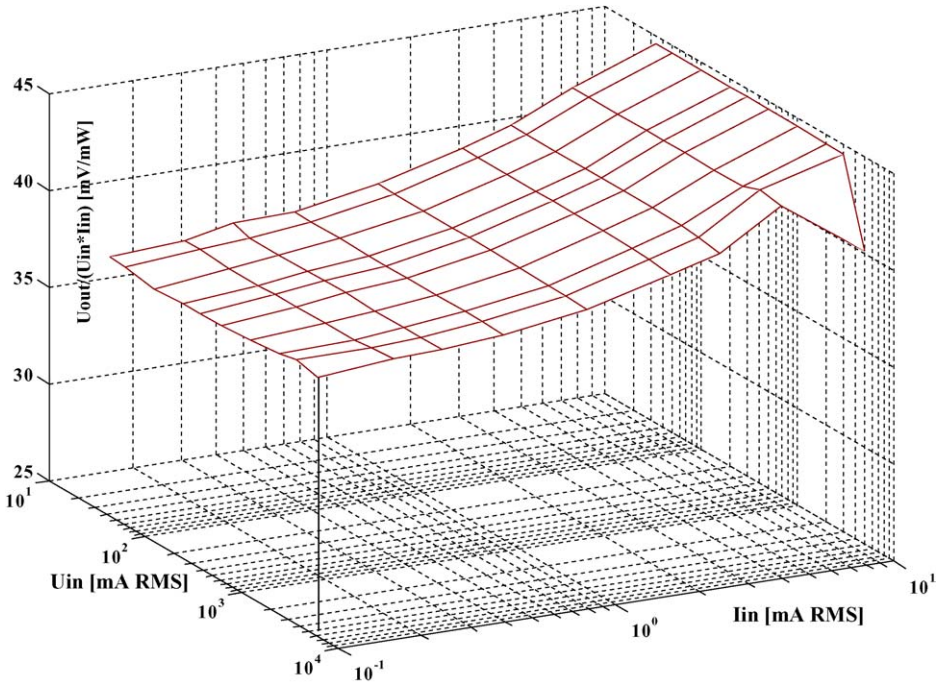

Fig. 3. The map of the sensitivity in dependence on the input values. Phase shift: 0° and frequency: 100 Hz.

the output of the device after amplification by 100 does not exceed 100 μV).

3.2. Input signal magnitude dependence

The linearity of the device with respect to the RMS values of the inputs *for the phase shift of 0°* in logarithmical series 1–2–3–5 over the whole dynamic ranges of the both inputs was measured. The ratio of the output voltage (proportional to the active power) to the product of the input RMS values, or simply the sensitivity of the multiplier, is one of the most indicative parameters. In another words, the output voltage U_{out} of the multiplier should be given as

$$U_{\text{out}}(\varphi = 0) = kU_{\text{in,RMS}} I_{\text{in,RMS}} \quad (4)$$

where the sensitivity k [V/W] should be constant for any values of U_{in} and I_{in}.

The 'sensitivity map' measured at 100 Hz is shown in Fig. 3. It is obvious that the sensitivity almost does not depend on the voltage at a fixed current, but unfortunately the same is not valid for the varying current at a fixed voltage.

3.3. Frequency range and feedthrough

The frequency dependence of the sensitivity was measured at a 'medium range' of 300 mV, 1 mA RMS and the phase shift 0°. The −3 dB bandwidth of the amplifier is typically 200 kHz [9]. The device measures well up to a relatively high frequency of 100 kHz. When measuring at higher frequencies, we have to consider some serious complications. The first one is the impedance mismatch of the 50 Ω output of the generators, the cable and its termination. Another problem that has to be taken into account is considerable leakage of the input signals of the multiplier to the output. The leakage of one of the input signals of a multiplier to the output, when the second input is grounded, is called "feedthrough" [10]. In our case, the feedthrough of the supplying voltage of the bridge is considerable, caused probably by the imaginary parts of bridge elements impedances. Their compensation is possible just for a certain frequency and thus the feedthrough is strongly frequency dependent. If there are feedthroughs from the both input channels, the reliability of the output is affected, as the product of two sine functions at the same frequency is not zero in general, and thus the resulting dc component contributes to the useful output. If there is just one channel feeding through to the output, it does not affect the mean value (or active power, which is measured); however, the output value in certain time moment does not correspond to the instantaneous power anymore. The maximum feedthrough leakage of the supplying voltage is 320 mV RMS at 200 kHz for the supplying voltage $U_{\text{i}} = 2$ V RMS, whereas the maximum feedthrough of the current channel is 8 mV RMS at 1 MHz for $I_{\text{i}} = 2$ mA RMS.

4. Conclusion

We have demonstrated that a commercial magnetoresistive sensor can be successfully used as a simple analog signal multiplier or wattmeter. Amongst the main advantages of the AMR used in this area belongs the wide bandwidth (1 MHz typically after the producer). As the compensation

coil is placed very near to the sensitive bridge of the sensor, we can reach an extreme sensitivity of the sensor to the measured current. Estimated from the magnetic applications of the used sensor, the resolution should be in the order of units of microampere in the current channel. The linearity error with respect to the phase shift of the input signals is approximately 0.1% in the range of $\pm 70^{\circ}$. A serious problem is the change of the sensitivity with the current flowing through the compensation coil of the sensor, probably a consequence of the heating within the sensor structure and the intrinsic nonlinearity of the field response of the sensor. The leakage of the supplying voltage of the bridge to the output is evident, and it can be explained considering the non-negligible reactance character of the bridge elements.

Further improvement could be done using a proper way of the periodical flipping and synchronous detection [11] of the output signal. Also, we suppose that the dependence of the sensitivity on the current could be reduced using some type of magnetic compensation mode of the sensor. However, two excitation coils in the sensitive axis of the bridge would be necessary.

References

[1] K. Iwansson, G. Sinapius, W. Hoornaert (Eds.), Measuring Current, Voltage and Power, first ed., Elsevier, Amsterdam, 1999, p. 41.
[2] Patent US 4,199,696, Multiplier using Hall element.
[3] S. Tumanski, Thin Film Magnetoresistive Sensors, first ed., Institute of Physics Publishing, London, 2001, pp. 347–352.
[4] Patent EP 0218905, Low-cost self-contained transformerless solid state electronic watthour meter having thin film ferromagnetic current sensor.
[5] Patent US 4,525,668, System for measuring electrical output or energy.
[6] KMZ51 Magnetic field sensor, Datasheet, accessible at http://www.semiconductors.philips.com/acrobat/datasheets/KMZ51_3.pdf.
[7] B. Pant, M. Caruso, Magnetic sensor cross-axis effect, Honeywell Application Note 205, accessible at http://www.ssec.honeywell.com/magnetic/datasheets/an205.pdf.
[8] H. Hauser, P.L. Fulmek, P. Haumer, M. Vopalensky, P. Ripka, Flipping field and stability in anisotropic magnetoresistive sensors, Sens. Actuators A106 (2003) 121–125.
[9] INA 129 Precision, Low power instrumentation amplifiers. Datasheet, accessible at http://focus.ti.com/lit/ds/symlink/ina129.pdf.
[10] MPY 634, Wide bandwidth precision analog multiplier. Datasheet, accessible at http://focus.ti.com/lit/ds/symlink/mpy634.pdf.
[11] M. Vopálenský, P. Ripka, A. Platil, Precise magnetic sensors, Sens. Actuators A106 (38) (2003) 42.

Biographies

Michal Vopálenský received an Ing. degree (equivalent to MSc) in 2002 at the faculty of electrical engineering at the Czech Technical University in Prague, Czech Republic. Began to study for his PhD degree at the Department of Measurement at the mentioned faculty under the supervision of Prof. Pavel Ripka immediately. During his pre-graduate study, he stayed at the Milwaukee School of Engineering, Wisconsin, USA (2000), and at the Vienna University of Technology (2001). In 2003, he was supported by the government of Mexico to make a research on magnetoresistive materials at the National University of Mexico, Mexico City. His research interests are magnetic sensors and magnetometers, especially the anisotropic magnetoresistive sensors, giant magnetoresistors and spin dependent tunneling sensors. At the time, he is an author or co-author of about 25 scientific papers.

Antonín Platil was born in Prague in 1972. He graduated from the faculty of electrical engineering, Czech Technical University in Cybernetics in 1997. He received PhD degree in measurements in 2002. His research interests cover magnetic measurements, sensors and application of computer systems in measurements.

Petr Kašpar received an Ing. degree (MSc equivalent) in 1981 and CSc (PhD equivalent) in 1988. Since 1999, he is associate professor at the Faculty of electrical engineering of Czech Technical University in Prague, laboratory of magnetic measurements. His research interests include PC controlled systems for magnetic measurements, measurements of magnetic disturbances and test methods of magnetic materials.